DELIVERY AND EFFICACY OF CDK4/6 INHIBITORS IN THE TREATMENT OF BRAIN TUMORS

A DISSERTATION

SUBMITTED TO THE FACULTY OF THE UNIVERSITY OF MINNESOTA

BY

KAREN EILEEN PARRISH

IN PARTIAL FULFILLMENT OF THE REQUIERMENTS

FOR THE DEGREE OF

DOCTOR OF PHIOLOSOPHY

WILLIAM F. ELMQUIST

JANUARY 2016

ACKNOWLEDGEMENTS

I would not be where I am today without the help of many people throughout my graduate work. First, I would like to thank my advisor, Dr. William F. Elmquist. His patience and enthusiasm for our work are just a few of the many qualities that make him a great advisor. I would like to thank Dr. Jann N. Sarkaria who is on my committee and has been a fantastic mentor as I have developed my scientific voice. His comments while preparing manuscripts were invaluable; he did not just make my writing better, but made me a better writer. Dr. Carolyn Fairbanks was a mentor early on in my schooling when I worked as an undergraduate in her lab. She gave me the first exposure to the Department of Pharmaceutics at the University of Minnesota and her support and guidance have been essential as I navigated graduate school. I would like to thank Dr. Richard Brundage for his guidance and thoughtful questions that have brought out the best of my research project. He has been a great mentor during my graduate studies and a constant reminder to think critically about my data.

Thank you to my colleagues in the Elmquist lab, both past and present: Dr. Rajendar Mittapalli, Dr. Ramola Sane, Dr. Shruthi Vaidhyanathan, Dr. Rajneet Oberoi, Dr. Shuangling Zhang, Brynna Wilken-Resman, Gautham Gampa, Minjee Kim, and Janice Laramy. Their support has enabled me to learn and grow as a scientist and I will always remember my times in the lab with these wonderful friends. This research would not have been able to be completed without the help of collaborators in the Sarkaria Lab at the Mayo Clinic. Brett,

Ann, Katie, and Mark were all instrumental in ensuring the studies in tumor-bearing mice went smoothly.

I would like to thank the Department of Pharmaceutics and the Graduate School at the University of Minnesota. The Rowell, Sawchuk, and Rippie fellowships enabled me to focus on my research and funding from the department gave me the opportunity to present my work at national and international conferences. I would like to thank the Graduate School at the University of Minnesota for the Doctoral Dissertation Fellowship which covered my stipend and funded the opportunity to travel to AAPS 2015. I would also like to thank AFPE for the Pre-Doctoral Fellowship from 2013-2015.

Finally, I would like to thank my husband, Anthony, for his support and encouragement. He has pushed me to be a better scientist and provided fresh eyes and entertainment when I needed it most. I would like to thank my brothers who supported me throughout my studies and lastly, I would like to thank my first teachers, my parents John and Maureen Riedl who allowed me to believe this was all possible.

DEDICATION

This thesis is dedicated to my father, John Thomas Riedl (1962-2013).

One my father's favorite quotations was from Thorstein Veblen:

> *"The outcome of any serious research can only be to make two questions grow where only one grew before."*

I hope my thesis project has done just that.

ABSTRACT

Primary and metastatic brain tumors have limited treatment options and long term survival is rare. Cyclin-dependent kinases (CDKs) are major regulators of the cell cycle and are commonly altered in tumors. The CDK4/6 pathway regulates the checkpoint between G1 and S phase of the cell cycle. When altered, cells are able to proliferate rapidly and independent of this checkpoint. The blood-brain barrier (BBB) is a network of cells and proteins that prevent the paracellular and transcellular passage of many therapeutic agents from systemic circulation into the brain. The efflux transporters P-glycoprotein (P-gp) and breast cancer resistance protein (BCRP) actively transport substrates back into systemic circulation. Previous studies have demonstrated that numerous molecularly-targeted agents are substrates of P-gp and/or BCRP and that these transporters are responsible for the limited brain delivery. The objective of this work was to evaluate the role of efflux transport at the BBB in the brain delivery of CDK4/6 inhibitors and assess the relationship between brain delivery and efficacy in a glioblastoma (GBM) patient-derived xenograft. There are three CDK4/6 inhibitors, palbociclib, ribociclib and abemaciclib, currently in clinical development for the treatment of a variety of solid tumors. We show that palbociclib has limited brain delivery to active efflux transport by P-gp and BCRP at the BBB. Furthermore, we demonstrate that the concentrations of palbociclib reaching the brain are also subtherapeutic in the treatment of a subcutaneous GBM tumor. We then used a pharmacological inhibitor of efflux transport and

improved the brain delivery of palbociclib in tumor-naïve and tumor-bearing mice. We demonstrated that chronic use of this combination therapy was well tolerated and significantly improved the brain delivery of palbociclib in an intracranial tumor model to the same levels that were achieved in the subcutaneous GBM model. Despite improving the brain delivery of palbociclib, there was no improvement in efficacy. Using the *in situ* brain perfusion technique, we compared the brain delivery of palbociclib, ribociclib and abemaciclib and the data suggest that abemaciclib may saturate efflux at lower concentrations that palbociclib or ribociclib and have improved brain delivery. These studies show that improving the brain delivery of palbociclib alone is not sufficient to improve survival in the intracranial GBM model. Future studies that reveal other factors besides delivery that are altered in subcutaneous models of brain tumors will be essential in understanding the use of preclinical models to study experimental GBM therapies.

TABLE OF CONTENTS

LIST OF TABLES

LIST OF FIGURES

CHAPTER I

IMPROVING DRUG DELIVERY TO PRIMARY AND METASTATIC BRAIN TUMORS: STRATEGIES TO OVERCOME THE BLOOD-BRAIN BARRIER

This chapter has been published as a manuscript in Clinical Pharmacology and Therapeutics. 2015; 97(4):336-346.

www.wileyonlinelibrary/cpt

Abstract

Brain tumor diagnosis has an extremely poor prognosis, due in part to the blood-brain barrier (BBB) that prevents both early diagnosis and effective drug delivery. The infiltrative nature of primary brain tumors and the presence of micro-metastases lead to tumor cells that reside behind an intact BBB. Recent genomic technologies have identified many genetic mutations present in glioma and other CNS tumors, and this information has been instrumental in guiding the development of molecularly-targeted therapies. However, the majority of these agents are unable to penetrate an intact BBB, leading to one mechanism by which the invasive brain tumor cells effectively escape treatment. The diagnosis and treatment of a brain tumor remains a serious challenge and new therapeutic agents that either penetrate the BBB or disrupt mechanisms that limit brain penetration, such as endothelial efflux transporters or tight junctions, are required in order to improve patient outcomes in this devastating disease.

1.1 INTRODUCTION TO DISEASE

In the United States over 10,000 patients are expected to be diagnosed with glioblastoma multiforme in the year 2015 and over ten times that number will be diagnosed with metastatic brain tumors (Ostrom et al., 2014). Brain tumor diagnosis is devastating to patients and their families with median survival after diagnosis between 4 and 15 months (Stupp et al., 2005; Maher et al., 2009). Promising experimental agents continue to fail in clinical trials and the incidence of primary and metastatic brain tumors continues to rise. The vast majority of available therapeutic agents are unable to reach tumor cells that reside behind an intact blood-brain barrier (BBB), and this failure to treat these invasive tumor cells significantly contributes to the abysmal prognosis for brain tumor patients. As systemic therapy continues to improve peripheral tumor treatment, the number of patients affected by brain tumors will continue to increase (Gállego Pérez-Larraya and Hildebrand, 2014). Thus, it is imperative that future therapies developed for brain tumors are specifically designed to penetrate an intact BBB in order to treat the tumor cells that are invariably “left behind” after surgical resection (Berens and Giese, 1999).

1.1.1 PRIMARY BRAIN TUMORS

Glioblastoma multiforme (GBM) is the most common primary brain tumor in adults (81% of malignant CNS tumors) with a five-year survival rate of less than

5% (Ostrom et al., 2014). As a grade IV astrocytoma, GBM is a rapidly growing tumor that typically forms in the cerebral hemisphere (**Figure 1.1.A**). Primary brain tumors are often only diagnosed following symptoms that may include headache, seizure or altered mentation (Gállego Pérez-Larraya and Hildebrand, 2014). The incidence rate for GBM is 3.19 per 100,000 with a median age at diagnosis of 65 (Ostrom et al., 2014). Since 2005, the standard therapy for patients with newly diagnosed GBM is surgery followed by radiation and treatment with the alkylating agent temozolomide (Stupp et al., 2005). Large-scale sequencing studies have defined signature molecular alterations in GBM including mutations and/or copy number alterations in multiple genes including those coding for CDKN2A (50%), TP53 (40%), EGFR (37%) and PTEN (30%) (Parsons et al., 2008). These detailed studies have helped define promising molecular targets that could be beneficial in the treatment of GBM by not only guiding drug discovery efforts, but also in determining subpopulations of patients that will be sensitive to a given therapy (Vitucci et al., 2011). Despite the discovery of these common alterations in GBM, small molecule inhibitors of pathways such as EGFR have not demonstrated significant therapeutic efficacy in the clinic (Roth and Weller, 2014).

1.1.2 BRAIN METASTASES

Brain metastases remain a devastating complication of systemic cancer that is becoming more prevalent as detection methods continue to improve and

treatment of systemic disease extends survival (Fokas et al., 2013). The mechanism by which brain metastases occur is not well understood, but undoubtedly metastases are present for a variable duration of time before they are detectable by modern imaging methods. The cancers with the highest propensity to metastasize to the brain are lung (50%), breast (15%) and melanoma (5-10%), which account for nearly 80% of all brain metastases (Gállego Pérez-Larraya and Hildebrand, 2014). Non-small cell lung cancer (NSCLC) is the most common systemic cancer to metastasize to the brain and nearly one-third of NSCLC patients will develop brain metastases without evidence of metastasis to any other organ (Nayak et al., 2012). Although only 10% of breast cancer patients are found to have brain metastasis, breast cancer is the second most common cancer to metastasize to the brain due to the large patient population. It has been suggested that the incidence of breast cancer is increasing, and this will likely lead to a further increase in breast cancer patients with brain metastases (Stemmler and Heinemann, 2008). Finally, while melanoma is not as prevalent as lung and breast cancer, its propensity to metastasize to the brain is extremely high (Gállego Pérez-Larraya and Hildebrand, 2014). Given that over 100,000 brain metastases are diagnosed each year, the efficacy of brain tumor treatment is critical to improving patient care (Gállego Pérez-Larraya and Hildebrand, 2014).

The incidence of brain metastases is increasing and the number of patients affected by metastatic disease has risen. However, due to complications that are associated with brain tumor treatment and the poor survival rates, this patient population is often excluded from clinical trials and is left with few options (Gállego Pérez-Larraya and Hildebrand, 2014). In addition, after initial detection of a brain metastasis, there is a very high likelihood of other undetectable micro-metastases that may be 'protected' from most therapies by a relatively intact BBB in these regions. These smaller brain metastases have been referred to as "subclinical" since they are not detectable by current methods. Despite this, the effective treatment of micro-metastases is critical for durable responses in brain tumor patients.

1.1.3 CURRENT PRIMARY BRAIN TUMOR TREATMENT

Clinical trials for primary and metastatic brain tumor treatment have only marginally improved overall survival in the last thirty years. Since the landmark 2005 study defining the benefit of TMZ for newly diagnosed GBM patients, there have been no treatments that have improved primary brain tumor patient progression free survival other than bevacizumab (Stupp et al., 2005). Importantly, in the past decade, during which dozens of new targets have been discovered and provided significant gains for patients with peripheral tumors, none of these new targeted therapies have provided any significant improvement in overall patient survival (Cloughesy et al., 2014).

Without any treatment, the average patient survival following diagnosis is three months. Even with the standard of care, median survival is only 12-15 months following diagnosis (Wen and Kesari, 2008). Patients with unresectable tumors (approximately 35-40% of GBM patients) due to tumor location or medical comorbidities have an even worse prognosis with a median survival of 31 weeks (Fazeny-Dörner et al., 2003). Optimal surgical resection is an important component of therapy, and the extent of tumor resection has a direct, positive correlation to patient outcome (Keles et al., 1999; Fazeny-Dörner et al., 2003). Despite this relationship, even historical experience with hemispherectomy was associated with tumor recurrence, demonstrating the remarkable invasive nature of these tumor cells and the lack of a cure with surgery alone (Zollinger, 1935). The standard care of newly diagnosed GBM patients in 2014 is surgery, followed by adjuvant radiation therapy (2 Gy for 5 days per week for 6 weeks) and temozolomide (Stupp et al., 2005). Irrespective of the treatment received, it is clear that every patient with GBM will have infiltrative tumor cells that are not removed by surgery, and are protected from chemotherapy behind an intact BBB.

After surgical de-bulking, some patients receive BCNU through the implantable wafers called Gliadel(R). These were approved by the FDA in 1996 for recurrent GBM, and, although the therapy does not provide an increase in overall survival,

in 2004 they were approved for primary GBM treatment as well (Bregy et al., 2013). The reasons for failure of this local delivery method are related to the permeability of the compound across the BBB, such that the drug can readily diffuse back into the blood as it is released from the wafer, creating a “sink” effect that limits effective delivery to tumor cells at any distance from the implanted wafer (described below).

Bevacizumab is a monoclonal antibody that targets vascular endothelial growth factor (VEGF). This growth factor is hyperactivated in GBM and is associated with the highly angiogenic nature of these tumors (a hallmark of GBM is the formation of new vasculature) (Chamberlain, 2011). Through targeting VEGF, bevacizumab leads to a rapid reduction in the appearance of tumor volume, as assessed by contrast accumulation within the tumor by conventional magnetic resonance imaging techniques (Chamberlain, 2011). This “reduction” in tumor is not believed to be a physical reduction in tumor size, but rather a normalization of the vasculature preventing the distribution of imaging contrast agents to the tumor (Thompson et al., 2011). Therefore, the use of bevacizumab in the treatment of GBM has been controversial since it difficult to tease out the difference between reduction in tumor burden and normalization of the vascular such that the tumor appears to have reduced in size (Thompson et al., 2011). Bevacizumab was approved for recurrent GBM in 2009, but two recent randomized, double-blind, placebo-controlled trials with radiation therapy and

temozolomide were done to determine if the addition of bevacizumab would improve survival in newly diagnosed patients. In both studies, although progression free survival was extended in the bevacizumab group (10.7 vs. 7.3 months), the primary endpoint of improving overall survival was not met (15.7 vs. 16.1 months) (Gilbert et al., 2014). In addition, neurocognitive decline, symptom severity and decreased quality of life were greater in the bevacizumab treatment group (Gilbert et al., 2014). These studies, taken together, indicate unanswered questions with the use of bevacizumab for primary and secondary brain tumors.

Given the remarkable lack of efficacy of current treatments for primary brain tumors (especially GBM) and the discovery of new targets, there has been a concerted effort to develop molecularly targeted small molecule kinase inhibitors that target commonly mutated genes in brain tumors. These agents have repeatedly shown promise against xenograft models in *in vitro* or *in vivo* systems only to fail in the patient. The failure of these experimental therapies has left patients with few options and demonstrates the tremendous unmet need for effective treatments for GBM.

1.1.4 CURRENT TREATMENTS FOR METASTATIC BRAIN TUMORS

The treatment for metastatic brain tumors closely mirrors the treatment of primary brain tumors. Surgery or gamma knife radiosurgery is typically explored as a first option when there are only a few metastases present. In many cases, due to the

number, location, or size of tumors, focal surgery or gamma knife are not options, and in these cases patients are treated with whole brain radiation therapy. While the first pharmacological treatment of GBM is usually temozolomide, there are no proven chemotherapeutic options specifically effective for brain metastasis therapy.

Even in the face of aggressive treatment, metastatic brain tumor growth and recurrence is unavoidable due in part to ineffective delivery of therapeutic agents across the BBB to the invasive tumor cells. In addition to ineffective brain delivery of chemotherapeutics, metastatic brain tumors can be invasive, aggressive, and can possibly mutate leading to the development of resistance, a common characteristic of peripheral metastases. An example of rapid development of resistance has been studied in the peripheral treatment of melanoma. In the last three years, four new therapies have been approved for the treatment of metastatic melanoma (vemurafenib and dabrafenib, BRAF inhibitors, trametinib, a MEK inhibitor, and ipilimumab, an anti-CTLA4 antibody). Despite this recent progress in the treatment of peripheral metastatic melanoma, the standard of care for patients with brain tumor metastasis remains radiation and surgery. Tumor recurrence, however, was inevitable after 4-8 months of treatment with vemurafenib and the development of resistance led to newly altered signaling pathways (Trunzer et al., 2013). Furthermore, the use of these small molecule inhibitors has demonstrated conflicting results in the clinic for its impact on brain

metastases (Rochet et al., 2012). In one study that followed 86 patients from 2010-2013 receiving 960 mg of vemurafenib twice daily, 59% developed brain metastases while their peripheral tumors were under control (Peuvrel et al., 2014). Patients treated with systemically delivered treatments for peripheral metastatic disease that have limited brain distribution, such as vemurafenib for melanoma and trastuzumab for HER2-positive breast cancer, have an increase in the incidence of brain metastases (Mittapalli et al., 2012; O'Sullivan and Smith, 2014; Peuvrel et al., 2014). In order to better treat systemic cancers, new molecular targets are being identified and more drugs are being developed that target these specific mutations. However, as these drugs extend patient survival by controlling peripheral disease, the limited brain penetration for many of these drugs will result in a pharmacological sanctuary in the brain that should lead to an increase in the incidences of brain tumors. Thus, new therapeutic modalities that either penetrate the BBB or attack the mechanisms that limit brain penetration are required in order to improve patient outcomes.

1.2 INTRODUCTION TO THE PROBLEM - THE BLOOD-BRAIN BARRIER

The failure of novel drug therapy trials for brain tumors may be at least partially due to the presence of tumor cells that escape treatment behind an intact BBB. The BBB plays an important role in regulating the environment of the brain by both protecting the neurons from toxic substances in the systemic circulation as well as providing the brain with a delicate balance of ions, glucose, and other

nutrients necessary for normal brain function (Abbott, 2013). The endothelial cells that form the brain capillaries are held together by a complex network of proteins (tight junctions) to generate a physical blood-brain barrier that prevents paracellular transport of molecules, including many xenobiotics, into the brain (**Figure 1.1.B**) (Abbott, 2013). In addition to the tight-junction proteins, the endothelial cells express active efflux proteins that have wide substrate specificity to provide a biochemical blood-brain barrier by preventing transcellular transport of xenobiotics into the brain. ATP-binding cassette (ABC) transporters such as P-glycoprotein (P-gp), multidrug resistance-associated proteins (MRPs) and breast cancer resistance protein (Bcrp) are efflux transporters that are highly expressed at the BBB (Uchida et al., 2011). These efflux transporters actively transport xenobiotics back into the systemic circulation, preventing these molecules from reaching the brain (Agarwal et al., 2010). The expression of these transporters on the luminal side of the endothelial cells of the brain microvasculature limits substrates in the systemic circulation from accumulating within the brain, thus providing the infiltrative tumor with a protected microenvironment.

The BBB has long been thought to be compromised in brain tumors to such a degree that drug delivery to the tumor was believed to be uninhibited. A key reason for this misconception is that contrast-enhanced magnetic resonance imaging (MRI) is used as a diagnostic tool for brain tumors. In contrast-enhanced

MRIs, brain regions that have a leaky BBB allow the contrast agent (frequently gadolinium-DTPA, a 938 MW contrast agent unable to cross an intact BBB) to diffuse into the brain parenchyma, indicating “tumor” location. While this technique can indicate location of the brain tumor central mass, or tumor core, it does not describe the invasiveness of the tumor since it is unable to indicate the highly infiltrative tumor cells behind an intact BBB (**Figure 1.2**). **Figure 1.2** compares three imaging techniques used to diagnose patients with brain tumors and to determine tumor location. On each image, the tumor area, as determined by a particular imaging technique, is outlined: T1-GAD in red, T2-FLAIR in blue, and F-DOPA positron emission tomography (PET) in yellow. T1-GAD (red) images indicate the necrotic tumor core (i.e., where the BBB is leaky) and describe the area that is typically resected during surgery (Pafundi et al., 2013). Bright regions on T2-FLAIR images (blue) indicate increased water (i.e., edema, inflammation, etc.) and while it is known that there are tumor cells in this region, there is also a high density of normal brain tissue and therefore the entire area described by T2-FLAIR is not typically removed at surgery but is targeted with radiation. The tumor volume determined by the labelled F-DOPA (yellow) describes the area of the tumor that has LAT1-mediated uptake of the F-DOPA ligand (Pafundi et al., 2013; Youland et al., 2013). Initial studies demonstrate that F-DOPA PET may identify regions of high-density tumor in patients and, while not routinely used in clinic, studies at Mayo Clinic and elsewhere are evaluating whether F-DOPA PET may be useful for defining the extent of surgical resections

or radiation therapy fields (Pafundi et al., 2013). These data highlight the potentially large regions of tumor with an intact BBB that must be effectively targeted. As such, the success of a treatment will be closely related to its ability to target the tumor cells “left behind” (Berens and Giese, 1999). This requires effectively delivering therapy to all the remaining tumor cells, many of which are behind an intact BBB (Agarwal et al., 2011).

The misconception that drug delivery to brain tumors is not impeded by the BBB due to disruption of the tumor vasculature has been furthered by studies that fail to consider the invasive nature of brain tumors and these studies use “tumor core” concentrations to indicate effective drug delivery to the tumor (Blakeley et al., 2009; Grossman et al., 2013). Clinical studies in the last decade have measured brain and tumor concentrations of small molecules such as gefitinib and methotrexate in brain tumor patients (Hofer and Frei, 2007; Blakeley et al., 2009). Intratumoral gefitinib concentrations in seven GBM patients were found to be about ten times higher than plasma concentrations, however drug accumulation was measured in the resected brain tumor ”core” (Hofer and Frei, 2007). The assumption made was that the BBB is leaky in the region measured, the tumor core and, therefore, drug delivery to brain tumors is unrestricted. This same group used microdialysis to measure methotrexate concentration in regions adjacent to the tumor core (Blakeley et al., 2009). As is often the case, the authors found the concentration of methotrexate in the contrast enhancing

region, or tumor core, was significantly higher than the noncontrast-enhancing tumor regions (Blakeley et al., 2009). The BBB in the tumor core is often leaky and therefore delivery to the tumor core alone is insufficient to improve patient outcomes, since the invasive cells remain untreated. These few clinical studies, as well as numerous studies in animal models, indicate that concentrations in the tumor core are inadequate to predict a useful concentration-response relationship, and that the concentration achieved around the invasive cells is critical for improved response.

Extensive work has been done to recapitulate human brain tumor development in animal models used for preclinical studies. Although preclinical brain tumor models have been studied for decades, the translation into the clinic has been poor. While there are many potential reasons for the poor preclinical-to-clinical translatability, one problem is the heterogeneity of tumors both in the model and in patients. Efficacy in one model will not necessarily correlate to efficacy in a large patient population due to tumor heterogeneity. Using inadequate models to study brain tumors will result in misguided drug development (de Vries et al., 2009). For example, a commonly used xenograft derived from long-term cell culture GBM cell line, U87, exhibits features that are not reflective of human GBM such as homogeneously leaky tumor vasculature, and a non-invasive growth pattern in the brain (de Vries et al., 2009). In addition to GBM heterogeneity, the murine BBB has notable differences from the human BBB.

The variable expression of transporters at the mouse and human BBB has been analyzed through quantitative targeted absolute proteomics. P-gp and MRP4 expression were found to be higher at the BBB in mice than in human whereas Bcrp is expressed at higher levels at the human BBB (Uchida et al., 2011). Information about the differences in activity of these transporters at the BBB remains unknown. The best GBM model for preclinical studies will be not only reproducible, but also display human-like pathology, genetic lesions and an aggressive growth pattern. Such a model will be able to help select the right drug for the target as well as a drug that can be effectively delivered to the invasive tumor cells. Patient-derived xenografts (PDX) maintain the same genetic characteristics (methylation status, mutations, resistance to therapy, etc.) observed in the patient from whom they were derived (Carlson et al., 2011). Tumor cells derived from PDX models can be implanted into the cerebral hemisphere of immunodeficient mice in order to study the efficacy of small molecule therapies. However, since they must be established in immunocompromised mice, they are not suitable for studying immunotherapies. Genetically engineered mice (GEM) that harbor mutations common to GBM are another tool used to study GBM development that enables preclinical studies to be completed in immunocompetent mice (Wiesner et al., 2009). In either case, these models display key characteristics of GBM including a highly invasive nature of the disease, that results in tumor cells migrating from initial site of tumor development. These improved GBM models that are more similar in growth

patterns to human disease, should provide a better platform to study the efficacy of new treatments, including the influence of drug delivery.

1.3 SYSTEMIC TREATMENTS

In the treatment of brain tumor patients, there are two options for drug delivery to tumor cells. The first option is systemic therapy (**Figure 1.1.C**) in which the therapeutic agent is delivered either orally or intravenously and able to travel from the systemic circulation into the brain. The other option is local delivery (**Figure 1.1.D-G**), where the treatment is delivered directly to the brain parenchyma and the agent needs to diffuse through the brain tissue in order to treat invasive tumor cells throughout the brain. Both local and systemic therapies have advantages as well as challenges to overcome.

Extensive genetic screening of tumors has identified genetic mutations and both large and small molecule drugs have been synthesized to target these mutations that lead to unregulated proliferation. Nearly all large molecules are unable to accumulate within the brain and the majority of small molecules are unable to penetrate the BBB. Effectively treating a primary brain tumor with systemic therapy requires therapeutic concentrations of drug to reach the brain before off-site toxicity becomes dose-limiting. Achieving an adequate “targeted bioavailability” to the brain is essential in the treatment of brain tumors. Currently, there are two types of drugs that can reach the brain from the systemic

circulation: (1) small, highly lipophilic drugs, such as diazepam, are able to passively diffuse across the endothelial cells; and (2) drugs, such as L-DOPA, are able to utilize an active influx transport system at the BBB to reach the brain (del Amo et al., 2008). Unfortunately, the majority of cancer therapies do not achieve therapeutic levels in brain tissue leading to ineffective therapy. Molecular mutations causing unregulated tumor proliferation and growth are often conserved across many tumors. This leads to target-based clinical trials that are conducted without first adequately understanding the brain delivery of a molecularly-targeted agent. The hypothesis tested time and again is that drugs targeting mutations in other cancers as well as GBM that provide a therapeutic benefit in peripheral cancer *should* work in brain tumors. The clinical results, however, have been disappointing. This shows that *in vitro* efficacy against tumor lines, and even *in vivo* efficacy against tumors in inappropriate animal models, is insufficient to guide the use of experimental therapies in clinical trials. This is due to, in part, to the fact that, for many drugs, only 1-10% of the concentration in the plasma reaches the brain. Given this, it is unlikely that therapeutic brain concentrations will be achieved before off-site toxicity in the periphery limits dose escalation. One reason for lack of brain delivery for many candidate treatments is that these compounds are actively effluxed at the BBB by P-gp, Bcrp and MRPs.

1.3.1 MAJORITY OF SMALL MOLECULE DRUGS ARE EFFLUXED

Five of the most commonly mutated pathways in GBM are Cdk 4/6, epidermal growth factor receptor (EGFR), platelet-derived growth factor receptor (PDGFR), phosphoinositide 3-kinase (PI3K), and tumor protein p53 (TP53) (Parsons et al., 2008). Of these five pathways, four have small molecular inhibitors that are either undergoing clinical trials or have already been tested in the clinic for efficacy against GBM. Gefitinib, erlotinib, dasatinib, and imatinib are all examples of tyrosine kinase inhibitors (TKIs) that target some component of the EGFR or PDGFR pathway, which are commonly amplified together in patient tumors in different tumor subpopulations (Szerlip et al., 2012). In preclinical studies, these TKIs showed promising results that have not been translated into the clinic (Franceschi et al., 2012; Reardon et al., 2012). The majority of TKIs are actively effluxed by P-gp and Bcrp on the luminal side of endothelial cells, and never reach therapeutic levels in the brain (Agarwal et al., 2011). Erlotinib failed in a Phase II trial testing the efficacy of temozolomide, radiation and erlotinib and was discontinued due to toxicity (Peereboom et al., 2010). In a Phase II trial testing gefitinib efficacy in nearly 100 recently diagnosed GBM patients, gefitinib did not provide a therapeutic benefit (Uhm et al., 2011). Since efflux is a problem in the treatment of brain tumors, effective therapies could be improved by reducing efflux. Recently, there has been a study in a genetically-engineered mouse model of gliomas showing that the genetic deletion of both P-gp and Bcrp significantly improved the efficacy of dasatinib (Agarwal et al., 2012). There are two methods to overcome the efflux transporters: modifying the structure of the

drug such that there is reduced efflux liability, as was done in the in silico-guided design of a brain penetrant phophoinositide 3-kinase (PI3K) inhibitor, or pharmacologically inhibiting the efflux transporters (Heffron et al., 2012). The clinical efficacy of pharmacological inhibition of efflux transporters to increase brain distribution remains unknown. If very potent inhibitors are used to improve CNS delivery of toxic compounds, a careful assessment of CNS toxicity due to the increase in brain delivery will be required (Kalvass et al., 2013).

1.3.2 CHEMICAL MODIFICATION TO REDUCE EFFLUX LIABILITY

There has been significant interest in testing PI3K inhibitors in GBM, given the dysregulation of PTEN/PI3K pathway. Unfortunately, most PI3K inhibitors are robust substrates for efflux and have limited brain penetration. Given this, specific attempts have been made to design a brain penetration PI3Ki through SAR studies to reduce efflux liability (Heffron et al., 2012). In preclinical efficacy studies, pictilisib (an efflux substrate) demonstrated efficacy only in a non-invasive model with a broken-down BBB, whereas GNE-317 (engineered to lack efflux substrate activity) was efficacious in both a preclinical model with an intact BBB and the non-invasive model. Matrix-assisted laser desorption ionization (MALDI-TOF) was used to examine relative accumulation of two inhibitors, pictilisib and GNE-317, throughout a brain slice and correlate brain distribution with efficacy (Salphati et al., 2014). As a P-gp and Bcrp substrate, pictilisib was only detectable in the region of tumor core of the non-invasive tumor model with

a disrupted BBB and was not detectable in the invasive preclinical model with an intact BBB. In contrast, GNE-317 was uniformly distributed throughout tumor and normal brain regions (Salphati et al., 2014). These results support the hypothesis that effective drug delivery to the whole brain is required to improve patient survival. This also serves as an example for the clinical development of other small molecule inhibitors that could be used in the treatment of brain tumors.

1.3.3 INFLUX TRANSPORT SYSTEMS

An alternative to overcoming efflux transporters is designing drugs to take advantage of innate influx transporter systems already expressed at the BBB. Carrier-mediated transport of amino acids from the systemic circulation into the brain is necessary to maintain the correct balance of nutrients for the brain microenvironment. Endogenous ligands for LAT1 (large-neutral amino acid transporter) are phenylalanine, leucine, isoleucine, valine, tryptophan, histidine and methionine. Targeting a transport system at the BBB for drug development and improved delivery has been used for other diseases. For example, dopamine was discovered as a potential therapy for Parkinson's but was unable to reach the brain. A prodrug of dopamine, L-DOPA, was synthesized and reaches the brain through LAT1 and is activated into dopamine in the brain parenchyma (Gomes and Soares-da-Silva, 1999). The LAT1 influx transport system also improves the brain delivery of the anti-epileptic, gabapentin (Dickens et al., 2013). In addition to amino acid transport systems, glucose is transported into

the brain via glucose transporter (GLUT1). GLUT1 (SLC2A1) is expressed on brain capillary endothelial cells and has the potential to transport sugar-like molecules into the brain. To date, this method has not been successful in achieving therapeutic levels of chemotherapeutics, but can increase the brain uptake of ketoprofen and indomethacin in rats (Gynther et al., 2009). These studies illustrate that taking advantage of guided drug design in an intentional drug development scheme can lead to molecularly-targeted small molecule drugs that do not suffer from drug delivery limitations. If this is done early in the process, finding a drug that is effective against its target, with the ability to reach that target at invasive brain tumor sites, is much more likely.

The number of large molecule drugs such as peptides and antibodies developed is increasing, especially in the oncology field. Half of the approved cancer therapeutics in 2014 were large molecules (2014). One example of large molecule drugs that has shown promising clinical results are the angiopeps, a family of peptides related to aprotinin (Demeule et al., 2008). These have been identified as potential peptides that can be conjugated to a drug of interest that will allow for transport into the brain via low-density lipoprotein receptor-related protein (LRP1). LRP1 is a receptor that is involved in the transcytosis of aprotinin relatives across the BBB. It has received attention recently for its abluminal expression and involvement in the clearance of amyloid beta in the development of Alzheimer's disease. In the context of cancer treatment, angiopep-2 was

selected from 96 peptides as the most promising candidate for increasing brain delivery (Demeule et al., 2008). ANG1005 is a 19 amino acid long peptide (angiopep-2) conjugated to paclitaxel, a mitotic inhibitor that prevents the stabilization of microtubules. ANG1005 is currently in a Phase 2 clinical trial for recurrent GBM.

Another potential brain uptake mechanism used for targeted brain delivery is the transferrin receptor (TfR). TfRs are highly expressed on the BBB and transport transferrin, a glycoprotein which binds iron, through receptor-mediated transcytosis. Iron transport mediated by transferrin provide neurons with the majority of the iron needed for function and a significant proportion of transferrin-conjugated iron is provided from the systemic circulation and delivered through the BBB by receptor-mediated transcytosis. To exploit this system, several groups have developed agents which use this innate influx system. In the treatment of Alzheimer's Disease, the TfR has gained attention due to the development of therapeutic antibodies which are transported into the brain via the TfR (Yu et al., 2011). Interestingly, in the development of a bispecific anti-BACE1/transferrin antibody, it was discovered that the affinity for the TfR mediates the extent of brain delivery. In particular, antibodies with high affinity for the TfR were unable to be released on the brain side, whereas antibodies with moderate affinity were transported across the BBB more efficiently (Yu et al., 2011). In addition to Alzheimer's Disease where a bispecific antibody was found

to cross the BBB, the brain delivery of drugs conjugated to transferrin has been studied. When methotrexate was conjugated to transferrin, significantly higher methotrexate brain delivery was achieved (Friden et al., 1991). In addition to methotrexate, transferrin-modified paclitaxel conjugates penetrated the BBB significantly better than paclitaxel alone or paclitaxel loaded micelle in preclinical models (Zhang et al., 2012). A Phase II clinical studies testing the efficacy of Tf-CRM107 (transferrin conjugated to diphtheria toxin that contains a point mutation) delivered locally (microinfusion in the parenchyma) showed promise, but a Phase III trial was not conducted (Yoon et al., 2010). Given these results, the clinical utility of transferrin-conjugated drugs for brain tumors remains to be seen.

1.3.4 CHANGING FORMULATIONS TO IMPROVE DRUG DELIVERY TO BRAIN

Nanoparticles, such as liposomes, have shown some promise in increasing brain delivery of drug molecules. One example is doxorubicin, which is a cytotoxic chemotherapy that prevents tumor cell replication by intercalation into DNA base pairs and prevents protein synthesis. Doxorubicin is used in the treatment of breast cancer and, due to high rates of brain metastases in this type of cancer, the brain delivery of doxorubicin has been studied. PEGylated liposomal-doxorubicin has higher and prolonged brain concentrations that resulted in higher brain concentrations than nonliposomal-doxorubicin formulations and a survival

increase was observed in a preclinical intracranial model of breast cancer brain metastasis (Anders et al., 2013). In the context of liposomal delivery, addition of a targeting ligand, such as glutathione, can improve brain delivery (Gaillard et al., 2014). In preliminary results from a Phase 1/2a clinical study, a glutathione pegylated liposomal doxorubicin formulation (2B3-101) has shown promising results in breast cancer brain metastasis patients with no disease progression for 3 months in 58% of patients treated (Brandsma et al., 2014). Readers are directed to a comprehensive review (Kreuter, 2014) of the use of nanoparticles to enhance brain drug delivery. These early results indicate that large-scale clinical trials testing brain-targeted nanoparticles can shape the future use of these formulations in the clinic.

1.4 LOCAL DELIVERY METHODS

In the systemic treatment of brain tumors, there is a dynamic relationship between the concentration of drug in the blood and the concentration of drug in the microenvironment of the tumor core, as well as the invasive tumor cells. This relationship is determined in large part by the permeability of the BBB in each of these locations. If a drug has poor BBB permeability in the regions that have an intact barrier, such as the infiltrative GBM cells, then inadequate delivery can be expected. Because of this fact, and to improve targeting of the drug to all of the tumor cells, direct administration to the brain parenchyma has been studied. This method has been explored for decades, and has the potential benefit of both

decreasing systemic toxicities and overcoming the lack of permeability through the BBB. In contrast to systemic therapies, local treatment options are often more invasive since the drugs are delivered directly to the tumor and the surrounding brain tissue.

1.4.1 CONVECTION ENHANCED DELIVERY

Convection Enhanced Delivery (CED) allows for continuous drug delivery through infusion catheters that are implanted during surgery and relies on a hydrostatic pressure gradient for the drug to reach the all tumor cells via convective flow through the parenchyma (**Figure 1.1.E**). The theoretical basis for this approach is that drug will disperse via bulk flow leading to an extensive distribution of drug throughout the brain (**Figure 1.3**) (Morrison et al., 1994). In the clinic, the issue with this invasive method is that the tissue directly around the catheter may receive effective delivery, but, depending of the drug, concentrations further away from the catheter tip may diminish rapidly. The distribution pattern following CED depends on competing forces of convective flow through the parenchyma and the capillary diffusion of the drug from the extracellular fluid into the blood. After local delivery, if a drug molecule readily diffuses, or is actively effluxed, into the blood, it is effectively “swept away” from the brain. This is known as the “sink effect” of the brain circulation and can influence the volume of brain captured by any local delivery technique, including CED. Drugs with high passive permeability, or are avidly transported by active

efflux into the blood, will be severely limited in the volume of distribution of the compound in the brain. This will certainly limit efficacy at those invasive sites that are distant from the site of administration. Recent advances in this method include the co-administration of contrast agents to track the volume captured upon manipulation of the infusion parameters, including catheter design and flow rates (Sampson et al., 2010). Many of the advantages and limitations of the use of CED for brain tumors have been discussed in a recent review by Lonser et al (Lonser et al., 2014). Importantly, there have been no reported studies using CED that have resulted in a positive effect on patient outcomes. In a recent phase III trial, the use of CED to deliver IL-13 conjugated to a *Pseudomonas* endotoxin was tested in GBM patients, and no significant effect was seen compared to Gliadel wafers (Kunwar et al., 2010). This trial was done without the benefit of co-administered contrast agents, and therefore an estimate of the targeted volumes could not be correlated to effect (Lonser et al., 2014). CED may find a role in the treatment of brain tumors if the right compounds are chosen, i.e., those that are not subject to the sink effect, and the infusate parameters are carefully worked out to capture an adequate volume of the brain.

1.4.2 GLIADEL WAFERS

Approved in 1995 for the treatment of recurrent glibolastoma and in 2002 for the treatment of newly diagnosed GBM, Gliadel wafers are dime-sized implantable polymer wafers than encase carmustine. These drug-loaded wafers are placed at

the site of tumor resection and slowly release carmustine over 2-3 weeks. Although these have been approved for nearly 20 years, they are not routinely used by most surgeons due, in part, to complications and high cost of therapy (Bregy et al., 2013). In a trial studying 240 patients, median survival was 13.9 and 11.6 months for patients treated with Gliadel wafers or placebo, respectively (Westphal et al., 2003). While other studies have observed an increase in adverse events, the slight increase in survival in this study was not accompanied by an increase in adverse events such as seizures, brain edema, healing abnormalities and intracranial infections (Brem et al., 1995; Westphal et al., 2003). The effectiveness of this therapy relies on the diffusion of carmustine from the Gliadel wafer, into the brain parenchyma (**Figure 1.1.D**). As a lipophilic drug, carmustine is able to diffuse through membranes with relative ease, but this also means that carmustine diffuses rapidly into systemic circulation. The average distance between adjacent capillaries in the brain is approximately 40 microns which means that at any given time, a drug molecule is a maximum of 20 microns from a capillary (Pardridge, 2012). Gliadel wafer efficacy requires that carmustine rapidly diffuses to all areas with tumor, while not diffusing from parenchyma and into a capillary. Therefore, as seen with CED, Gliadel wafers also face the “sink effect” problem where the drug is washed away in systemic circulation, creating a steep concentration-distance gradient a few microns from the wafer.

1.4.3 OSMOTIC BLOOD-BRAIN BARRIER DISRUPTION

In 1972, the first observation of Evans Blue penetrating CNS tissue due to intra-arterial infusion of hypertonic arabinose was observed (Rapoport et al., 1972). This led to the concept of osmotic blood-brain barrier disruption (BBBD) which has since been used clinically to open the tight junctions between the endothelial cells by causing shrinkage of the endothelial cells to disrupt the tight junctions and broadening of the paracellular space (**Figure 1.1.G**). This technique was brought to the clinic by Dr. Ed Neuwelt in 1979 when mannitol was infused via a catheter in the carotid artery (Bellavance et al., 2008). Following the hyperosmolar mannitol infusion, chemotherapy is administered to increase the concentration in the brain relative to systemic delivery. Preclinical studies in dogs demonstrated that osmotic BBBD could increase the brain distribution 50- to 100-fold (Neuwelt et al., 1981). In the treatment of primary CNS lymphoma (PCNSL), a chemosensitive brain tumor, this technique has shown promising results. 149 recently diagnosed PCNSL patients were treated with osmotic BBBD followed by intra-arterial methotrexate chemotherapy between 1982 and 2005. The results from this multi-center clinical trial were positive, demonstrating a durable response without the use of radiation (Angelov et al., 2009). BBBD is an invasive technique and requires a highly trained team of neurosurgeons to have the

greatest chance of therapeutic benefit. For this reason, it is not a widely used treatment, although there are centers where this method is routinely used.

1.4.4 ULTRASOUND-INDUCED BLOOD-BRAIN BARRIER OPENING

For decades, the majority of oncology drugs in clinical development were small molecule inhibitors. Over the last ten years, there has been a shift to incorporate large molecules in the form of antibodies and antibody-drug conjugates into treatments for brain tumors. Given this, it is critical to examine delivery techniques that may improve the penetration of large molecule drugs into the brain. One possibility is a recent method of BBBD that uses an ultrasound-induced approach in which the BBB is opened transiently and can be monitored via MRI (**Figure 1.1.F**) (Fan et al., 2014). In animal models, ultrasound-induced BBBD is able to produce consistent opening while avoiding damage to tissues. In ultrasound-induced BBBD, preformed microbubbles (2-6 um in diameter) are injected intravenously prior to ultrasound exposure. The underlying mechanism that causes BBBD is not well understood, but studies have shown that focused-ultrasound causes cavitation of the microbubbles. This cavitation can either be inertial (leading to microbubble collapse and shockwave release causing mechanical stress on surrounding vessels) or stable (leading to oscillating microbubbles causing shear stress on surrounding vessels). Either mechanism would lead an increase in BBB permeability (Mitragotri, 2005; Liu et al., 2014).

Focused ultrasound-induced BBBD is able to provide local BBB opening in a selected region of the brain. In a study to determine the optimal focused ultrasound to disrupt the BBB that would allow an antibody-sized molecule to cross into the brain, a 155kDa-dextran was used and the dextran distribution 100-200 μm below the pia mater was monitored (Shi et al., 2014). As a control, neither microbubble injection nor focused ultrasound alone proved to increase BBB permeability; however when microbubbles were administered prior to focused ultrasound, a 14-fold increase in BBB permeability was observed. Currently, BBBD by ultrasound should be considered a potential method to effect a transient, local and noninvasive improvement in drug delivery to the brain, although there are still important challenges to overcome in translating this method to the clinic.

1.5 CONCLUSIONS AND FUTURE DIRECTIONS

Although there have been marked improvements in the treatment of peripheral cancers, the treatment of glioblastoma multiforme, the most common primary brain tumor in adults, has not changed over the last decade and effective treatments for metastatic brain tumors are limited. Diagnosis with either a primary or metastatic brain tumor is associated with abysmal prognosis and current therapies are unable to provide a long-lasting therapeutic benefit. The infiltrative and aggressive nature of these tumors makes complete surgical resection impossible and the BBB prevents the majority of therapies from reaching the

tumor cells “left behind” following resection. Molecularly targeted agents that target a specific pathway mutated in the tumor have continued to fail in clinical trials. There can be multiple reasons for this failure and lack of adequate delivery to the invasive cells behind an intact BBB may be an important shortcoming of these new therapies. As systemic treatment continues to prolong survival in patients with peripheral cancers, the population of patients with brain tumors will increase. In order to effectively treat these patients, therapies which penetrate an intact BBB are required to treat micro-metastases and tumor cells left behind after surgery.

There are two broad categories of treatments for brain tumors: systemic therapy and local delivery. Each of these broad approaches has their advantages and disadvantages. In systemic therapy, drugs are delivered either orally or intravenously and adequate delivery to the brain relies on BBB penetration. This type of therapy is less invasive and the recently developed molecularly targeted compounds are often delivered orally. However, the systemic route is often plagued by offsite toxicity and the concentration reaching the brain often falls to sub-therapeutic levels. The targeted brain bioavailability is often less than ten percent of the systemic exposure due to the BBB. Currently, there are two ways systemically administered drugs can overcome the BBB: (1) small lipophilic drugs which are not substrates for efflux transporters (or concurrent inhibition of efflux);

or (2) drugs which are able to utilize an influx transport system to gain access to the brain.

In local delivery, drugs are placed directly into the brain in order to achieve higher concentrations in the brain and to avoid the dose-limiting toxicities in peripheral organs. This route of administration relies on the diffusion of drugs through the brain parenchyma in order to reach tumor cells throughout the brain. Gliadel wafer and convection-enhanced delivery have high drug concentrations near the wafer or catheter implantation site, but the sink effect can cause the concentration to rapidly decline, and be insufficient at sites away from implantation if the drug is highly BBB penetrable. Blood-brain barrier disruption techniques such as osmotic or focused-ultrasound BBBD transiently open the BBB in either one hemisphere (osmotic BBBD) or a region (focused-ultrasound BBBD). While osmotic BBBD has been around for decades, and has shown promising results in the treatment of chemosensitive brain tumors such as primary CNS lymphoma, it has yet to become standard of care at most institutions. The potential clinical use of focused-ultrasound BBBD remains to be tested in large clinical trials.

In conclusion, the treatment of brain tumor patients requires new therapies that: 1) avoid active efflux by transporters such as P-gp and Bcrp, 2) have high passive permeability that overcomes the efflux liability, 3) take advantage of an

influx transport system, or 4) can be delivered using effective local delivery methods. In order to improve brain tumor patient outcomes, it is critical that new drugs and delivery methods be developed that allow adequate drug concentrations to reach all invasive tumor cells left behind following resection, especially those residing behind an intact BBB.

Conflict of Interest:

J.N.S. has received research funding from Eli Lilly, Genentech, Sanofi Aventis, Beigene, and Basilea. W.F.E. and K.E.P declare no conflict of interest.

Figure Legends

Figure 1.1: Schematic representation of brain tumors and delivery strategies.

(A) Primary brain tumors are infiltrative in nature and typically occur in the parenchyma. Metastatic brain tumors are often variable in size and brain micro-metastases, the spread of cancer from original location to the brain before they reach a detectable size, are a significant problem in the treatment of patients. (B) Brain delivery of most systemically administered molecularly-targeted agents is limited due to the blood-brain barrier (BBB). The neurovascular unit regulates the brain microenvironment. Astrocytes, pericytes, endothelial cells, basal lamina and neurons all play critical roles in the BBB. Through the expression of tight junctions and transport proteins, such as P-gp and Bcrp, many therapeutic agents are excluded from the brain and unable to reach infilitrative tumor cells. The BBB prevents drugs from entering brain tissue behind an intact BBB. (C) Systemic delivery to brain tumors results in a higher drug delivery to tumor core lower concentrations reaching the edge of the tumor due to the presence of an intact BBB. Local delivery relies on diffusion through brain parenchyma in order to reach tumor cells. (D) Gliadel wafer are implantable polymer discs which release drug into surrounding tissue. (E) Convection-enhanced delivery (CED) infuses drug through a catheter and relies on the hydrostatic pressure gradient to diffuse drug into the tumor tissue. (F) Focused ultrasound microbubble disruption breaks the tight junctions and transiently opens the paracellular space.

(G) Osmotic blood-brain barrier disruption uses an osmotic agent (mannitol) via intracarotic injection in order to shrink the endothelial cells and allow drug to pass into the brain through the paracellular space.

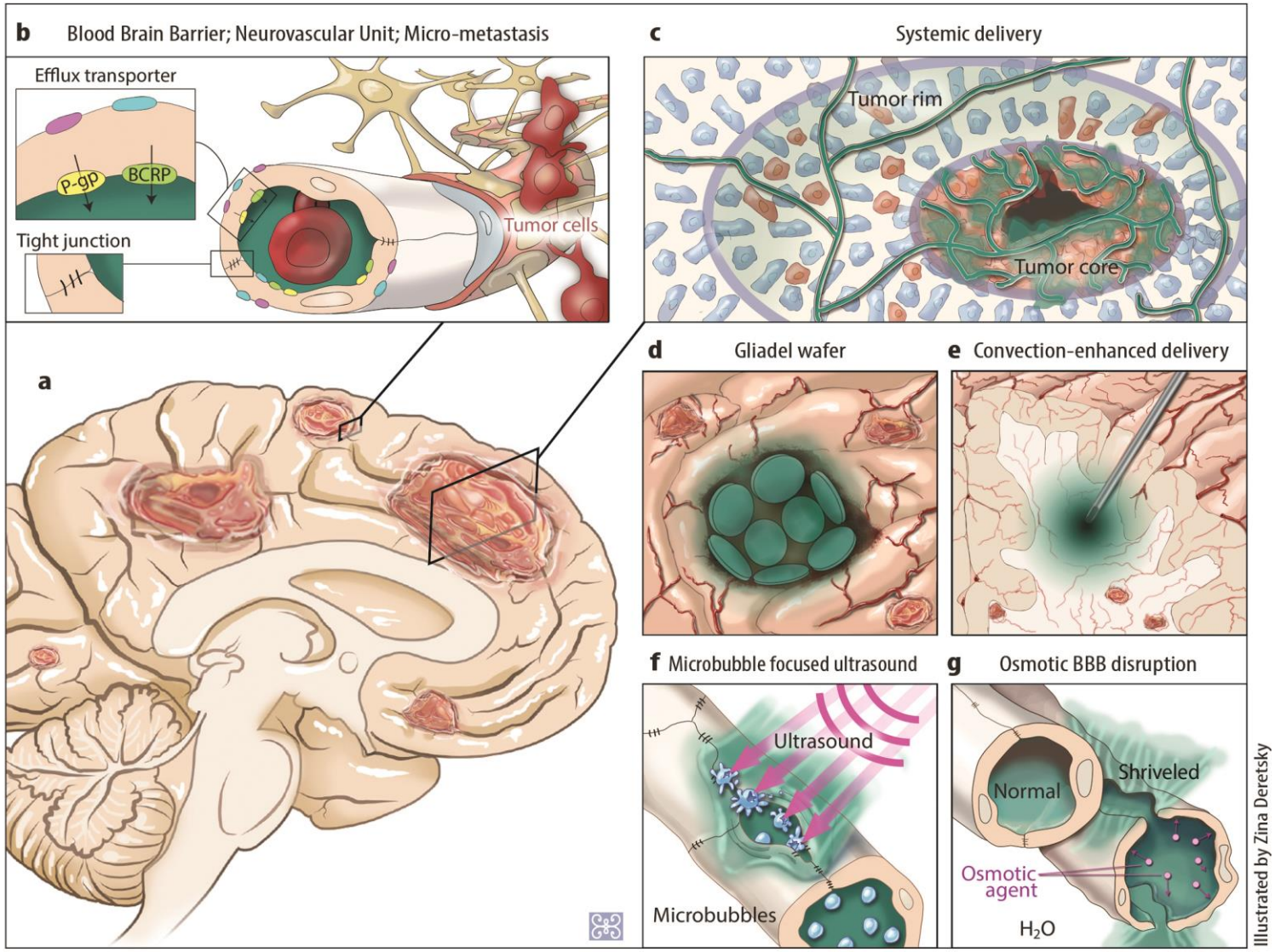
b Blood Brain Barrier; Neurovascular Unit; Micro-metastasis
Efflux transporter
P-gp
BCRP
Tight junction
Tumor cells
c Systemic delivery
Tumor rim
Tumor core
a
d Gliadel wafer
e Convection-enhanced delivery
f Microbubble focused ultrasound
Ultrasound
Microbubbles
g Osmotic BBB disruption
Normal
Shriveled
Osmotic agent
H_2O
Illustrated by Zina Deretsky

Figure 1.2: Current diagnostic tools fail to adequately describe entire tumor location.

(A) T2-FLAIR image of GBM patient with tumor area outlined in BLUE; (B) T1-GAD image of patient tumor with GBM (outlined in RED). Contour includes post-operative cavity (not just enhancement); (C) PET image with active tumor outlined in YELLOW. Tumor volume comparison of T1-GAD, T2-FLAIR and PET.

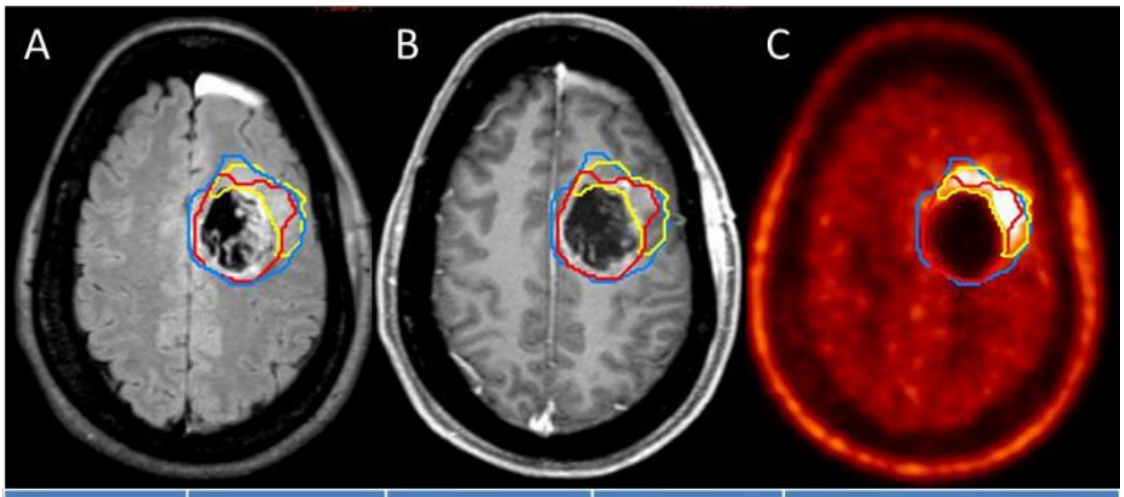

Structure	Structure Volume (cc) *from Eclipse*	PET Volume outside of T1-GAD (cc) *from Eclipse*	PET Volume outside of FLAIR (cc) *from Eclipse*	MR Volume outside of PET (cc) *from Eclipse*
T1-GAD	47.7	N/A	N/A	33.2
FLAIR	54.3	N/A	N/A	36.4
PET	21.7	7.1	3.8	N/A

Figure 1.3: Relationship between extracellular concentration and distance from cannula.

Convection-enhanced delivery allows for a broader distribution of therapeutic agent than a bolus injection because of the sink effect.

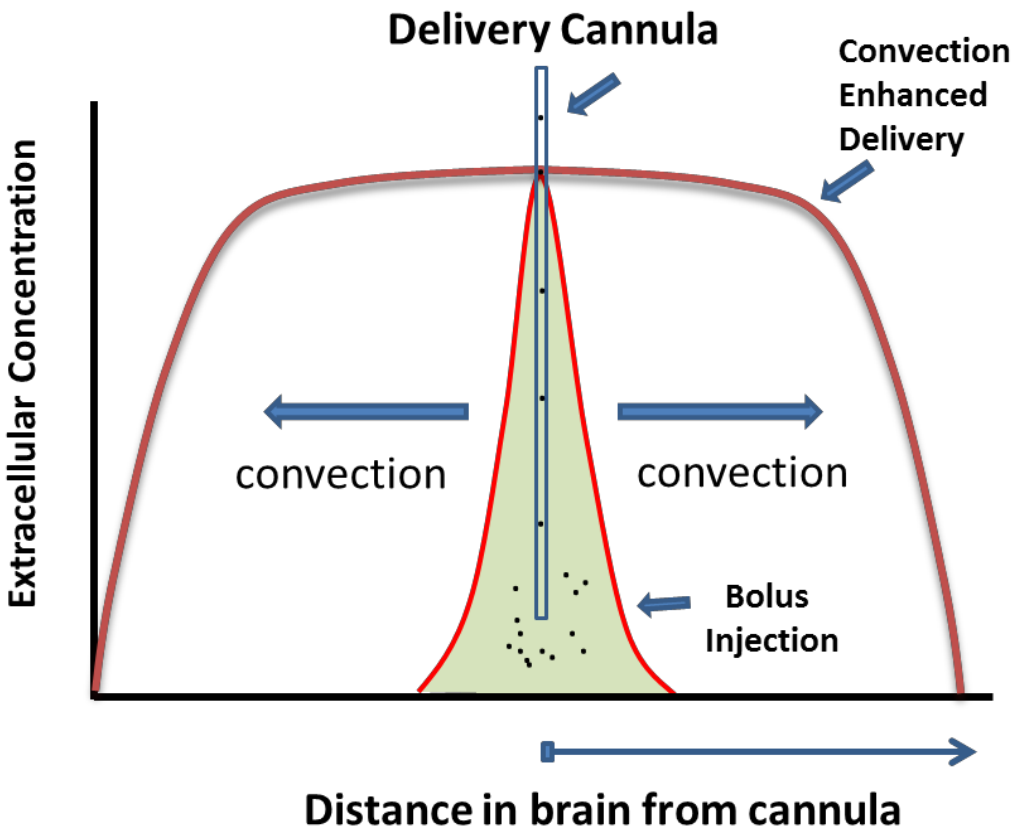

CHAPTER II

THE ROLE OF CYCLIN-DEPENDENT KINASE INHIBITORS IN CANCER THERAPY

2.1 INTRODUCTION

A hallmark of cancer is uncontrolled cell growth. Pathways involved in the cell cycle become dysregulated and often drive tumor cell proliferation (Hanahan and Weinberg, 2000). In recent years, there has been a shift from using non-targeted chemotherapeutics that attempt to nonspecifically kill any rapidly proliferating cell to using molecularly-targeted agents that target a specific mutation involved in tumor growth (Cloughesy et al., 2014; Prados et al., 2015a). This change has led to the identification of numerous abnormal pathways that can be specifically targeted with molecularly-targeted agents. Despite identifying dysregulated pathways that drive tumor growth, tumor resistance remains a major challenge for the targeted therapies (Taylor et al., 2012; Yadav et al., 2014a; Yadav et al., 2014b). One potential way to overcome resistance is the use of multiple targeted therapies (Dickson, 2014; Jhanwar-Uniyal et al., 2015). This chapter will briefly summarize the challenges in treating brain tumors stated in **Chapter 1** and review the most commonly dysregulated pathways in primary and metastatic brain tumors with a focus on the cyclin-dependent kinases (CDKs), which play a major role in regulating the cell cycle and are often involved in tumor cell proliferation.

2.2 TREATMENT OF BRAIN TUMORS

2.2.1 BLOOD-BRAIN BARRIER

The blood-brain barrier (BBB) is highly involved in regulating the distribution of therapeutic agents into the brain (Abbott, 2013). In the treatment of brain tumors, the BBB often limits the brain distribution of therapeutic agents through the efflux activity of P-glycoprotein (P-gp) and breast cancer resistance protein (BCRP) (Agarwal et al., 2011). These two transporters have broad substrate specificity and are able to actively transport substrates back into systemic circulation, preventing these molecules from reaching tumor tissue in the brain. As discussed in detail in **Chapter 1**, the BBB integrity is variable in the tumor regions of patients with glioblastoma (GBM) (Parrish et al., 2015). In the clinic, tumors are visualized by regions of BBB disruption where a gadolinium contrast agent is able to be seen by magnetic resonance imaging (MRI). Gadolinium is only able to diffuse into the brain in regions where the BBB is disrupted and this does not adequately describe the entire tumor (van Tellingen et al., 2015). Importantly, gadolinium-based MRI fails to provide a visual representation of the tumor regions that reside behind an intact BBB (Dhermain et al., 2010). Since these regions are left behind following surgical resection, it is paramount to target these invasive tumor cells in the treatment of GBM (Berens and Giese, 1999).The goal of this thesis project is to study the brain delivery of anti-cancer agents and aims to improve the brain delivery of these agents to tumors that reside behind an intact BBB.

2.2.2 GENETIC HETEROGENEITY OF GLIOBLASTOMA

GBM, the most common primary brain tumor in adults, was one of the first tumors characterized as part of The Cancer Genome Atlas (TCGA) project (2008). This characterization confirmed that GBM is a particularly difficult type of tumor to treat because of its highly heterogeneous nature. Large-scale genomic analyses like TCGA have led to the discovery of subclasses of GBM as well as genetic alterations that have the potential to be targeted through molecularly-targeted therapies (Cloughesy et al., 2014). Current treatment of GBM is surgery followed by nonspecific chemotherapy (temozolomide) followed by radiation therapy (Stupp et al., 2005). While this treatment targets cells that are rapidly dividing, it fails to target tumor-specific mutations. The identification of specific mutations common among GBM has provided opportunities in the treatment of GBM, and has the potential to allow for precision medicine to be applied to the treatment of GBM patients (Jhanwar-Uniyal et al., 2015).

Precision medicine is a relatively new approach that personalizes treatments to patients based on genetic information (Reardon et al., 2015). Current therapy for nearly all newly diagnosed GBM patients in surgery followed by radiations which is nonspecific treatment of the disease. GBM is a complex tumor with genetic aberrations that subdivide the patient population into different subgroups that may benefit from different treatment regimens (Reardon et al., 2015). As treatment of GBM moves towards precision medicine, the number of clinical trials that combine therapeutic agents will grow and the selected treatment regimen will become patient-specific (Prados et al., 2015a) .

2.3 COMBINATION THERAPY IN TREATMENT OF CENTRAL NERVOUS SYSTEM TUMORS

Effectively selecting specific molecularly-targeted agents will be critical in improving the treatment of heterogeneous tumors such as GBM. It is unlikely that one targeted agent will be sufficient to provide a durable response and therefore the development of rational combination therapies will likely be critical in the treatment of GBM (Alifieris and Trafalis, 2015; Prados et al., 2015a). Precision medicine is driving the development of combination therapies and it is likely that small molecule inhibitors will be used in combination with other therapies in order to better target the tumor and slow or prevent the development of resistance (Asghar et al., 2015). Numerous genetic alterations are commonly observed in GBM and a few of the most frequently altered pathways in GBM are described below (**Figure 2.1**).

One characteristic of GBM is the formation of new blood vessels, which is critical for tumor growth beyond 0.125 mm (Chamberlain, 2011). GBM is one of the most highly vascularized type of tumors and numerous tumor growth factors are upregulated in GBM (Reardon et al., 2008b). This angiogenesis is regulated by growth factors, such as vascular endothelial growth factor (VEGF), that are released and taken up by tumor and endothelial cells (Takano et al., 2010). Studies have demonstrated that the level of VEGF in the tumor is 200- to 300-fold higher than in normal brain regions in order to provide new vasculature that

will supply the tumor with the nutrients necessary for continued growth (Takano et al., 1996). Bevacizumab (Avastin) is a monoclonal antibody that targets VEGF and has been approved for the treatment of recurrent GBM and, although bevacizumab is an approved therapy, it showed no improvement in overall survival (Vredenburgh et al., 2007; Cohen et al., 2009). Bevacizumab inhibits VEGF from activating VEGF receptor and slows the formation of new vasculature that is central to GBM. This leads to normalization of the vasculature and appears to rapidly reduce the tumor burden as monitored by MRI. The use of bevacizumab has been controversial because although the tumor burden appears to be reduced, the imagine methods that are currently used are unable to monitor true tumor growth and bevaciumab does not improve overall survival (Reardon et al., 2008a).

The phosphatidylinositol 3-kinase/mammalian target of rapamycing (PI3K/mTOR) pathway is mutated across many tumor types and in GBM, approximately 80% of tumors have an alteration in this pathway (2008; Akhavan et al., 2010; Duzgun et al., 2016). The binding of VEGF to its receptors triggers a signaling cascade via phosphorylation events. This pathway is critical in GBM because it interferes with apoptosis of endothelial cells and is involved in a feedback process to further release VEGF (Karar and Maity, 2011; Onishi et al., 2011). Preclinical studies have demonstrated that inhibition of this pathway markedly improves survival. Furthermore, preclinical studies have shown that a brain penetrant PI3K/mTOR is more efficacious than a molecule with poor brain penetration (Salphati et al.,

2012; Salphati et al., 2014). Ongoing clinical trials are examining that use of PI3K/mTOR inhibitors in GBM patients.

The majority of GBMs have alterations in receptor tyrosine kinases such as the epidermal growth factor receptor (EGFR), which is altered in 40-50% of GBMs (Taylor et al., 2012). In normal cells, EGFR is activated in response to growth factors, but in tumors such as GBM, this cell-surface receptor is constitutively activated and drives tumor growth. The aggressive nature of GBM is attributed in part to EGFR variant EGFRvIII (Brennan et al., 2013; Prados et al., 2015a). Numerous small molecule EGFR inhibitors have failed to provide a therapeutic benefit in the clinical treatment of GBM and these same inhibitors have been shown to be substrates of efflux transporters at the BBB (Agarwal et al., 2010; Kodaira et al., 2010; Agarwal et al., 2013).

The mitogen-activated protein kinase (MAPK) pathway has been reported to be frequently altered in GBM and a variety of other tumors (Pandey et al., 2015). Alterations, such as constitutive activation of MAPK, have been shown in the majority of gliomas and therefore has potential as a therapeutic target (Jhanwar-Uniyal et al., 2011). Poor tumor progression and the development of resistance have both been linked to MAPK expression and this indicates that this pathway is involved in the invasive or aggressive nature of GBM (Wong et al., 2009; Pandey et al., 2015). Inhibitors of the MAPK pathway have not provided a breakthrough in GBM treatment, but it is possible that a more in depth understanding of other

activation pathways may lead to combinations of therapies with MAPK inhibitors playing an important part in these treatment regimens, preventing a possible pathway for resistance.

VEGF, PI3K/mTOR, EGFR, and MAPK are four pathways that are currently being explored as therapeutic targets in the treatment of cancers. As cancer treatment focuses on precision medicine, combination therapies that are patient specific will become increasingly common to try and eradicate the entire tumor while avoiding the development of resistance (Prados et al., 2015f). Effective treatment of GBM will require all therapeutic agents administered to effectively reach the invasive tumor cells residing behind an intact BBB. Although there are numerous molecularly-targeted therapies currently being explored in the treatment of GBM, the focus of this dissertation will be the brain delivery and efficacy of CDK4/6 inhibitors in the treatment of GBM.

2.4 CYCLIN-DEPENDENT KINASES

CDKs are serine/threonine kinases that are dependent on the binding of cyclin in order to activate, and this heterodimeric complex is involved in a diverse set of functions (Cicenas et al., 2014). Throughout the cell cycle, upregulation and downregulation of specific CDKs control cellular proliferation. CDK2 is involved in DNA replication and starting histone synthesis, whileCDK1 is involved in regulating G2-M phase cell cycle progression (Sánchez-Martínez et al., 2015).

Basal transcriptional processes for RNA processing are, in part, controlled by CDK7, 8, 9, and 11. CDK4/6 are major regulators of G1-S phase cell cycle progression (Malumbres et al., 2009; Malumbres, 2014) and will be the focus of this thesis project.

2.4.1 CYCLIN-DEPDENT KINASE 4/6

CDK4 and 6 are major regulators of the transition from G1 to S phase in the cell cycle and this pathway is commonly altered in tumors (Brower, 2014). Single deletion of either CDK4 or CDK6 is not lethal, however simultaneous deletion of both CDK4 and CDK6 is embryonic lethal, showing that these two proteins share cell cycle functions. More recently, some differences between CDK4 and CDK6 have been noted, but are outside the scope of this review. CDK4/6 activity is controlled by association with D-type cyclins and tumor suppressor proteins (Sherr and Roberts, 2004). Cyclin D1 is the most researched D-type cyclin and forms a complex with CDK4 or CDK6 in response to mitogenic signals (Sherr and Roberts, 1999). This CDK4/6-cyclin D1 complex phosphorylates the tumor suppressor protein retinoblastoma (RB1), releasing the E2F family of transcription factors (Sherr and Roberts, 2004). This family of transcription factors activates synthesis of the proteins that are necessary for the S phase of the cell cycle. CDK4/6 activity is also controlled by cyclin-dependent kinase inhibitors, such as p16 and p18 (Ruas and Peters, 1998).

2.5 CYCLIN-DEPENDENT KINASE ACTIVITY IN CANCER

The p16-CDK4-RB1 axis is commonly dysregulated in many types of cancers (Schmidt et al., 1994; Zuo et al., 1996; Malumbres and Barbacid, 2005), but the predominant mechanism of altered cell cycle regulation is not uniform across this pathway. For example, RB1 loss is commonly observed in small cell lung cancer (50-60% of tumors), but amplification of cyclin D1 is more common in breast cancer (15-20% of tumors) (Peyressatre et al., 2015). In glioblastoma, homozygous deletion of CDKN2A, the gene that encodes for p16, is the most common alteration observed (approximately 70% of tumors) (Peyressatre et al., 2015).

The most common tumors to metastasize to the brain (lung, breast and melanoma) frequently have alterations in CDK4/6, making it an attractive therapeutic target (Zuo et al., 1996; Yu et al., 2006; Puyol et al., 2010). Glioblastoma, the most common brain tumor in adults, commonly has loss of p16 (Schmidt et al., 1994). Therefore, studying the brain delivery of CDK4/6 inhibitors is critical in assessing the potential clinical efficacy of these therapeutic agents.

2.6 CDK4/6 INHIBITORS

Three CDK4/6 inhibitors palbociclib, abemaciclib, and ribociclib are currently undergoing clinical trials for their potential use in multiple tumor types such as

breast cancer, melanoma and childhood GBM (Vidula and Rugo, 2015). Specific details about published results and ongoing clinical trials are described below.

2.6.1 PALBOCICLIB

Palbociclib (PD-0332991) is a potent CDK4/6 inhibitor and is currently the only CDK4/6 inhibitor that is FDA approved (**Table 2.1**). Palbociclib was approved in early 2015 for the treatment of hormone receptor positive breast cancer in combination with letrozole (Dhillon, 2015). *In vitro* palbociclib has been shown to cause cell cycle arrest in the G1 phase of the cell cycle by preventing the cyclin D-CDK4/6 complex from phosphorylating RB (Michaud et al., 2010; Rivadeneira et al., 2010). The induction of *in vitro* cell cycle arrest by palbociclib treatment has been demonstrated in numerous breast cancer cell lines as well as in GBM and melanoma cell lines (Michaud et al., 2010; Young et al., 2014). Initial preclinical reports have shown that palbociclib has great potential to be used in the treatment of a variety of tumors from breast cancer to brainstem glioma (Barton et al., 2013). Previous studies have demonstrated that P-gp and BCRP are involved in the brain delivery of palbociclib and that these efflux transporters restrict the brain exposure (de Gooijer et al., 2015; Raub et al., 2015). The potential clinical use of palbociclib for the treatment of GBM remains to be seen (Schröder and McDonald, 2015). Palbociclib is dosed at 125 mg daily for three of four weeks and the most common toxicities are anemia, neutropenia and thrombocytopenia (Cadoo et al., 2014).

2.6.2 ABEMACICLIB

Abemaciclib (LY2835219) is another selective CDK4/6 inhibitor that is currently in clinical trials for the treatment of breast cancer and lung cancer (**Table 2.2**). Previous reports have demonstrated that abemaciclib is a substrate for P-gp and BCRP efflux transport at the BBB, but the ability of P-gp to efflux abemaciclib was found to be saturable at physiologically relevant concentrations (Raub et al., 2015). This suggests that the brain distribution of abemaciclib could improve its own delivery and potentially provide a greater therapeutic benefit than compounds that do not have this characteristic. Abemaciclib is dosed at 150 mg or 200 mg twice daily and can be dosed continuously for 28 days (Vidula and Rugo, 2015). The most common toxicities observed are neutropenia, thrombocytopenia leukopenia, diarrhea, and nausea (Cicenas et al., 2014).

2.6.3 RIBOCICLIB

The third CDK4/6 inhibitor is ribociclib (LEE-011) which is currently being evaluated in the clinic for the treatment of breast cancer as well as advanced solid tumors (**Table 2.3**, ClinicalTrials.gov). The brain delivery of palbociclib and abemaciclib has been previously explored in the literature, but little is known about the brain delivery of ribociclib. Ribociclib is dosed at 600 mg daily (three out of four weeks) in the clinic and the main toxicities were neutropenia, anemia, diarrhea, and nausea (Asghar et al., 2015).

CDK4/6 inhibitors have great potential in the treatment of both primary and metastatic brain tumors because of the high frequency of alteration in this pathway in GBM, breast cancer, non-small cell lung cancer, and melanoma (Peyressatre et al., 2015). Precision medicine has the potential to vastly change treatment of cancer patients by understanding the underlying genetic lesions that drive cancer growth (Prados et al., 2015a). Since most tumors have multiple lesions, combination therapies are becoming increasingly common and may change the way cancers are treated. The brain delivery of drugs to regions of tumor that reside behind an intact BBB will be necessary in the treatment of brain tumors. Therefore, the brain delivery of small molecule drugs needs to be understood in order to develop therapeutic regimens that have the greatest potential to improve brain tumor patient outcomes (Parrish et al., 2015). Understanding the role of the BBB in the brain delivery of CDK4/6 inhibitors and the relationship between delivery and efficacy will be critical in designing rational clinical trials with the highest probability of improving brain tumor patient prognosis.

Table 2.1: Physicochemical properties summary of palbociclib.

Drug	Palbociclib
Company	Pfizer
Molecular Weight	447.53
IC_{50}	CDK4: 11 nM; CDK6: 16 nM
LogP	2.8
Clinical Dose	125 mg daily
Aqueous Solubility	50 mg/mL
Clinical Trials	▪ Childhood CNS tumors ▪ Carcinoma of the head and neck ▪ Breast cancer ▪ KRAS mutant and ALK-positive NSCLC ▪ Solid tumors (BRAF wild-type melanoma)
Structure	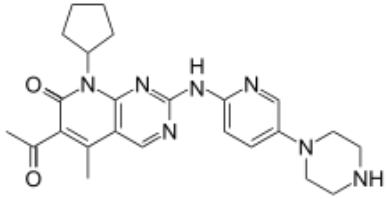
References	(Flaherty et al., 2012; Raub et al., 2015; VanArsdale et al., 2015)

Table 2.2: Physicochemical properties summary of abemaciclib.

Drug	Abemaciclib
Company	Eli Lilly
Molecular Weight	506.59
IC_{50}	CDK4: 2 nM; CDK6: 10 nM
LogP	4.3
Clinical Dose	150 or 200 mg twice daily
Aqueous Solubility	100 mg/mL
Clinical Trials	▪ Non-small cell lung cancer ▪ Brain metastases of breast cancer, non-small cell lung cancer, or melanoma ▪ Breast cancer ▪ ALK-positive non-small cell lung cancer
Structure	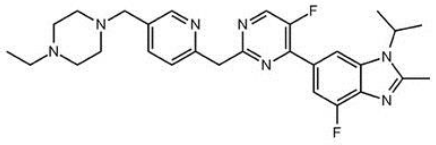
References	(Raub et al., 2015; VanArsdale et al., 2015)

Table 2.3: Physicochemical properties summary of ribociclib.

Drug	Ribociclib
Company	Novartis
Molecular Weight	434.54
IC_{50}	CDK4: 10 nM; CDK6: 39 nM
LogP	2.2
Clinical Dose	600 mg daily
Aqueous Solubility	<1 mg/mL
Clinical Trials	▪ Breast cancer ▪ ALK-positive non-small cell lung cancer
Structure	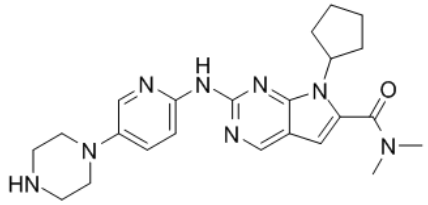
References	(Mariaule and Belmont, 2014; Sánchez-Martínez et al., 2015; VanArsdale et al., 2015)

Figure 2.1: Commonly altered pathways in glioblastoma and corresponding molecularly-targeted therapies.

VEGFR, vascular endothelial growth factor receptor; PDGFR, platelet-derived growth factor receptor; EGFR, epidermal growth factor receptor; RTKs, receptor tyrosine kinases.

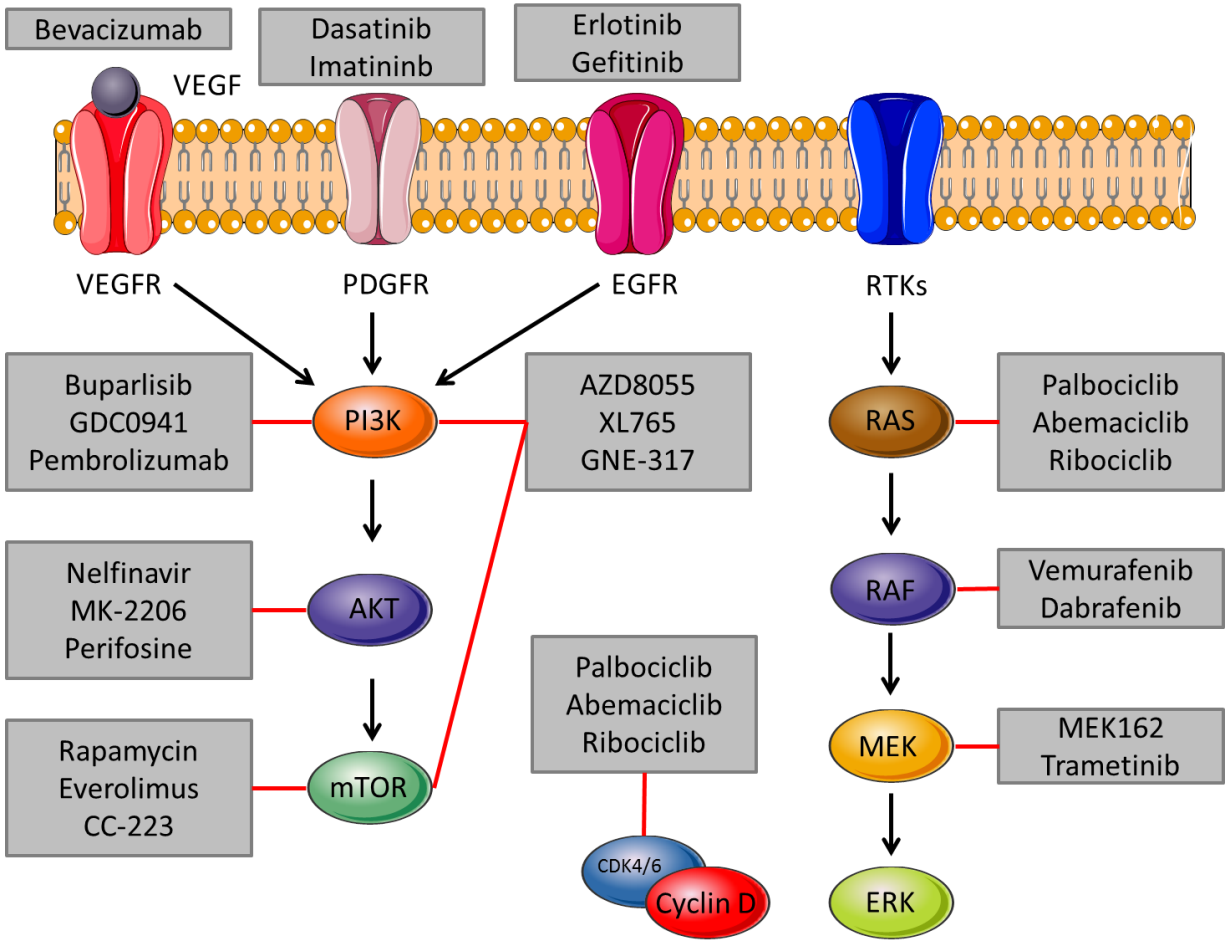

Figure 2.2: Schematic of CDK4/6 inhibition.

CDK4/6 inhibitors prevent CDK4/6 from dimerizing with Cyclin D, which inhibits the phosphorylation of RB. This sequence of events prevents G1-S phase cell cycle progression and causes cell cycle arrest.

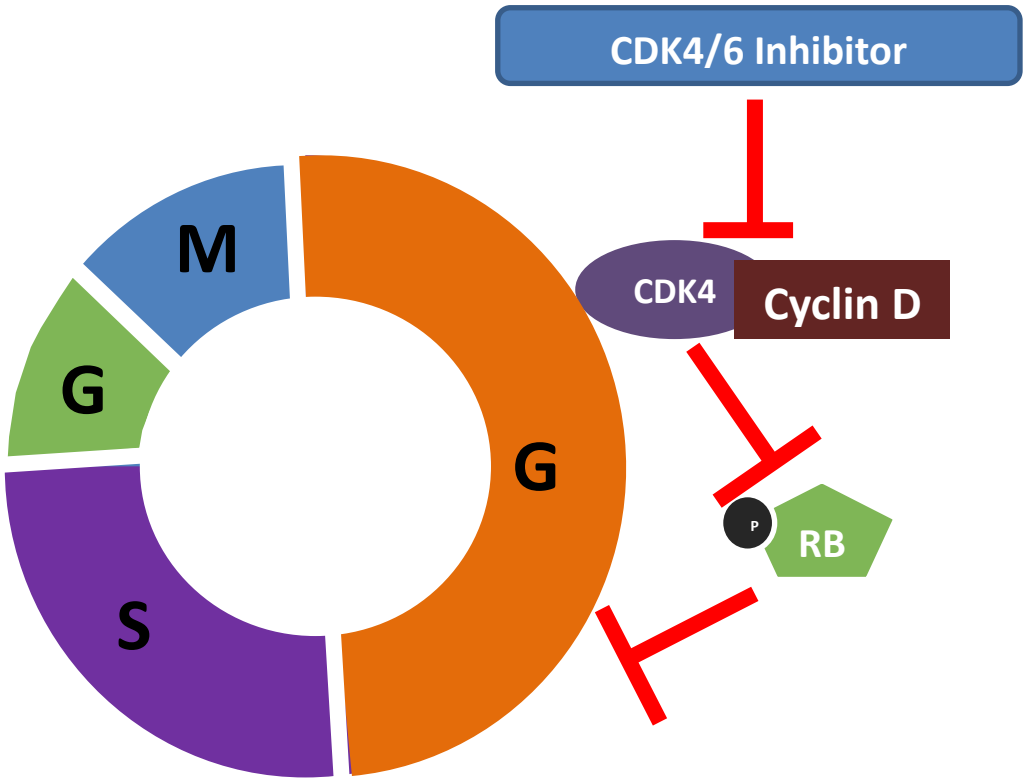

Figure 2.3: Schematic of CDK4/6 pathway regulation.

(A) Regulation of G1-S phase cell cycle progression in normal cells. p16 inhibits the dimerization of CDK4/6 with Cyclin D which prevents the E2F family of transcription factors.

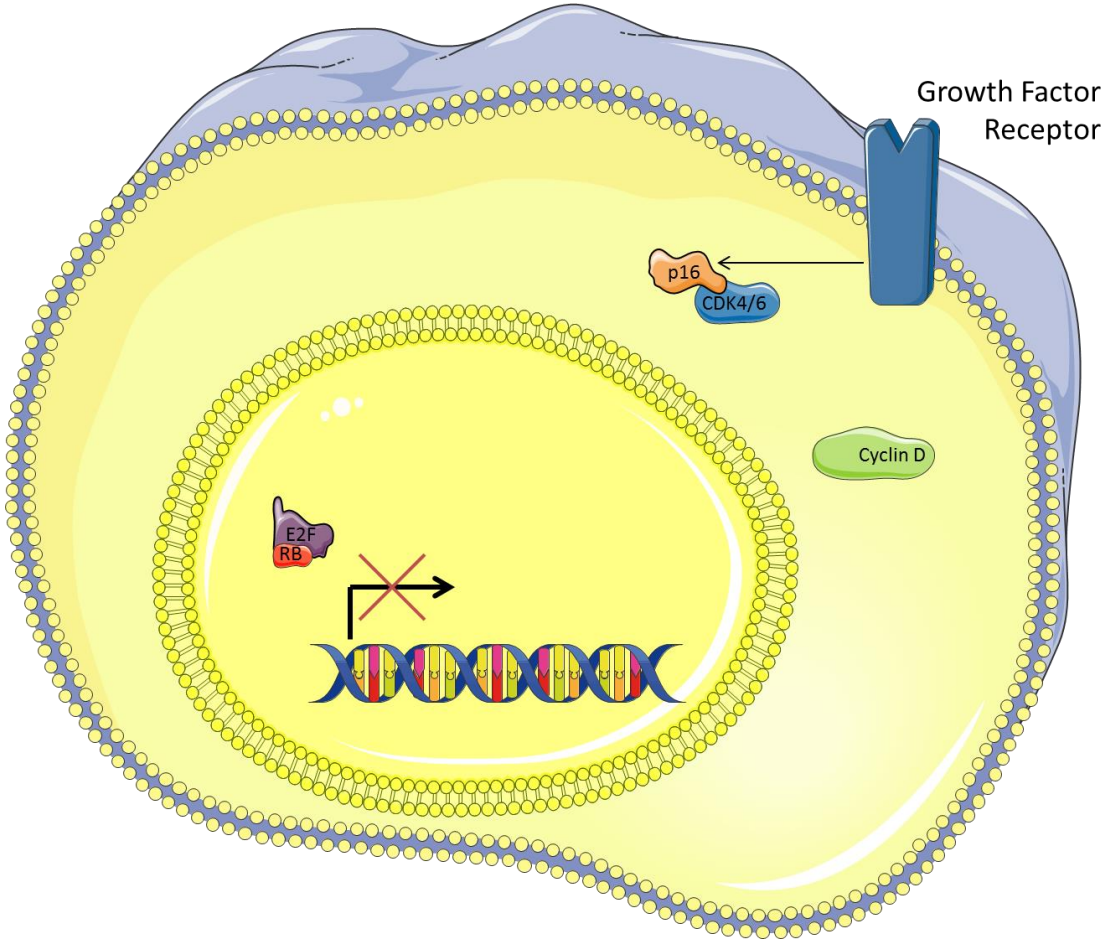

Figure 2.3: Schematic of CDK4/6 pathway regulation.

(B) Deregulation of G1-S phase cell cycle progression in tumor cells. Deletion of the gene encoding for p16 is a common alteration that prevents G1-S phase regulation. Amplification of CDK4, CDK6, and/or Cyclin D is also commonly observed.

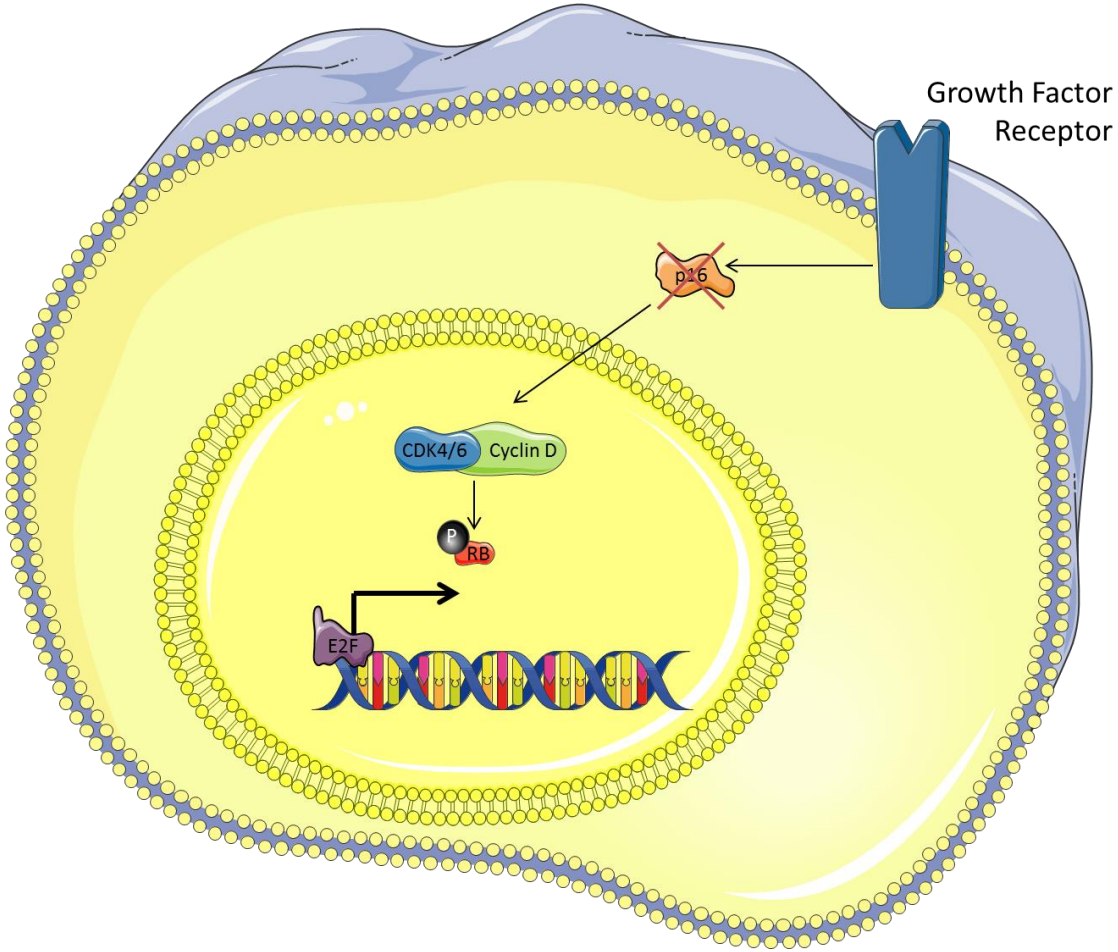

2.7 STATEMENT OF THE PROBLEM

Glioblastoma (GBM) is the most common primary brain tumor in adults and there is a great need for the development of new therapies to treat this devastating disease. Following diagnosis, patients are left with limited treatment options and, even with aggressive treatment, survival is approximately one year (Stupp et al., 2005). Clinical trials targeting GBM patients continue to provide little to no therapeutic benefit due, in part, to the presence of the blood-brain barrier (BBB) (Oberoi et al., 2015). Magnetic resonance imaging (MRI) visualizes tumor regions that are near a disrupted BBB, but the MRI described region does not adequately describe the tumor burden as there are tumor cells residing outside of the MRI enhancing region (Pafundi et al., 2013). Therefore, it is crucial to deliver drugs to tumor cells that reside behind an intact BBB in order to effectively treat brain tumor patients.

GBMs have a number of unique genetic lesions that are present only in tumor tissue and absent in surrounding normal brain tissue. The discovery of these characteristics has led to the development of molecularly-targeted therapies that target a specific alteration in GBM. One such mutation is the p16-CDK4/6-RB pathway that is mutated in over 75% of GBM patients (2008).

The CDK4/6 pathway is an attractive target in GBM because it is commonly altered in patients and has the potential to be used in combination with other

therapies. Palbociclib, abemaciclib and ribociclib are three CDK4/6 inhibitors that prevent G1-to-S phase cell cycle progression (VanArsdale et al., 2015).

Efflux transporters at the BBB are one possible reason for the failure of many molecularly-targeted agents in clinical trials for the treatment of GBM (Parrish et al., 2015). P-gp and BCRP are two efflux transporters with wide substrate specificity that actively transport drug substrates into systemic circulations, preventing these drugs from reaching the tumor site (Agarwal et al., 2011). Brain tumor diagnosis is devastating and prognosis is poor due to genetic heterogeneity of tumor cells, rapidly mutating cells that become resistant to therapy and the BBB preventing adequate delivery. The studies presented will address the issue of drug delivery to tumor cells that reside behind an intact BBB.

2.8 RESEARCH OBJECTIVE

The overall research objective of this thesis is to explore the role of P-glycoprotein and breast cancer resistance protein, two active efflux transporters at the blood-brain barrier (BBB), in the brain distribution, and hence efficacy, of CDK4/6 inhibitors in the treatment of glioblastoma (GBM). To achieve this research objective, the following studies were conducted:

1) To study the time-course of plasma and brain distribution of the CDK4/6 inhibitor palbociclib and assess the relationship between drug distribution and efficacy using a patient-derived xenograft model of GBM (**Chapter 3**).

2) To evaluate the pharmacokinetics and pharmacodynamics of enhancing the brain distribution of palbociclib using elacridar, a pharmacological inhibitor of active efflux at the BBB (**Chapter 4**).

3) To compare the relative brain distribution of palbociclib, ribociclib and abemaciclib using the *in situ* brain perfusion technique and evaluate the role of efflux transport in the relative brain distribution (**Chapter 5**).

These objectives are driven by the hypothesis that efflux transporters at the BBB prevent CDK4/6 inhibitors from reaching the tumor cells residing behind an intact

BBB, and that enhancing the brain delivery of CDK4/6 inhibitors to these "protected" tumor regions will improve efficacy.

2.9 RESEARCH PLAN

The focus of **Chapter 3** is to understand the brain delivery of palbociclib and the mechanisms involved in limiting the brain distribution. Transgenic knockout mice were used to study the role of active efflux at the blood-brain barrier (BBB) by P-glycoprotein (P-gp) and breast cancer resistance protein (bcrp) in the brain delivery of palbociclib. Patient-derived xenograft cells were used to study the effect of tumor location on efficacy and it was found that lack of delivery to the brain is responsible, at least in part, for the lack of efficacy. Importantly, flank tumor concentrations made to mimic brain concentrations are also subtherapeutic indicating that limited delivery could be solely responsible for the lack of efficacy observed in an orthotopic (intracranial) model of glioblastoma.

In **Chapter 4**, the limited brain delivery of palbociclib is further studied. Escalating doses of elacridar, a pharmacological inhibitor of P-gp and bcrp at the BBB, were used to increase the brain delivery of palbociclib and understand the concentrations of elacridar necessary to enhance delivery. An optimized dosing regimen was used to study efficacy and pharmacodynamic effect of palbociclib alone and in combination with elacridar.

Chapter 5 compares the brain delivery of the three CDK4/6 inhibitors, palbociclib, ribociclib and abemaciclib. The role of active efflux transport in the brain distribution of abemaciclib and ribociclib was examined after a 48 hour

constant rate infusion, showing that P-gp and/or bcrp are also involved in the brain delivery of these two CDK4/6 inhibitors. In this chapter, *in situ* brain perfusion is used to study the differences in the interaction of P-gp and bcrp with abemaciclib, palbociclib and ribociclib. Interestingly, palbociclib and ribociclib are unable to saturate efflux transport at the BBB at any of the concentrations studied, however abemaciclib is able to saturate efflux activity, thereby enhancing its own brain delivery. Furthermore, these studies indicate that at lower concentrations, there may be an influx transporter system that actively transports these CDK4/6 inhibitors into the brain.

To summarize, these studies establish that palbociclib, abemaciclib and ribociclib have limited brain distribution due to active efflux at the BBB by P-gp and bcrp. Furthermore, these studies demonstrate that the limited brain distribution of palbociclib is related to the observed efficacy in the preclinical patient-derived xenograft model of GBM. Both the use of the pharmacological inhibitor of BBB efflux transport (elacridar) and the differential interaction of abemaciclib with efflux transport at the BBB give potential therapeutic strategies to improve the brain delivery of a CDK4/6 inhibitor. Taken together, these studies provide a clear rationale for the need to study the brain delivery of anti-cancer agents prior to use in the clinical treatment of brain tumors.

CHAPTER III

EFFLUX TRANSPORTERS AT THE BLOOD-BRAIN BARRIER LIMIT DELIVERY AND EFFICACY OF CDK4/6 INHIBITOR PALBOCICLIB (PD-0332991) IN AN ORTHOTOPIC BRAIN TUMOR MODEL

This chapter has been published as a manuscript in the Journal of Pharmacology and Experimental Therapeutics. November 2015 355:264-271.

ABSTRACT

Palbociclib is a cyclin-dependent kinase (CDK) 4/6 inhibitor approved for the treatment of metastatic breast cancer and is currently undergoing clinical trials for many solid tumors. Glioblastoma (GBM) is the most common primary brain tumor in adults and has limited treatment options. The CDK4/6 pathway is commonly dysregulated in GBM and is a promising target in treating this devastating disease. The blood-brain barrier (BBB) limits delivery of drugs to invasive regions of GBM, where efflux transporters P-glycoprotein (P-gp) and breast cancer resistance protein (BCRP) can prevent treatments from reaching the tumor. The purpose of this study was to examine the mechanisms limiting the effectiveness of palbociclib therapy in an orthotopic xenograft model. *In vitro* intracellular accumulation results demonstrated that palbociclib is a substrate for both P-gp and BCRP. *In vivo* studies in transgenic mice confirmed that efflux transport is responsible for the limited brain distribution of palbociclib. There was a ~115-fold increase in brain exposure at steady-state in the *Mdr1a/b*$^{-/-}$*Bcrp1*$^{-/-}$ mice when compared with wild-type and the efflux inhibitor elacridar significantly increased palbociclib brain distribution. Efficacy studies demonstrated that palbociclib is an effective therapy when GBM22 tumor cells are implanted in the flank, but ineffective in an orthotopic (intracranial) model. Moreover, doses designed to mimic brain exposure were ineffective in treating flank tumors. These results demonstrate that efflux transport in the BBB is involved in limiting the brain

distribution of palbociclib and this has critical implications in determining effective dosing regimens of palbociclib therapy in the treatment of brain tumors.

3.1 INTRODUCTION

The cyclin-dependent kinase (CDK) 4/6 pathway is a major regulator of G1-to-S phase transition in the cell cycle (Peyressatre et al., 2015). The p16-CDK4-cyclinD-Rb axis is commonly dysregulated in many cancers and this pathway is a promising target for cancer therapy. During normal cell cycle progression CDK4 complexes with Cyclin D and phosphorylates retinoblastoma (Rb) (VanArsdale et al., 2015). This phosphorylation event leads to downstream signaling to continue via the E2F family of transcription factors and is linked to G1/S phase cell cycle progression (Fry et al., 2004; Baughn et al., 2006; Barton et al., 2013). This pathway is hyperactive in many types of cancers, and inhibitors of this pathway, such as palbociclib, have the potential to be widely used across many solid tumors (Finn et al., 2014). Tumor suppressor proteins, such as p16, regulate the cell cycle by preventing CDK4 from forming a complex with Cyclin D. Amplification of CDK4, CDK6 or Cyclin D as well as the deletion of CDKN2A (the gene that encodes for p16) is commonly observed in glioblastoma (GBM). Any one of these alterations leads to dysregulation of this critical pathway in cell cycle progression (Thangavel et al., 2013).

Palbociclib (PD0332991) is a promising CDK4/6 inhibitor for malignancies with alterations in this pathway. Palbociclib was approved for the treatment of metastatic breast cancer in early 2015 for patients with estrogen-receptor positive, Her2 negative tumors (Turner et al., 2015). Although palbociclib is

currently approved for breast cancer, the potential use of palbociclib in other indications is under investigation. This p16-Cyclin D-CDK4/6-Rb pathway is commonly dysregulated in breast cancer (hormone-receptor positive), melanoma (90%), and GBM (78%) tumors, making it an attractive therapeutic target (Cancer Genome Atlas Research, 2008; Peyressatre et al., 2015; Turner et al., 2015). Previous studies have examined the effectiveness of palbociclib therapy against GBM xenograft cell lines (Michaud et al., 2010). Michaud et al. determined that of the 21 GBM xenografts they examined, 16 (76%) were sensitive to palbociclib treatment *in vitro*. The five tumor lines that were resistant to palbociclib therapy all had mutations in Rb, which is downstream of CDK4/6. These data indicate there is a clear rationale to consider palbociclib and other CDK 4/6 inhibitors to treat brain tumors.

A critical factor in the use of palbociclib in the treatment of brain tumors is achieving effective drug delivery to all tumor cells, including those invasive cells which reside behind an intact blood-brain barrier (BBB) (Agarwal et al., 2011b). The BBB acts as both a physical and biochemical barrier, limiting the brain delivery of numerous treatments (Abbott, 2013). Tight junction proteins, such as occludin and claudin, prevent the paracellular transport of compounds from the blood into the brain and efflux transporters actively prevent compounds from reaching the brain via the transcellular route (Abbott, 2013). P-glycoprotein (P-gp) and breast cancer resistant protein (BCRP) are two efflux transporters that are highly expressed at the BBB (Uchida et al., 2011) and can prevent potentially

effective agents from reaching the brain. GBM is the most common primary brain tumor in adults and survival following diagnosis, even after aggressive treatment, is about 1 year (Stupp et al., 2005). Therefore, the purpose of this study was to determine the mechanisms that limit the delivery, and hence efficacy, of palbociclib therapy in an orthotopic xenograft model of a patient-derived GBM.

3.2 MATERIALS AND METHODS:

3.2.1 CHEMICALS: Palbociclib (PD-0332991) was purchased from Chemietek (Indianapolis, IN). [^{3}H]-prazosin and [^{3}H]-vinblastine were purchased from Perkin Elmer Life and Analytical Sciences (Waltham, MA) and Moravek Biochemicals (La Brea, CA), respectively. Ko143 was purchased from Tocris Bioscience (Ellisville, MO) and zosuquidar (LY335979) was kindly provided Eli Lilly and Co.(Indianapolis, IN). Cell culture reagents were purchased from Invitrogen (Carlsbad, CA), and all other chemicals were from Sigma-Aldrich (St. Louis, MO).

3.2.2 IN VITRO STUDIES: *In vitro* studies were conducted using Madin-Darby canine kidney II (MDCKII) cells. Vector control and Bcrp1-transfected MDCKII cells were gifts from Dr. Alfred Schinkel (The Netherlands Cancer Institute) and vector control and MDR1-transfected (MDCKII-MDR1) cell lines were provided by Dr. Piet Borst (The Netherlands Cancer Institute). Cell lines were cultured in Dulbecco's modified Eagle's medium (DMEM) with 10% (v/v) fetal bovine serum and penicillin (100 U/mL), streptomycin (100 µg/mL), and amphotericin B (250 ng/mL). MDCKII-MDR1 cells were cultured in media with colchicine (80 ng/mL) to maintain positive selection pressure for P-gp expression. Cells were maintained in 25 mL tissue culture flasks at 37º C in a humidified incubator with 5% CO_2.

Intracellular accumulation studies:

Palbociclib intracellular accumulation studies were performed as previously described (Mittapalli et al., 2012). Briefly, the cells were preincubated for 30 minutes with blank cell assay buffer or cell assay buffer containing 200 nM Ko143 or 1 □M zosuquidar. Following the preincubation, 2 μM palbociclib was added to each well for 60 minutes at 37º C. 1% Triton-X was used to lyse the cells and the lysate was analyzed via LC-MS/MS for drug concentration and protein concentration (BCA protein assay) to normalize accumulation.

3.2.3 *IN VIVO* STUDIES

3.2.3.1 Animals:

Concentration-time profile studies were conducted in Friend leukemia virus strain B (FVB) male and female wild type, *Mdr1a/b*$^{-/-}$ (P-gp knockout), *Bcrp1*$^{-/-}$ (Bcrp knockout), and *Mdr1a/b*$^{-/-}$*Bcrp1*$^{-/-}$ (triple knockout) mice (Taconic Farms, Germantown, NY). Animals were maintained in a 12 hour light/dark cycle with unlimited access to food and water and were 8 to 12 weeks old at the time of the experiment. *In vivo* studies were approved by the Institutional Animal Care and Use Committee (IACUC) at the University of Minnesota.

3.2.3.2 Brain distribution of palbociclib after a single oral dose:

Wild type, *Mdr1a/b*$^{-/-}$, *Bcrp1*$^{-/-}$, and *Mdr1a/b*$^{-/-}$*Bcrp1*$^{-/-}$ mice received an oral dose (10 mg/kg) of palbociclib (vehicle: 1% CMC and 1% Tween-80). Following euthanasia in a CO2 chamber, brain and blood samples were collected at 0.5, 1,

2, 4, 8, 12, and 24 hours post dose (n=4 per time point). Plasma was isolated from whole blood via centrifugation (3500 rpm for 15 minutes at 4 ºC), whole brain was removed and washed with ice cold water and superficial meninges were removed by blotting with tissue paper. Samples were stored at -80 ºC until analysis via LC-MS/MS.

3.2.3.3 Steady-state brain distribution of palbociclib:

Alzet osmotic mini-pumps (1003D, Durect Corporation, Cupertino, CA) were implanted in the peritoneal cavity of wild type, *Mdr1a/b*$^{-/-}$, *Bcrp1*$^{-/-}$, and *Mdr1a/b*$^{-/-}$ *Bcrp1*$^{-/-}$ mice to deliver 1 □L/hr as a constant infusion in order to determine the steady-state brain and plasma concentrations of palbociclib (n=4). Palbociclib (10 mg/mL in DMSO) was loaded into the pumps and primed at 37º C overnight in sterile saline. Pumps were implanted into the peritoneal cavity as described previously (Agarwal et al., 2010). Briefly, isoflurane was used to anesthetize mice and the hair was removed from the abdominal cavity. A small incision was made in the lower right abdominal wall and the peritoneal membrane was exposed then a small incision was made in the peritoneal membrane and the primed pump was inserted into the cavity. The peritoneal membrane was sutured and the skin incision was closed with surgical clips. The surgical procedure was conducted on a heating pad until the animals were fully recovered. 48 hours following pump implantation, the mice were sacrificed and blood and brain samples were isolated. Samples were stored at -80 ºC until analysis via LC-MS/MS.

3.2.3.4 Palbociclib efficacy in GBM22 xenograft:

Tumor-bearing studies were conducted in female athymic nude mice (Harlan Sprague Dawley Athymic Nude-Foxn1nu mice) as described in detail previously (Carlson et al., 2011; Pokorny et al., 2015). The patient-derived xenografts (PDX) were derived from individual primary human GBM at the Mayo Clinic, Rochester, Minnesota, and maintained through serial passages in the flank (Carlson et al., 2011). Short term explant cultures were maintained exclusively in the Sarkaria laboratory in DMEM containing 10% FBS and 1% penicillin/streptomycin media prior to intracranial or flank implantation. Mice were anesthetized using ketamine (100 mg/kg) and xylazine (10 mg/kg) and intracranial tumors were implanted 1mm anterior and 2 mm lateral from the bregma. GBM22 is a PDX that has homozygous deletion of CDKN2A/B, hemizygous deletion of CDK4, gain of CDK6 and loss of CDKN2C, CCND1, CCND2 and RB1 (Cen et al., 2012). GBM22 tumor cells were implanted either in the flank or intracranially. Eleven days following intracranial tumor implantation, palbociclib was dosed at 150 mg/kg until mice became moribund (n=10). Fourteen days following flank tumor implantation, palbociclib was dosed at either 150 or 10 mg/kg until tumors reached 1500 mm^3 (n=8-10). Mice were euthanized by CO_2.

3.2.3.5 In vivo pharmacological inhibition of efflux transporters:

A microemulsion formulation of elacridar, a dual inhibitor of P-gp and BCRP, was prepared as described previously (Sane et al., 2013). Cremophor EL, Carbitol and Captex 355 were formulated in a 6:3:1 ratio. On the day of the experiment, elacridar was added to this mixture and sonicated to form a 3 mg/mL solution that was then diluted with water to form a 1 mg/mL microemulsion for injection. Wild-type mice received blank microemulsion or 10 mg/kg elacridar via intraperitoneal injection and a single oral dose of palbociclib (10 mg/kg). Two hours following the administration of elacridar and palbociclib, blood and brain samples were collected and analyzed via LC-MS/MS.

3.2.4 LC-MS/MS ANALYSIS OF PALBOCICLIB

The concentration of palbociclib in cell lysate, plasma, tumor and brain homogenate samples was determined using a sensitive liquid chromatography coupled with tandem mass spectrometry (LC-MS/MS) assay. Brain and tumor homogenate samples were prepared by adding three volumes of 5% bovine serum albumin before homogenizing using a tissue homogenizer (PowerGen 125, Thermo Fisher Scientific). Samples were spiked with 25 ng dasatinib as internal standard and extracted by the addition of 1-2 volumes of pH 11 buffer and 5-10 volumes of ethyl acetate followed by vigorous shaking for 5 minutes, then 5 minutes of centrifugation at 7500 rpm. The organic layer was transferred to microcentrifuge tubes and dried under nitrogen. Samples were reconstituted in 100 µL of mobile phase and transferred to HPLC vials for analysis. An AQUITY

UPLC® system (Milford, MA, USA) was used with a Phenomenex Synergi Polar 4 µ polar-RP 80A column (75 x 2 m, Torrance, CA). The ionization was conducted in positive mode and the m/z transitions were 448.34 – 379.95 and 488.21 – 400.88 for palbociclib and dasatinib, respectively. The retention time was 2.8 minutes for palbociclib and 4.8 minutes for dasatinib. The mobile phase (73:27::1 mM ammonium formate with 0.1% formic acid: acetonitrile) was delivered at a constant flow rate of 0.25 mL/min.

3.2.5 PHARMACOKINETIC CALCULATIONS

Parameters from the concentration-time profiles in plasma and brain samples were obtained by non-compartmental analysis (NCA) performed using Phoenix WinNonlin 6.2 (Pharsight, Mountain View, CA). The area-under-the-curve for plasma (AUCplasma) and brain (AUCbrain) were calculated using the log-linear trapezoidal approximation ($AUC_{0\text{-}tlast}$). The standard error around the mean of AUCs was estimated using the sparse sampling module in WinNonlin. Relative brain exposure comparisons between wild type, *Mdr1a/b*$^{-/-}$, *Bcrp1*$^{-/-}$, and *Mdr1a/b*$^{-/-}$*Bcrp1*$^{-/-}$ mice were made using the drug targeting index (DTI = $(AUC_{brain}/AUC_{plasma})_{knockout}$ / $(AUC_{brain}/AUC_{plasma})_{wild\text{-}type}$).

3.2.6 STATISTICAL ANALYSIS

GraphPad Prism 6.04 (GraphPad, San Diego, CA, USA) software was used for statistical analysis. The sample sizes used were based on previous work and determined based on approximately 80% power to detect differences greater than ten-fold in distribution studies or two-fold in efficacy studies. Data in all experiments are represented as mean ± SD. Comparisons between two groups were made using an unpaired t-test. Multiple comparisons were made using one-way ANOVA, followed by Bonferonni's multiple comparisons test. A significance level of $p<0.05$ was used for all studies.

3.3 RESULTS

3.3.1 INTRACELLULAR ACCUMULATION OF PALBOCICLIB

MDCKII vector control and P-gp or Bcrp transfected cell lines were used to study the intracellular accumulation of the CDK4/6 inhibitor palbociclib. Functionality of efflux in the cell lines was validated using [^{3}H]-vinblastine as a positive control for P-gp mediated transport and [^{3}H]-prazosin as positive control for Bcrp mediated transport. The accumulation of [^{3}H]-vinblastine was 90% lower in the P-gp overexpressing cell line than vector control cells (**Figure 3.1.A**, Vector Control (normalized): 100 ± 6.7%; P-gp: 9.4 ± 0.8%, $p<0.0001$). This effect was abolished when P-gp was inhibited by 1 μM LY335979. Intracellular accumulation of palbociclib was 25% lower in the P-gp overexpressing cells than in vector-control cells (**Figure 3.1.A**, Vector Control: 100 ± 12.3%; P-gp: 74.8 ± 6.0%, $p=0.0333$) and the efflux was again reversed by LY335979. In the Bcrp overexpressing cells, the accumulation of [^{3}H]-prazosin was 73% lower than vector control cells (**Figure 3.1.B**, Vector Control: 100 ± 6.1%; Bcrp: 27.0 ± 2.4%, $p<0.0001$) and reversed by Ko143. Intracellular accumulation of palbociclib was significantly diminished in the Bcrp overexpressing cells vs. the vector control cells (**Figure 3.1.B**, Vector Control: 100 ± 7.9%; Bcrp: 23.7 ± 2.8%, $p<0.0001$). The reduced intracellular accumulation of palbociclib was reversed in the presence of a P-gp specific inhibitor, LY335979 (P-gp: 77.5 ± 6.0%; P-gp with LY3359779: 143.6 ± 13.8%, $p<0.0001$). Similarly, the difference in intracellular

accumulation of palbociclib was abolished in the presence of a Bcrp specific inhibitor, Ko143 (Bcrp: 23.7 ± 2.8%; Bcrp with Ko143: 85.6 ± 1.3%, $p<0.0001$). Taken together, these *in vitro* data demonstrate that palbociclib is a substrate of both P-gp and Bcrp, and the active efflux of palbociclib by each transporter can be inhibited by transporter-specific inhibitors.

3.3.2 CONCENTRATION-TIME PROFILES IN FOUR GENOTYPES

The brain and plasma concentration-time profiles were determined in FVB wild-type, *Bcrp1*$^{-/-}$, *Mdr1a/b*$^{-/-}$ and *Mdr1a/b*$^{-/-}$*Bcrp1*$^{-/-}$ mice following a single oral dose (10 mg/kg) of palbociclib. The plasma concentrations are elevated in the *Mdr1a/b*$^{-/-}$ and *Mdr1a/b*$^{-/-}$*Bcrp1*$^{-/-}$ mice and the brain concentrations are vary widely amongst the four genotypes with wild-type mice having the lowest brain exposure, followed by *Bcrp1*$^{-/-}$, *Mdr1a/b*$^{-/-}$ and *Mdr1a/b*$^{-/-}$*Bcrp1*$^{-/-}$ mice (**Figure 3.2**). The brain-to-plasma area-under-the-curve (AUC) ratios in the wild-type, *Bcrp1*$^{-/-}$, *Mdr1a/b*$^{-/-}$ and *Mdr1a/b*$^{-/-}$*Bcrp1*$^{-/-}$ mice were 0.064, 0.14, 1.42, and 7.36, respectively. The *Mdr1a/b*$^{-/-}$*Bcrp1*$^{-/-}$ mice have a 115-fold increase in the brain exposure of palbociclib when compared to wild-type (i.e., drug targeting index, DTI, $(AUC_{brain}/AUC_{plasma})_{knockout}$ / $(AUC_{brain}/AUC_{plasma})_{wild\text{-}type}$ (**Table 3.1**)).

3.3.3 BRAIN DISTRIBUTION OF PALBOCICLIB AT STEADY-STATE

The brain distribution of palbociclib at steady-state was determined after a constant rate infusion into the intraperitoneal cavity using Alzet^{TM} osmotic pumps for 48 hrs at 10 µg/hr. The steady-state brain-to-plasma ratios were 0.2 ± 0.07, 0.4 ± 0.1, 2.5 ± 0.1, 27.8 ± 5.9 for wild-type, *Bcrp1*$^{-/-}$, *Mdr1a/b*$^{-/-}$ and *Mdr1a/b*$^{-/-}$ *Bcrp1*$^{-/-}$ mice, respectively (**Figure 3.3**, **Table 3.2**). The brain-to-plasma ratio was ~ 140-fold higher in the *Mdr1a/b*$^{-/-}$*Bcrp1*$^{-/-}$ mice when compared to the wild-type mice.

3.3.4 FLANK VS. IC SURVIVAL STUDIES

GBM 22 tumor cells were implanted in either the flank or intracranially in athymic nude mice to assess the effect of the BBB on the efficacy of palbociclib treatment. Mice with established subcutaneous tumors (flank) were randomized to therapy (150 mg/kg/day) or vehicle control and the time to exceed 1500 mm^3 was measured. Palbociclib therapy provided a significant prolongation in the time to reach 1500 mm^3 (**Figure 3.4, Figure 3.5.A**, $p<0.0001$,). In stark contrast to what was seen in the subcutaneous model, the time to reach moribund in the treatment group was no different as compared to vehicle treated group in the intracranial tumor model (**Figure 3.5.B**, $p=0.55$).

The concentration of palbociclib in the brain following a 150 mg/kg dose was not significantly different than the concentration in the subcutaneous tumor following a 10 mg/kg dose (**Figure 3.6.A**). Following this study, mice with subcutaneous

tumors were randomized to two groups, palbociclib (10 mg/kg/day) or vehicle control. There was no effect on subcutaneous tumor growth in the 10mg/kg palbociclib treated group compared with the vehicle control (**Figure 3.6.B**, p=0.57). This informative study demonstrates that the concentrations reaching invasive tumor cells at the growing edge of a brain tumor were subtherapeutic. These results show the relationship between site-specific drug delivery and efficacy.

3.3.5 PHARMACOLOGICAL INHIBITION OF EFFLUX TRANSPORTERS IMPROVES PALBOCICLIB BRAIN DELIVERY

The effect of pharmacological inhibition of the efflux transporters on the brain exposure of palbociclib was studied in order to determine the feasibility of this strategy to enhance the brain delivery of palbociclib and possibly improve efficacy. Elacridar, a dual inhibitor of P-gp and Bcrp, was administered in a microemulsion formulation simultaneously with an oral dose of palbociclib. Two hours following dosing, plasma concentrations were no different in the wild-type plus elacridar microemulsion vehicle treated and wild-type plus elacridar treatment groups (**Figure 3.7.A**, vehicle: 867.7 ± 1187 nM; treatment: 363.1 ± 261.9 nM). The elacridar vehicle treatment provided no improved delivery when compared with the wild-type mice, however elacridar treatment significantly (p=0.0062) improved the brain delivery of palbociclib (**Figure 3.7.B**, wild-type + vehicle: 0.123 ± 0.072; WT + elacridar: 2.73 ± 1.56). These data indicate that

pharmacological inhibition of both BCRP and P-gp may be useful in enhancing the brain delivery, and hence the treatment efficacy of palbociclib in brain tumors.

3.4 DISCUSSION

GBM remains a lethal disease and there is a serious unmet need for better therapeutic options for these patients. Alterations in the p16-CDK4-cyclinD-Rb pathway are commonly found (~ 78%) in GBM and therefore CDK4/6 inhibitors, such as palbociclib, provide a promising targeted therapy in the treatment of GBM. In order to use palbociclib effectively in the treatment of brain tumors, it is critical to understand the mechanisms that may limit the brain distribution of palbociclib and the relationship between delivery and efficacy.

Efflux transport in the BBB restricts the brain delivery of numerous therapeutic agents (Agarwal et al., 2010; Agarwal et al., 2011d; Wang et al., 2012; Parrish et al., 2015). P-gp and BCRP actively transport substrate drugs back into systemic circulation and can especially prevent potentially effective drugs from reaching invasive tumor cells that reside behind an intact BBB. *In vitro* intracellular accumulation in MDCK-II transfected cells indicate that palbociclib is a dual substrate of both P-gp and BCRP. Consistent with this substrate status, *in vivo* studies characterizing the brain exposure of palbociclib in wild-type, *Mdr1a/b*$^{-/-}$, *Bcrp1*$^{-/-}$, and *Mdr1a/b*$^{-/-}$*Bcrp1*$^{-/-}$ mice demonstrate that both transporters are involved in limiting the brain delivery of palbociclib. Both P-gp and BCRP are also expressed in the intestine, and therefore the slight increase in systemic exposure after oral dose in the knockout mice may be

related to a decrease in efflux at the intestinal level leading to an increase in drug absorbed.

At steady state, no significant difference was observed in the brain distribution between the wild-type and *Bcrp1*$^{-/-}$ mice, likely because of P-gp mediated compensation for the lack of BCRP efflux (Agarwal et al., 2011a), however in *Mdr1a/b*$^{-/-}$ mice there is an approximately 10-fold increase in brain exposure. The largest increase in brain exposure was observed in the *Mdr1a/b*$^{-/-}$ *Bcrp1*$^{-/-}$ mice with a ~115-fold increase in brain distribution, again showing that both transporters are critical in limiting delivery. Consistent with recent reports (de Gooijer et al., 2015; Raub et al., 2015), we have shown that the efflux transporters P-gp and BCRP play a significant role in the brain delivery of palbociclib. Furthermore, our data in the current study indicate that the limited brain delivery of palbociclib may be the reason behind the lack of efficacy of palbociclib in the orthotopic GBM22 model.

The subcutaneous GBM22 model, that has homozygous deletion of CDKN2A/B as well as other alterations in the p16-CDK4-Rb pathway, demonstrated that palbociclib therapy is highly effective in prolonging time to reach 1500 mm^3, however using the same GBM22 cell line, there was no survival benefit in an orthotopic (intracranial) mouse model. Using these two different models to study the efficacy of therapy on the same patient-derived GBM cells, we observed two radically different outcomes based on tumor location. In the subcutaneous model, where there is no efflux barrier to impede delivery,

palbociclib therapy significantly hindered tumor growth. However these same GBM22 cells were insensitive to palbociclib therapy in the intracranial model, where efflux in the BBB is limiting delivery. The disconnect between the observed flank and intracranial efficacy demonstrates the essential role of the BBB in the treatment of brain tumors. There is a need for new treatment options for patients with primary and metastatic brain tumors and caution is needed when examining efficacy without recognizing the issue of delivery to invasive tumor cells behind an intact BBB.

We determined the dose that would expose a subcutaneous tumor to “brain-like” concentrations of palbociclib in order to understand the relationship between delivery and efficacy. In this study, a low dose of palbociclib (10 mg/kg/day) replicated concentrations in the subcutaneous tumor that were observed in the brain following a high dose (150 mg/kg/day) of palbociclib. This low dose of palbociclib, that mimicked the brain exposure of palbociclib, provided no therapeutic benefit in the flank tumor model of GBM. This demonstrates that the concentrations of a possibly effective drug, palbociclib, that reach the invasive edge of the tumor protected by an intact BBB, are subtherapeutic and, therefore, fail to provide therapeutic benefit.

The experimental paradigm of examining both delivery and efficacy in the heterotopic and orthotopic tumors results in powerful insights as to why a drug may fail in treating a tumor in the brain. On the one hand, if a drug at a maximally tolerated dose is ineffective in the flank tumor, then it is possible that

drug should no longer be considered as a treatment option for that tumor type. However, if a drug at the maximally tolerated dose is ineffective in treating a tumor in the brain, but effective in the flank, it is then important to recognize that the lack of efficacy in the brain may be due to inadequate delivery. These insights should guide the preclinical screening of compounds for GBM.

There may also be some inherent differences between brain tumors and subcutaneous tumors in addition to the BBB preventing adequate drug delivery to brain tumors. The possible changes in microenvironment between a subcutaneous tumor and an intracranial tumor have not yet been determined. These differences have not been explored in this paper, but are important to understand and may provide yet another reason to be cautious when using subcutaneous tumors for preclinical screening of compounds for GBM and other brain tumors. In this preclinical model, we show that inadequate brain drug delivery due to efflux at the BBB could be solely responsible for failure of palbociclib therapy.

Michaud et al. demonstrated the efficacy of palbociclib in both *in vivo* and *in vitro* models (Michaud et al., 2010). They proposed that since palbociclib was effective in their in vivo U87MG tumor model and GBM39 xenograft, the BBB was not a barrier for this molecule. In the U87MG model, the drug delivery to the tumor core was significantly greater than the delivery to the other regions of the brain (including brain around tumor and other hemisphere). It should be noted that U87MG model is a less invasive and more circumscribed tumor than many

PDX and genetically-engineered models, and as such serves as a poor model to study the invasive nature of glioma (de Vries et al., 2009). It is important to recognize that GBM is a disease of the whole brain, with invasive cells moving from the original tumor site to other areas of the brain (Agarwal et al., 2011b). Previous studies have demonstrated the importance of the BBB by MALDI-MS imaging where a drug that is a substrate for BBB efflux transporters is homogeneously distributed throughout the tumor for the U87 model, but that same drug is not distributed homogeneously in a GS2 model, a model which shares the invasive characteristics observed in human GBM (Salphati et al., 2014). For this reason, it is crucial to deliver therapies to the whole brain, not just the tumor core. This will require therapies that cross an intact BBB and overcome the liability of efflux transport.

Coadministration of elacridar with palbociclib significantly improves the brain delivery of palbociclib and provides a potential therapeutic strategy to overcome efflux transport in the BBB and achieve adequate brain delivery. These findings have important implications in the use of palbociclib in the treatment of GBM, as it may be necessary to employ adjuvant therapies that improve delivery to invasive tumor.

In addition to primary brain tumors such as GBM, metastatic brain tumors are associated with poor prognosis with limited treatment options (Maher et al., 2009). Lung, breast and melanoma are the three cancers with the highest propensity to metastasize to the brain and breast and melanoma often have

mutations in the CDK 4/6 pathway (Musgrove et al., 2011; Gállego Pérez-Larraya and Hildebrand, 2014). The clinical utility of CDK4/6 inhibitors in the treatment of cancer has been most extensively studied in the treatment of breast cancers (Turner et al., 2015). Since breast cancer is the second most common cause of brain metastasis, it is paramount that treatment modalities are able to penetrate the BBB. In melanoma, 38% of patients have genetic deletion of $p16^{INK4a}$ leading to unrestricted tumor growth via this pathway. Since well over half of melanoma patients are found to have brain tumors at autopsy (Fife et al., 2004), effectively delivering treatments to tumor cells behind an intact BBB, even at the stage of micrometastases, is critical. Furthermore, there have been studies which indicate that the incidence of brain metastasis can increase when treating cancers that have a high propensity to metastasize to the brain with agents that are unable to penetrate a BBB (O'Sullivan and Smith, 2014; Peuvrel et al., 2014). Understanding the delivery issues associated with using palbociclib therapy in the treatment of brain metastases will be essential in effectively treating this patient population.

Taken together, these results clearly demonstrate that the BBB plays a major role in limiting the brain delivery of palbociclib and limits the delivery of palbociclib to invasive tumor cells residing behind an intact BBB. Future work remains to determine the effect of palbociclib in combination with BBB efflux inhibition in tumor-bearing mice. Brain distribution studies comparing palbociclib

with other CDK4/6 inhibitors (such as ribociclib (LEE-011) and abemaciclib (LY2835219)) are also of significant importance.

ACKNOWLEDGEMENTS

The authors thank Jim Fisher, Clinical Pharmacology Analytical Services Laboratory, University of Minnesota, for support in the development of the palbociclib LC-MS/MS assay.

FOOTNOTES

Funding for this work was supported by the National Institutes of Health (RO1 CA138437, RO1 NS077921, and P50 CA108961). KEP was supported by the Ronald J. Sawchuk, Edward G. Rippie, Rowell, American Foundation for Pharmaceutical Education Pre-Doctoral, and the University of Minnesota Doctoral Dissertation Fellowships.

Part of this work was previously presented: Parrish KE, Pokorny JL, Mittapalli RK, Bakken K, Sarkaria JN, Elmquist WF (2013) Abstract C81: BBB efflux pump activity limits brain penetration of palbociclib (PD0332991) in glioblastoma. Mol Cancer Ther 12(11 Supplement):C81. doi:10.1158/1535-7163. Targ-13-C81

LEGENDS FOR FIGURES

Figure 3.1.A: Intracellular accumulation of palbociclib in vector controlled and MDR1 overexpressing MDCKII cells.

(A) The intracellular accumulation of vinblastine (positive control) and 2 µM palbociclib in MDCKII-vector controlled and MDR1 cells. *,*** represent $p<0.05$ and $p<0.001$, respectively, when compared to wild-type control and # represents $p<0.001$ when compared to transfected cells without inhibitor (n=3-6).

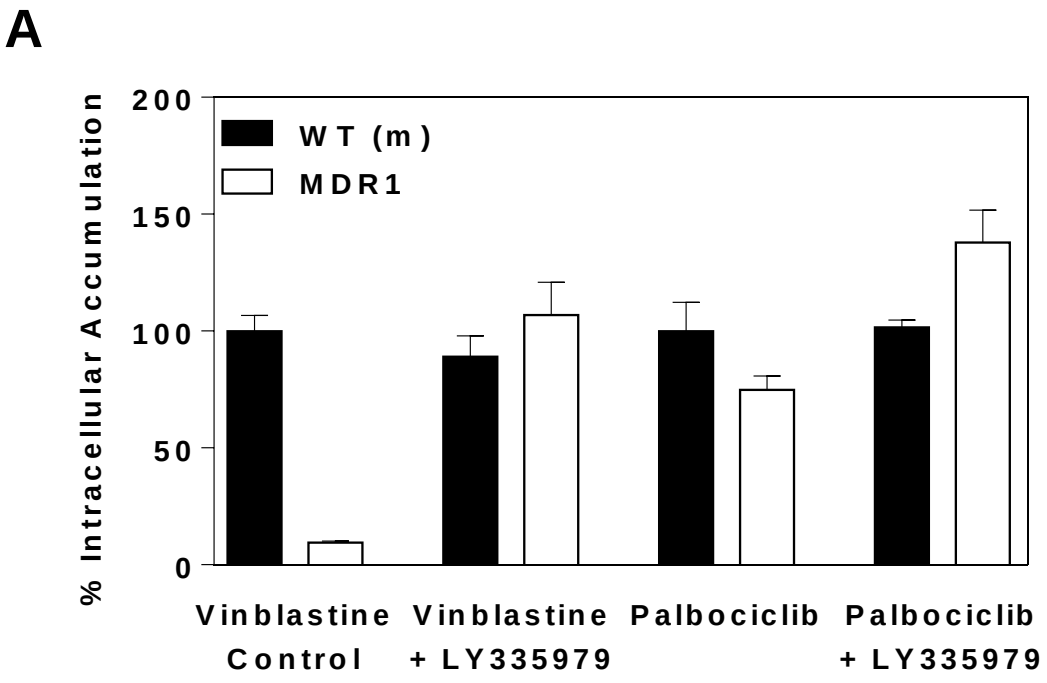

Figure 3.1.B: Intracellular accumulation of palbociclib in vector controlled and Bcrp1 overexpressing MDCKII cells.

(B) The intracellular accumulation of prazosin (positive control) and 2 µM palbociclib in MDCKII-vector controlled and Bcrp1 cells. *,*** represent $p<0.05$ and $p<0.001$, respectively, when compared to wild-type control and # represents $p<0.001$ when compared to transfected cells without inhibitor (n=3-6).

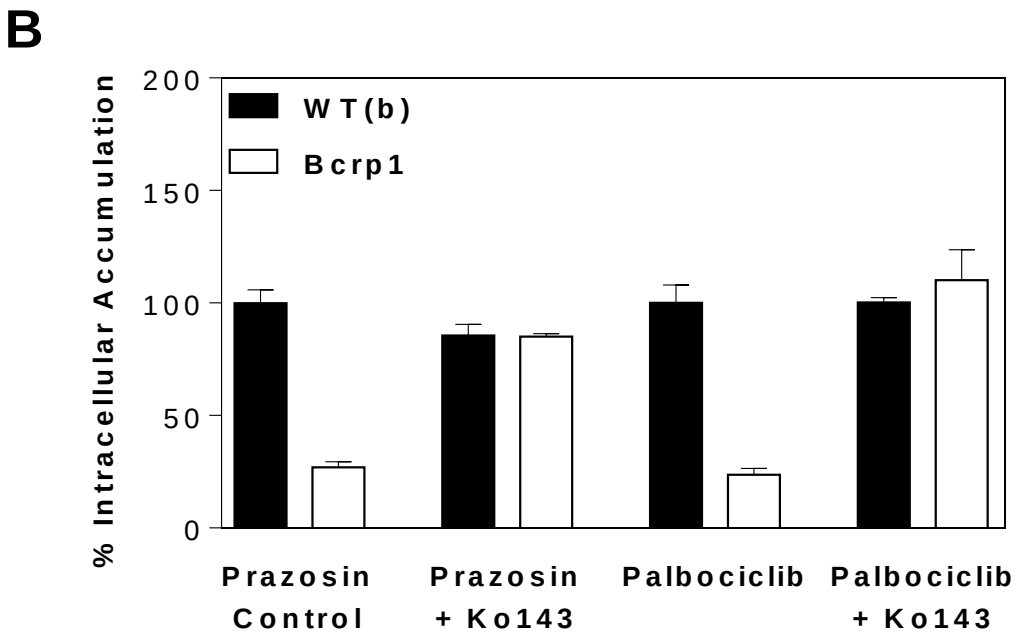

Figure 3.2.A: Concentration-time profiles in FVB wild-type mice.

Brain and plasma concentration-time profile in (A) wild-type mice (n=4 per time point).

A

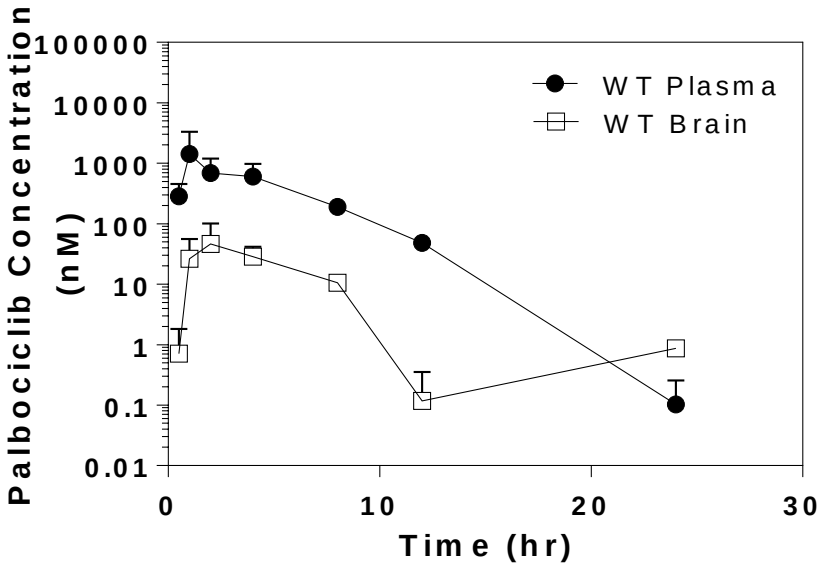

Figure 3.2.B: Concentration-time profiles in FVB *Bcrp1*$^{-/-}$ mice.

Brain and plasma concentration-time profile in (B) *Bcrp1*$^{-/-}$ mice (n=4 per time point).

B

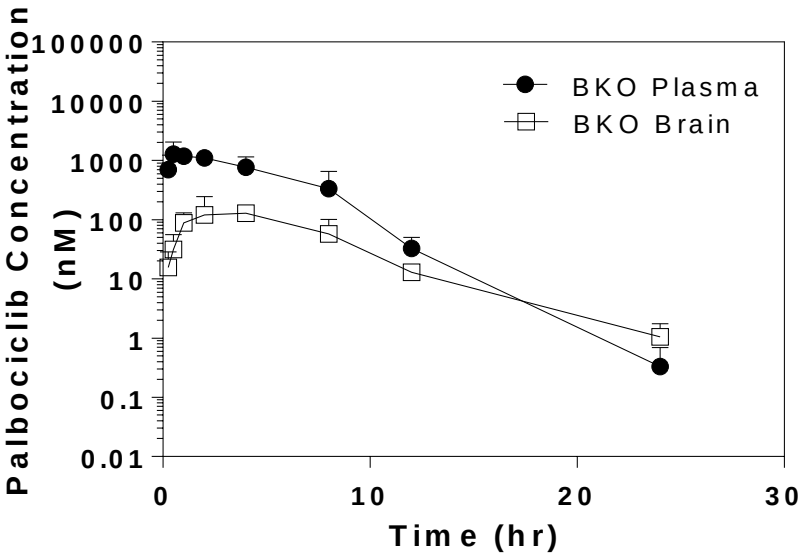

Figure 3.2.C: Concentration-time profiles in FVB *Mdr1a/b*$^{-/-}$ mice.

Brain and plasma concentration-time profile in (C) *Mdr1a/b*$^{-/-}$ mice (n=4 per time point).

C

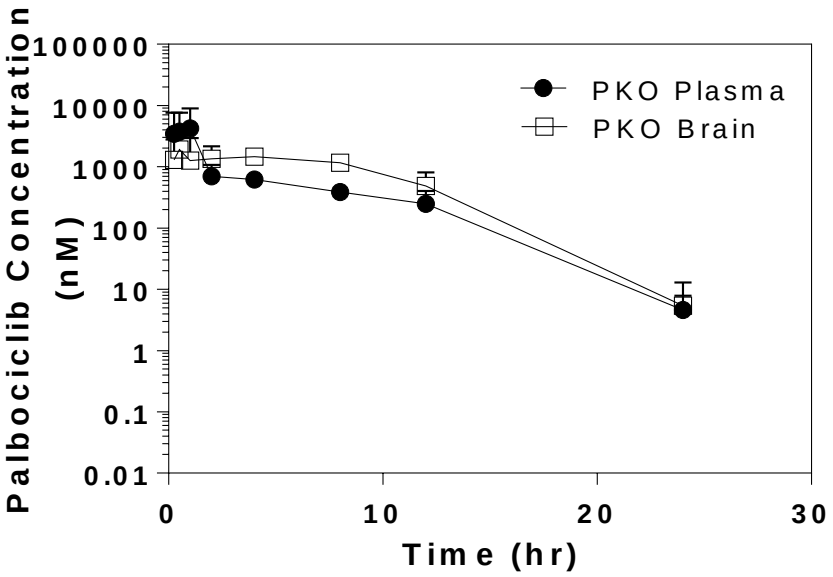

Figure 3.2.D: Concentration-time profiles in FVB *Mdr1a/b*$^{-/-}$*Bcrp1*$^{-/-}$ mice.

Brain and plasma concentration-time profile in (D) *Mdr1a/b*$^{-/-}$*Bcrp1*$^{-/-}$ mice (n=4 per time point).

D

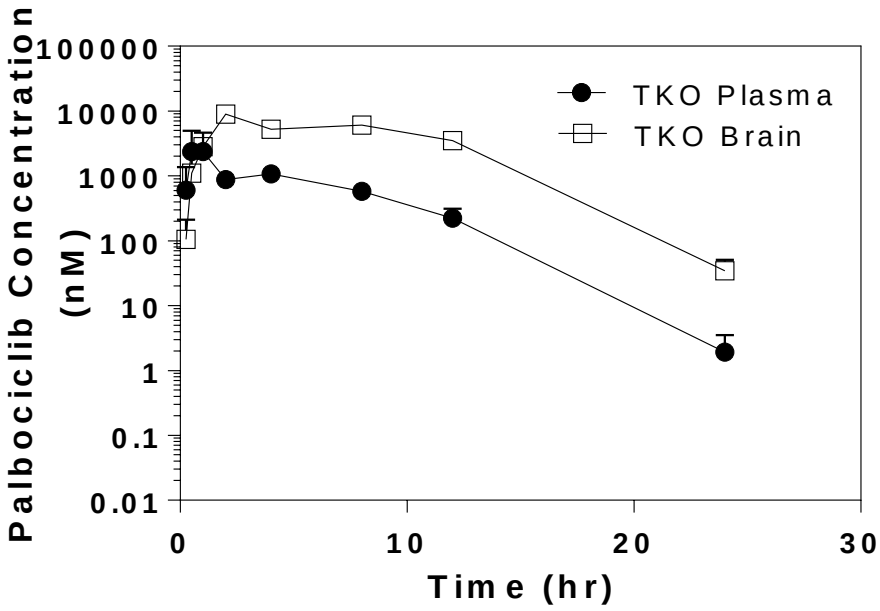

Figure 3.3.A: Steady-state distribution of palbociclib in FVB wild-type, *Bcrp1*$^{-/-}$, *Mdr1a/b*$^{-/-}$, and *Mdr1a/b*$^{-/-}$*Bcrp1*$^{-/-}$ mice.

,* represent p<0.01 and p<0.001, respectively (n=4).

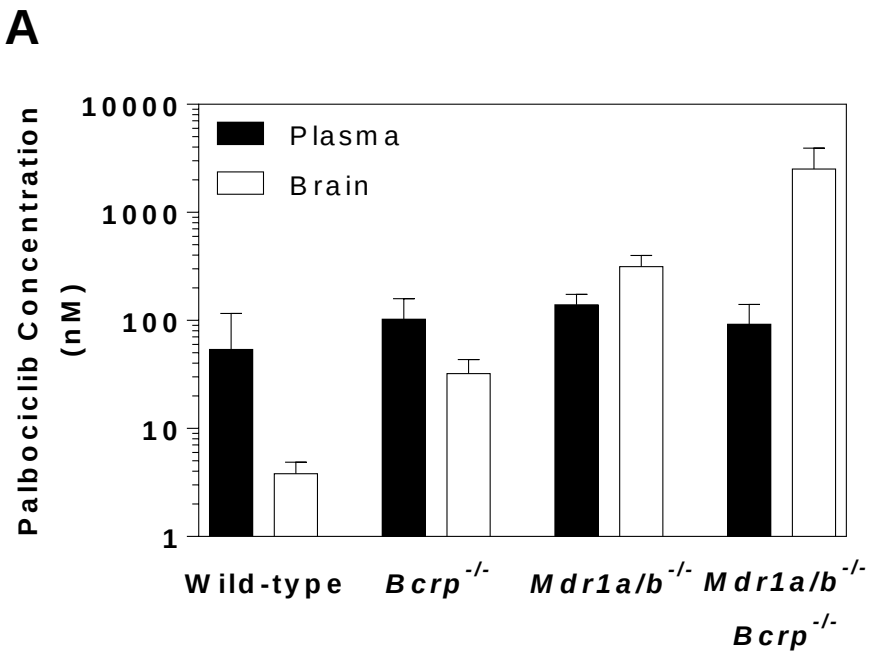

Figure 3.3.B: Steady-state brain-to-plasma ratio of palbociclib in FVB wild-type, *Bcrp1*$^{-/-}$, *Mdr1a/b*$^{-/-}$, and *Mdr1a/b*$^{-/-}$*Bcrp1*$^{-/-}$ mice.

(B) Brain-to-plasma ratio. **,*** represent p<0.01 and p<0.001, respectively (n=4).

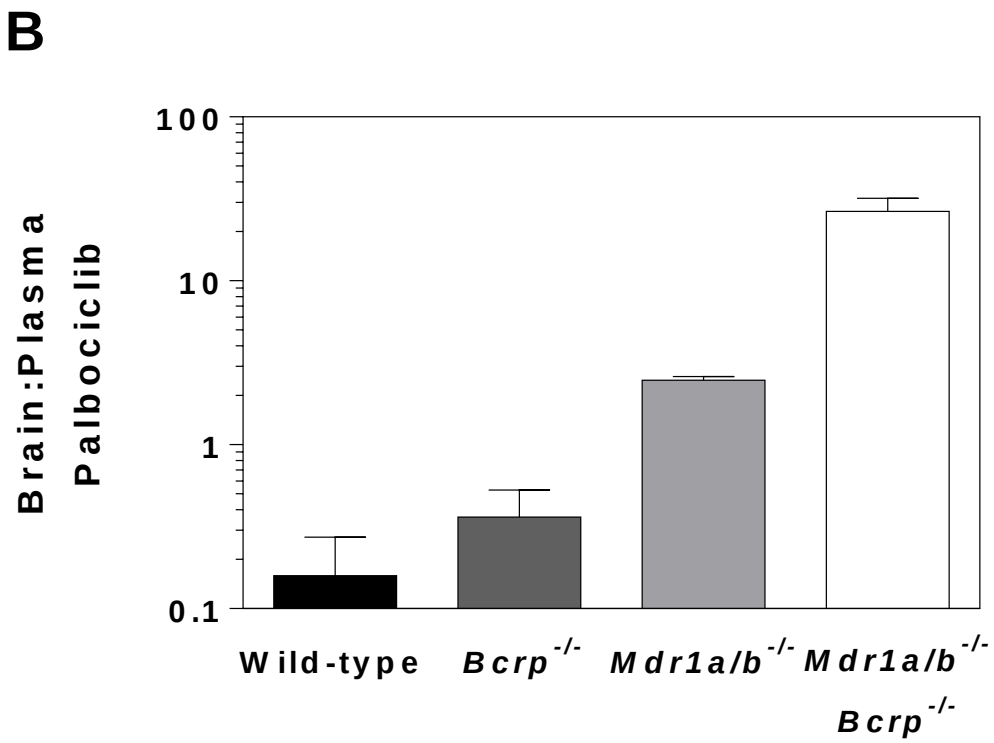

Figure 3.4: Xenograft (GBM22) tumor volume in subcutaneous tumor bearing mice following continuous treatment with 150 mg/kg/day palbociclib or vehicle (n=8-9).

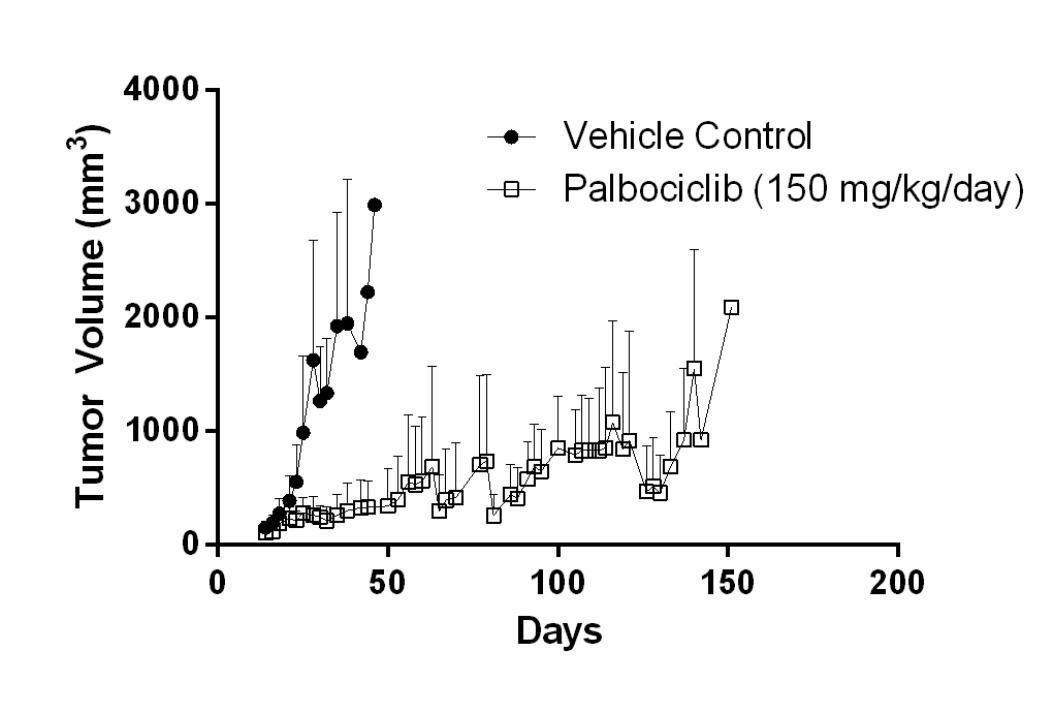

Figure 3.5.A: Efficacy of palbociclib therapy (150 mg/kg/day) in subcutaneous patient-derived xenograft (GBM22).

(A) Efficacy in subcutaneous GBM22 tumor bearing mice (n=8-9) based on time to exceed tumor size of 1500 mm^3.

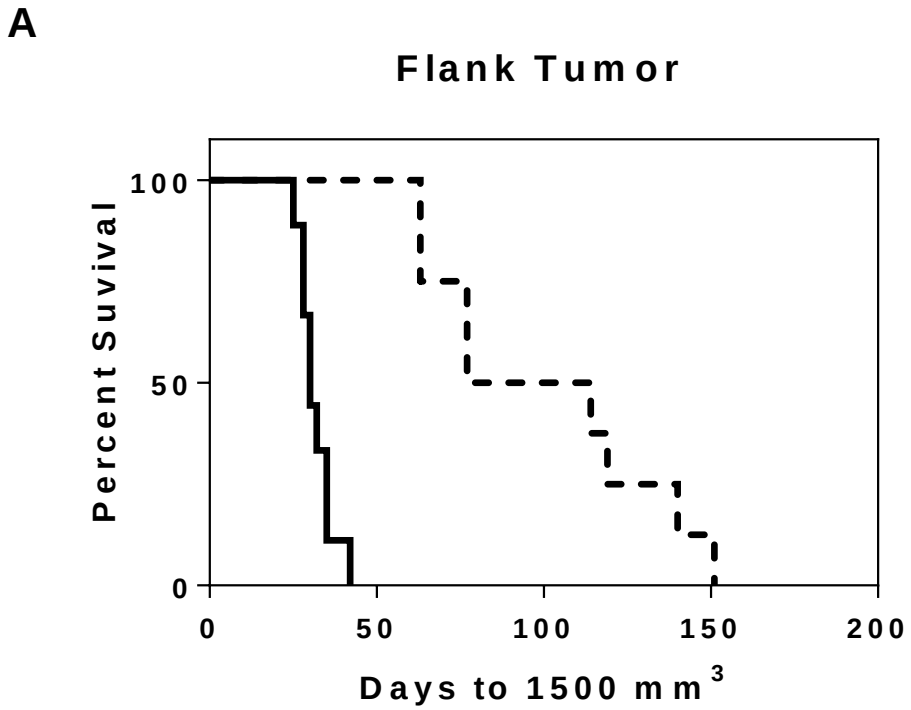

Figure 3.5.B: Efficacy of palbociclib therapy (150 mg/kg/day) in intracranial patient-derived xenograft (GBM22).

(B) Survival in GBM22 xenograft intracranial tumor model (n=10).

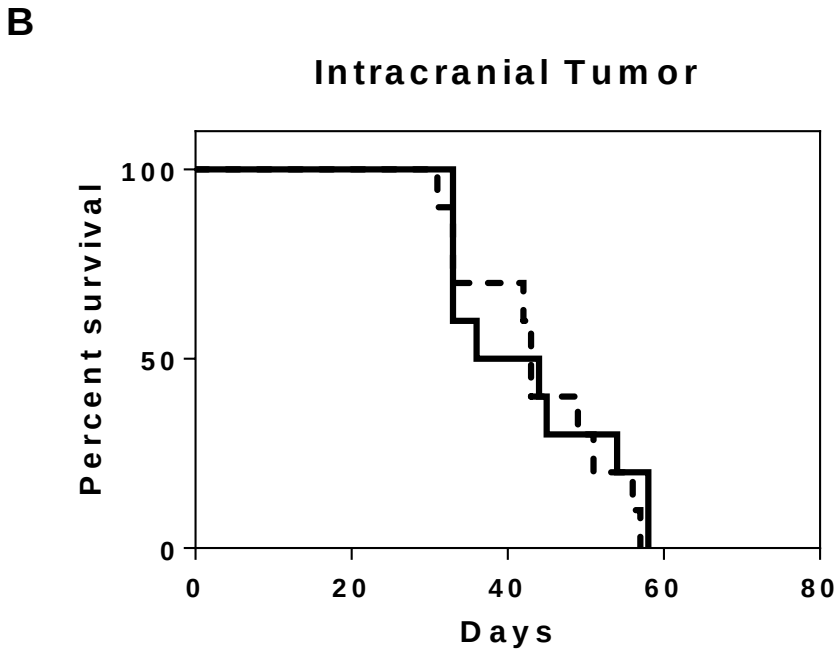

Figure 3.6.A: Flank tumor exposure to mimic brain delivery.

(A) Brain and flank tumor concentrations following either 10 (subcutaneous tumor) or 150 (brain) mg/kg oral dose (n=4);

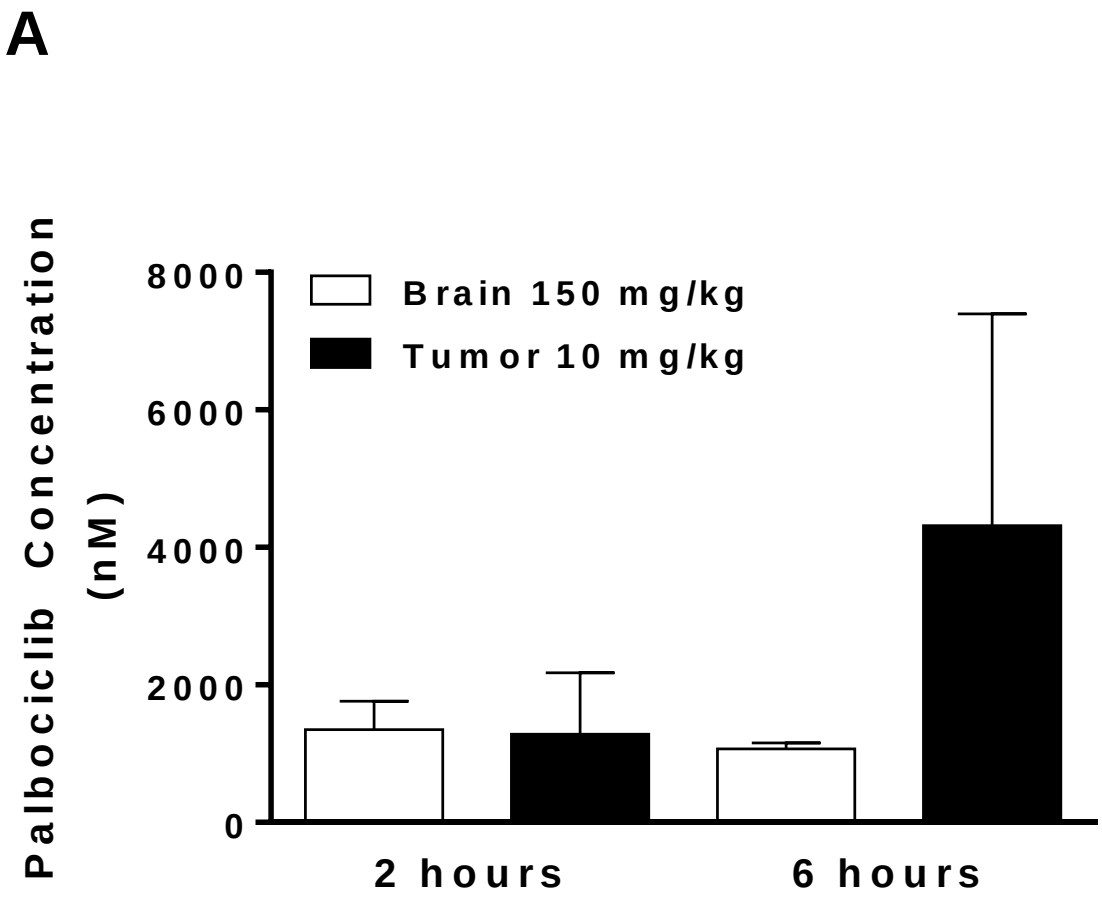

Figure 3.6.B: Flank tumor exposure to mimic brain delivery efficacy.

(B) Efficacy in GBM22 xenograft subcutaneous tumor with daily dosing of 10 mg/kg (n=8-10).

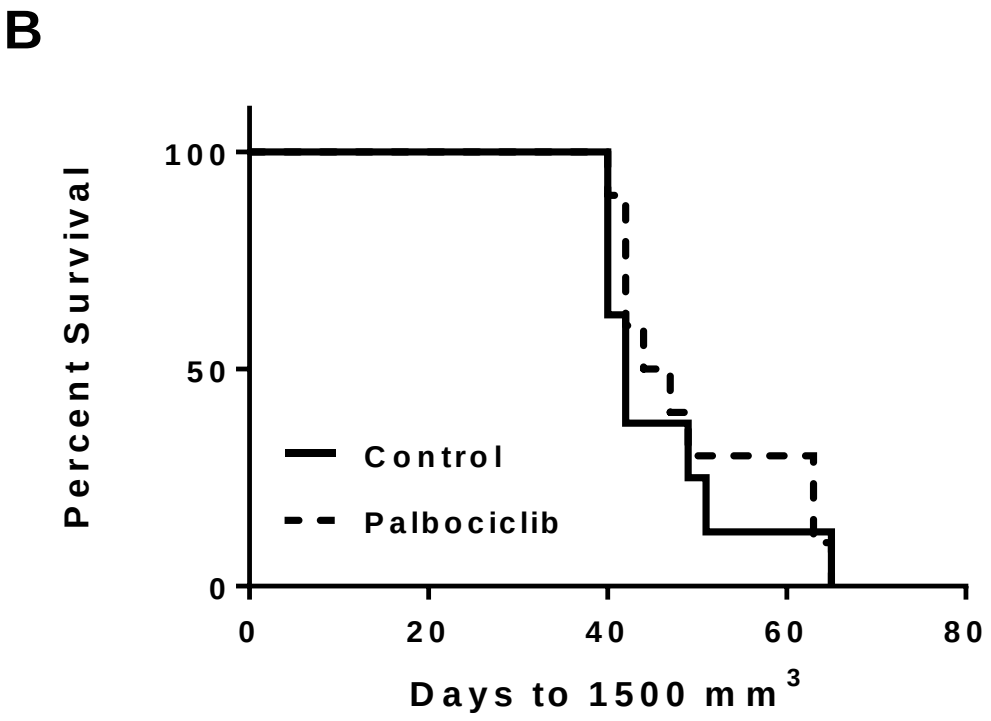

Figure 3.7.A: Effect of co-administration of elacridar, a dual inhibitor of P-gp and Bcrp, on the brain distribution of palbociclib.

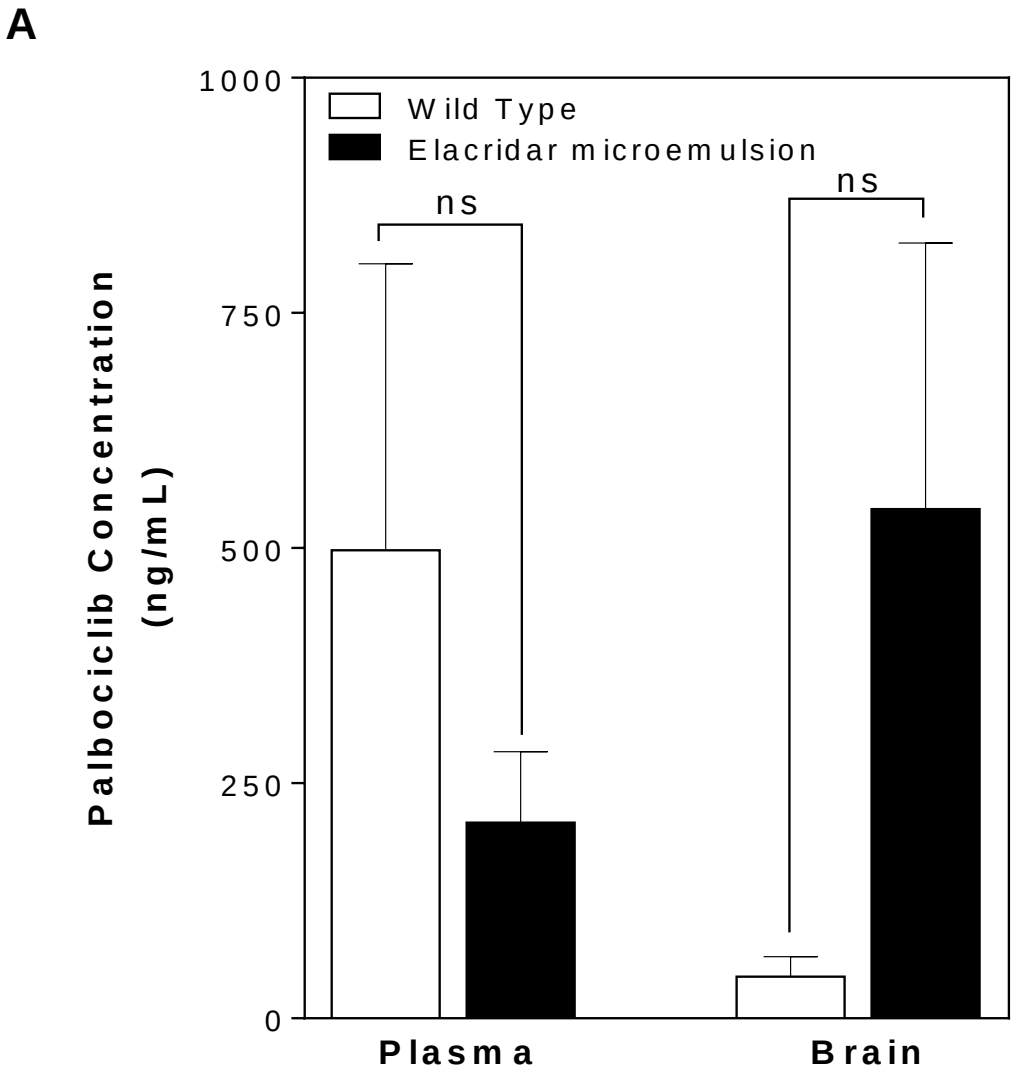

Figure 3.7.B: Effect of co-administration of elacridar, a dual inhibitor of P-gp and Bcrp, on the brain-to-plasma ratio of palbociclib.

(B) Brain-to-plasma ratio of palbociclib two hours post dose. (n=4-5).

B

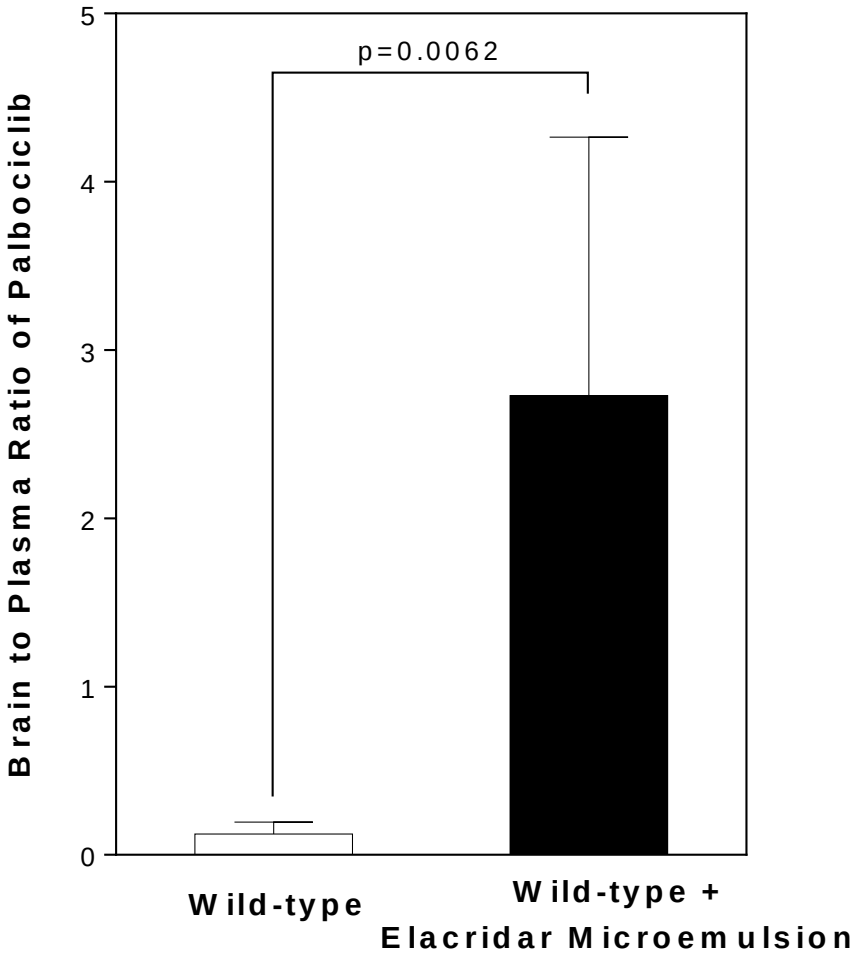

Table 3.1. Summary parameters from concentration-time profiles following 10 mg/kg oral dose.

Drug targeting index (DTI) = $(AUC_{brain}/AUC_{plasma})_{knockout}/(AUC_{brain}/AUC_{plasma})_{wild\text{-}type}$.

Strain	Plasma $t_{1/2}$ (hr)	Tissue	Cmax (μM)	AUC (μM*hr)	$\frac{AUC_{brain}}{AUC_{plasma}}$	DTI
Wild-type	1.5	Plasma	0.69 ± 0.3	4.5 ± 0.7	0.064	1.0
		Brain	0.047 ± 0.03	0.29 ± 0.05		
Bcrp1-/-	1.7	Plasma	1.27 ± 0.4	7.1 ± 0.9	0.14	2.2
		Brain	0.13 ± 0.02	0.99 ± 0.1		
Mdr1a/b-/-	2.4	Plasma	4.21 ± 2.4	11.9 ± 2.1	1.42	22
		Brain	1.91 ± 0.9	16.9 ± 1.7		
Mdr1a/b-/-Bcrp1-/-	2.1	Plasma	2.39 ± 1.3	11.4 ± 1.2	7.36	115
		Brain	8.9 ± 0.5	84.0 ± 6.1		

Table 3.2. Summary of steady-state concentrations.

Drug Targeting Index (DTI) = (Brain-to-plasma ratio)$_{knockout}$/(Brain-to-plasma ratio)$_{wild\text{-}type}$.

Strain	C_{ss} Plasma (nM)	C_{ss} Brain (nM)	Brain-to-Plasma Ratio	DTI
Wild-type	53.8 ± 63	3.82 ± 1.1	0.2 ± 0.07	1.0
Bcrp1$^{-/-}$	103 ± 57	32.3 ± 11	0.4 ± 0.1	2.0
Mdr1a/b$^{-/-}$	139 ± 35	315 ± 86	2.5 ± 0.1	12.5
Mdr1a/b$^{-/-}$*Bcrp1*$^{-/-}$	92.3 ± 49	2510 ± 1400	28 ± 6	140

CHAPTER IV

PHARMACOLOGICAL INHIBITION OF EFFLUX TRANSPORT AT THE BLOOD-BRAIN BARRIER IMPROVES DELIVERY OF PALBOCICLIB

ABSTRACT

Cyclin-dependent kinases (CDKs) are major regulators of the cell cycle and CDK4/6 play particularly important roles in G1-to-S phase cell cycle progression. Palbociclib is a potent CDK4/6 inhibitor that is currently approved for the treatment of breast cancer. Glioblastoma (GBM) is the most common primary brain tumor in adults and patients have limited treatment options following diagnosis. The CDK4/6 pathway is altered in over 75% of GBMs and is therefore an attractive target in the treatment of this devastating disease. Previous studies have demonstrated that palbociclib is effective in the treatment of GBM patient derived xenograft peripheral (non-brain) tumors, but ineffective in the treatment of orthotopic (intracranial) tumors, due in part to active efflux of palbociclib at the blood-brain barrier (BBB). The purpose of this study is to establish the relationship between pharmacological inhibition of BBB efflux transport and the brain delivery of palbociclib, monitor the tolerability of chronic pharmacological inhibition of BBB efflux transport, and evaluate the relationship between improved brain delivery and efficacy. Elacridar, a dual inhibitor of P-glycoprotein and breast cancer resistance protein, significantly improved the brain delivery of palbociclib. The brain-to-plasma ratio increased approximately 7-fold to 1.3 in the combination treatment group when compared with palbociclib monotherapy. Elacridar is well tolerated and had no adverse effect on body weight or ataxia as measured by rotarod. Furthermore, elacridar improved the brain delivery of palbociclib to the same concentrations previously observed in the flank tumor

model. Despite improved delivery, the palbociclib and elacridar combination therapy did not improve survival and did not provide a further reduction in phosphorylated-RB when compared with palbociclib monotherapy indicating that limited delivery is not the sole reason for the observed lack of efficacy in the intracranial GBM model.

4.1 INTRODUCTION

Cyclin-dependent kinases (CDKs) are major regulators of cell cycle control and CDK4 and CDK6 control G1-S phase cell-cycle progression (Asghar et al., 2015). This pathway is commonly altered in many solid tumors including breast cancer, melanoma and glioblastoma (GBM). Palbociclib is a potent CDK4/6 inhibitor that is approved for the treatment of metastatic breast cancer and is currently in clinical trials for other indications (Dickson, 2014; Finn et al., 2014; Dhillon, 2015). Previous reports by our group and others have demonstrated that palbociclib has limited brain delivery (de Gooijer et al., 2015; Parrish et al., 2015b). Furthermore, despite reducing tumor growth in a subcutaneous model of GBM, we have previously shown that this limited brain delivery resulted in limited efficacy in an orthotopic model of GBM (Parrish et al., 2015b). Importantly, the lack of efficacy observed in the model of GBM could be entirely explained by the limited delivery because the concentrations that were achieved in the brain also failed to provide a therapeutic response in the subcutaneous model (Parrish et al., 2015b).

GBM is the most common primary brain tumor in adults and the two-year survival is 30% following diagnosis (Ostrom et al., 2014). GBM is a particularly challenging type of cancer to treat because the tumor is able to grow in a protected environment behind the blood-brain barrier (BBB) (Parrish et al., 2015a). The BBB acts as both a physical and biochemical barrier to drug delivery

through tight junction proteins that prevent paracellular drug delivery and through efflux transporters that prevent transcellular drug delivery (Agarwal et al., 2011; Abbott, 2013). Numerous studies have demonstrated that following surgery, there are tumor cells that are “left behind” and in order to effectively treat GBM, it is crucial to deliver drugs to these tumor cells that are left behind, many of which reside behind an intact BBB (Berens and Giese, 1999).

Given that the limited brain delivery results in subtherapeutic palbociclib concentrations (Parrish et al., 2015b), strategies to improve the brain delivery are needed. Elacridar, a dual pharmacological inhibitor of P-gp and BCRP, may be used as a method to improve the treatment of GBM and overcome the limited brain delivery of palbociclib. The purpose of this study was to understand the relationship between delivery and efficacy of palbociclib treatment in a patient-derived xenograft model of GBM.

4.2 MATERIALS AND METHODS

All animal studies were approved by the Institutional Animal Care and Use Committees at either the University of Minnesota or the Mayo Clinic.

4.2.1 PALBOCICLIB AND ELACRIDAR COADMINISTRATION

Palbociclib was dosed at 150 mg/kg (PO; vehicle: pH 4 50 mmol/L sodium lactate) and elacridar was dosed in both male and female Friend leukemia virus strain B (FVB) mice at 1, 5, 10 and 20 mg/kg in a microemulsion formulation (IP; Cremophor EL, CaRBitol, and Captex 355::6:3:1, (Sane et al., 2013)). Two hours post dose, brain and whole blood samples were harvested (n=4). Plasma was isolated from whole blood by centrifugation (3500 rpm, 15 minutes) and samples were stored at -80˚C until analysis.

4.2.2 ELACRIDAR AND PALBOCICLIB TOLERABILITY FOLLOWING CHRONIC ADMINISTRATION

The tolerability of chronic administration of elacridar was evaluated in mice for 14 days at 5, 10 and 20 mg/kg (IP) in the microemulstion formulation. Prior to study initiation, mice were trained on the accelerating rotarod for three days before the baseline was recorded (Fairbanks et al., 2009). The benchmark for adequate performance on the rotarod was 300 seconds (Fairbanks et al., 2009; Stone et

al., 2014) and tested on days 4, 5, 9, 10, 15, and 16. In addition to rotarod performance, body weight was measured daily.

$$Latency\ to\ Fall\ (Normalized\ to\ \%\ Baseline) = \frac{Baseline - Experimental}{Baseline} \times 100$$

Following the chronic administration of elacridar, tolerability of the coadministration of elacridar and palbociclib was tested. Elacridar (PO; 10 mg/kg/day) was administered six hours before palbociclib (PO; 150 mg/kg/day). Two hours after the fifth dose of palbociclib, brain and whole blood samples were collected. Plasma was isolated from whole blood as described above and samples were stored at -80˚C until analysis.

4.2.3 PALBOCICLIB AND ELACRIDAR EFFICACY IN GBM22 XENOGRAFT

Survival studies in female athymic nude mice were conducted as described previously (Carlson et al., 2011; Pokorny et al., 2015). The patient-derived xenograft (PDX) GBM22 line was intracranially implanted from serial passages in the flank. Mice were anesthetized using ketamine (100 mg/kg) and xylazine (10 mg/kg) prior to tumor implantation (1 mm anterior and 2 mm lateral from the bregma). As previously described, GBM22 is sensitive to palbociclib both *in vitro* and in a subcutaneous model. Eight days following intracranial tumor implantation, mice were randomly assigned to one of four dosing regimens until moribund: vehicle control, palbociclib (150 mg/kg/day), elacridar (15 mg/kg/day),

or the combination of palbociclib and elacridar (n=10). Simultaneously, a separate group of mice were randomized to the same four treatment groups and dosed for nine days starting on day seventeen following tumor implantation. These mice were sacrificed two hours post the ninth dose of palbociclib and/or elacridar and samples were collected for LC-MS/MS or immunohistochemistry (IHC).

4.2.4 IMMUNOHISTOCHEMISTRY

Brain samples from mice with intracranial tumors were resected, placed in formalin, transferred to 70% ethanol, and then embedded in paraffin. Samples were sectioned at 5 µm thickness onto charged glass slides. Following rehydration, an unmasking solution (Vector Laboratories) was used to expose antigen epitopes. Hydrogen peroxide (3%) was used to remove peroxidase activity and blocking was conducted with 3% bovine serum albumin (BSA) overnight. Phospho-RB staining was performed with rabbit monoclonal antibody (dilution 1:150 in 1% BSA, Ser807/811, Cell Signaling Technologies) overnight. Following primary incubation, slides were washed with PBS before incubation with biotinylated goat anti-rabbit secondary antibody (1:200, Vector Laboratories) for 1 hour at room temperature. Slides were again washed with PBS and avidin/biotinylated enzyme complex conjugated to horseradish peroxidase (Vectastain Elite ABC kit, Vector Laboratories) was added for 30 minutes at room temperature. Following 2 washes with PBS, slides were treated with 3,3′-

diaminobenzidine (DAB) substrate (Vector Laboratories) and allowed to develop for 45 seconds. The slides were placed in water to stop the reaction and sections were counterstained with hematoxylin, dehydrated and mounted (Permount, Fisher Scientific). Images of each tumor-bearing animal (n=3-4) were taken on a Nikon AZ100M microscope (Melville, NY). Quantification of phosphorylated-RB was conducted in ImageJ. The IHC toolkit was used to locate positive DAB sites and six samples per tumor were quantified on the growing edge of the tumor.

4.2.5 LC-MS/MS

Elacridar plasma samples and palbociclib plasma and brain samples from FVB mice were analyzed as described previously (Sane et al., 2012; Parrish et al., 2015b). Brain samples from tumor-bearing athymic nude mice were sliced on a cryostat (Leica CM3050 S). Cresyl violet staining on 30 µm sections was used to determine tumor location in each sample. Brain samples were then sectioned at 300 µm and punch biopsies were used to sample regions of tumor core, tumor rim and normal brain tissue. Palbociclib was extracted from brain and tumor pooled punch biopsies through the addition of pH 11 buffer and ethyl acetate. Samples were vortexed and centrifuged (7500 rpm) and the supernatant was isolated and dried. Samples were then reconstituted in mobile phase and analyzed as described previously. A Phenomenex Synergi Polar 4 µ polar-RP 80 Å column (75 x 2 mm; Torrance, CA) with an AQUITY ultra performance liquid chromatography system (Waters, Milford, MA) was used for sample analysis.

The ionization was conducted in positive mode and the m/z transitions for palbociclib and dasatinib were 448.34-379.95 and 488.21-400.88, respectively. The mobile phase was 73:27::1 mM ammonium formate with 0.1% formic acid: acetonitrile was delivered at 0.25 mL/min.

4.2.6 STATISTICAL ANALYSIS

GraphPad Prism 6.04 (San Diego, CA) was used for statistical analysis and data is represented as the mean ± SD. Comparisons between two groups were made using an unpaired *t* test, and multiple comparisons were made using one-way analysis of variance using Bonferonni's multiple comparison test.

4.3 RESULTS

4.3.1 ELACRIDAR IMPROVES THE BRAIN DELIVERY OF PALBOCICLIB

Elacridar was delivered in increasing doses with palbociclib and brain samples were collected two hours post dose. Although there was no significant increase in brain delivery when elacridar was dosed at 1, 5, or 10 mg/kg IP, due in part to variability in the plasma concentrations of elacridar, elacridar at 20 mg/kg IP significantly improved the brain-to-plasma ratio of palbociclib two hours post dose (**Figure 4.1.A**). The brain-to-plasma ratio of palbociclib increased as a function of the plasma concentration of elacridar; the brain delivery of palbociclib reached a maximal brain-to-plasma ratio of 1.3 that was achieved when the plasma concentration was 1 µg/mL or higher (**Figure 4.1.B**). This is a five-fold increase in the brain-to-plasma ratio in the palbociclib monotherapy treatment group. Two hours following palbociclib administration (150 mg/kg), flank tumor concentrations were approximately 50 µM which is comparable to the concentrations achieved in the elacridar treated group.

4.3.2 CHRONIC ADMINISTRATION OF ELACRIDAR IS WELL TOLERATED

Chronic alteration of the BBB may have adverse side effects and elacridar, a dual inhibitor of P-gp and BCRP at the BBB, could alter BBB transport in such a way that the side effects are detrimental to the therapy and/or the patient. Since

chronic administration of elacridar would affect transport at the BBB, the effect of daily elacridar doses was examined by rotarod and changes in body weight. Elacridar was dosed at 5, 10 and 20 mg/kg/day for two weeks in FVB mice. There were no outward signs of toxicity and no significant changes in body weight over the two weeks of dosing (**Figure 4.2.A**). Rotarod was used to measure ataxia and 300 seconds was used as the baseline. There were no observable changes in ataxia as measured by rotarod at any dose of elacridar examined (**Figure 4.2.B**) indicating that elacridar is well tolerated for chronic administration.

The combination of elacridar and palbociclib for five days was examined in FVB mice. There were no significant changes in body weight over the five days of dosing (**Figure 4.3.A**) and the average plasma concentration two hours following the fifth dose of palbociclib was 17.8 ± 8.7 μM in the palbociclib alone group and 12.2 ± 2.0 μM in the combination group (**Figure 4.3.B**, p=0.25). The brain concentration of palbociclib increased approximately five-fold in the elacridar treated group and resulted in a six-fold increase in the brain-to-plasma ratio (**Figure 4.3.C**, p=0.0495).

4.3.3 ELACRIDAR AND PALBOCICLIB COMBINATION THERAPY IN TUMOR-BEARING MICE

In athymic nude mice, elacridar was dosed at 15 mg/kg to ensure that the plasma concentrations were sufficient to significantly increase the brain delivery of palbociclib. The dosing levels of palbociclib and elacridar were the maximum tolerated doses in order to maximize the effect. The body weight did not significantly change over the nine days of dosing (**Figure 4.4.A**). Brain and plasma samples were removed two hour after the ninth dose of palbociclib and elacridar. Half of the brain samples were flash frozen for LC-MS/MS analysis and half were paraffin embedded for IHC. Flash frozen samples were sliced on the cryostat at 30 µm for cresyl violet staining to determine tumor location and 300 µm for punch biopsies (2.5 mm diameter) (**Figure 4.5**). Regional samples were taken from the tumor core, normal brain (**Figure 4.5.C**), and tumor rim samples which were adjacent to the tumor core region. These samples were pooled together across 300 µm slices and analyzed via LC-MS/MS. The tumor rim and tumor core had significantly higher levels of palbociclib than the normal brain in both the palbociclib monotherapy and combination treatment groups (**Figure 4.4.B-C**). Elacridar significantly improved the brain delivery of palbociclib to these regions and palbociclib levels are comparable to the levels achieved in the flank tumor that provided a therapeutic benefit (**Figure 4.4.B**). IHC analysis from this study demonstrated a significant reduction in phospho-RB in both palbociclib and the combination treatment groups (**Figure 4.6**). Although there was a reduction in phospho-RB in the palbociclib treated group, there was no further effect in the combination treatment group (**Figure 4.7**). The improved brain delivery of

palbociclib through pharmacological inhibition of efflux transport did not correspond to improved survival (**Figure 4.8**).

4.4 DISCUSSION

The CDK4/6 pathway is frequently altered in GBM and it is an attractive therapeutic target in the treatment of this devastating disease (2008; Peyressatre et al., 2015). Previous studies have demonstrated that palbociclib, a potent CDK4/6 inhibitor, has limited brain delivery due to active efflux transport at the BBB (de Gooijer et al., 2015; Parrish et al., 2015b; Raub et al., 2015). Furthermore, we have previously reported that the palbociclib concentration achieved in the brain is subtherapeutic in the treatment of a GBM subcutaneous tumor (Parrish et al., 2015b). Therefore, there is a clear rationale for developing treatment modalities that increase the delivery of palbociclib to the brain in order to explore the relationship between delivery and efficacy in an orthotopic (intracranial) model of GBM. Pharmacological inhibition of BBB efflux transporters is one method to enhance the brain delivery of therapeutic agents (Sane et al., 2013).

Elacridar improved the brain delivery of palbociclib and this was a saturable effect, where the maximum brain-to-plasma ratio of palbociclib was 1.3. Since elacridar affects the BBB, which is fundamentally important in protecting the brain, the effect of elacridar on balance, coordination and motor status over a chronic dosing regimen was explored. Elacridar caused no observable changes in body weight or ataxia, indicating that elacridar is tolerated in long-term dosing. Furthermore, coadministration of elacridar and palbociclib also caused no

significant changes in body weight and significantly improved the brain delivery of palbociclib when compared to palbociclib monotherapy. The concentrations of palbociclib achieved in the brain following elacridar and palbociclib coadministration were similar to the concentrations of palbociclib achieved in a flank tumor model. These concentrations of palbociclib provided a therapeutic benefit in the flank tumor model. Therefore, a study was designed that would look at palbociclib concentration, pharmacodynamic effect (phospho-RB), and survival.

As anticipated, the regional distribution of palbociclib was higher in the core of the tumor than in the normal brain, indicating that the integrity of the BBB is compromised in the tumor core (Agarwal et al., 2013; Vartanian et al., 2014). Furthermore, the brain delivery was significantly improved in the elacridar treated group in all regions of the brain. The brain concentrations achieved in this study mimicked the flank tumor concentrations of palbociclib that provided a therapeutic benefit. The phospho-RB was reduced on in both groups treated with palbociclib (combination and monotherapy), however there was no further reduction in phospho-RB in the combination treated group when compared with the palbociclib monotherapy. Palbociclib did provide a modest improvement in survival GBM6, another patient-derived xenograft that is sensitive to palbociclib therapy (Cen et al., 2012). In this model, phospho-RB was reduced to approximately 20% of the vehicle control (Cen et al., 2012), compared with approximately 50% in this study. Consequently, despite the improved delivery,

there was no increase in the measured pharmacodynamic effect or overall survival in the palbociclib and elacridar combination therapy group.

A few potential reasons for the observed disconnect between the flank and intracranial efficacy were not looked at in the present study. One possible explanation is that the delivery of palbociclib to the specific target site within the tumor cells may be inadequate. While we do see a reduction in phospho-RB, it was not correlated to palbociclib delivery. In order to look at this question, we would need to look at the reduction in phospho-RB in flank tumor samples to determine if the extent of phospho-RB reduction is different even if the palbociclib concentrations are similar. Another possible reason for the lack of efficacy in the intracranial model is that the drivers of tumor growth may be different depending upon tumor location. It may be that the differences between the conditions in the flank tumor and brain tumor will need to be better understood. This study demonstrates that a flank tumor comprised of GBM cells is not the same as the same GBM cells in the brain. This study indicates that subcutaneously implanting GBM cells may not be a good screening technique. The lack of a BBB has been discussed previously (de Vries et al., 2009), but the idea that a tumor comprised of GBM cells may respond differently to similar concentrations of a therapeutic agent depending on tumor location has not yet been explored.

This study demonstrates that GBM cells implanted into the flank do not adequately represent a brain tumor without a BBB. Studies have shown that in

metastatic disease, there can be changes that occur and the tumor cells found in the brain are not identical to the tumor cells in the periphery (Da Silva et al., 2010; Svokos et al., 2014). Breast cancer brain metastases, for example, were found to have increased expression of enzymes that are involved in glycolysis and oxidative phosphorylation pathways (Chen et al., 2007). These results indicate that tumor cells in the brain have either adapted or been selected for their ability to use glucose oxidation for energy. It is possible that subcutaneous implantation of GBM xenograft cells has the opposite effect; rather than selecting or adapting for brain growth, the tumor cells may be selecting and adapting for non-brain growth. The other possibility is that the tumor cells have not adapted for non-brain growth and that is one of the reasons that the subcutaneous tumor was more sensitive to palbociclib therapy. It is possible that either of these changes could have caused the lack of efficacy of palbociclib therapy despite improved delivery.

Another reason for the differences in efficacy in the subcutaneous and intracranial tumor models could be tumor size. The primary endpoint in flank studies is time to reach a specific tumor volume, for example 1500 mm^3. This volume is about three times the size of a mouse brain and well over six times larger than the largest brain tumor observed in this study. Therefore, the differences in efficacy in the flank and intracranial studies could be due to tumor size. Previous studies have demonstrated that hypoxia is correlated to both subcutaneous and intracranial tumor size and larger tumors have lower oxygen

levels (Wang et al., 2003). In addition to the relationship between tumor size and oxygen levels, the microenvironment also plays a role. The hypoxia-responsive transcription factor HIF-1α is the major regulator of growth in response to hypoxic conditions and has been shown to be altered in GBM (Mayer et al., 2012). Previous studies have reported that the loss of HIF-1α slows tumor growth and progression in various tumors, mainly by reducing vascular density (Maxwell et al., 1997; Ryan et al., 1998). A study that explored HIF-1α changes in astrocytomas found that HIF-1α response was dependent on the microenvironment (Blouw et al., 2003). These studies found that the effect of the loss of HIF-1α was dependent on tumor location. In the brain, tumors that lacked HIF-1α were more invasive, but these same tumors were less invasive in the flank (Blouw et al., 2003). This demonstrates that the invasive nature of tumors can be dependent on the microenvironment and reinforces the need for an accurate preclinical model when assessing treatment regimens. In another study, the expression of antigens was found to be affected by the tumor location (Alonso-Camino et al., 2014). These studies indicate that the cellular pathways that drive tumor growth are likely dependent on tumor location. Taken together, there is growing evidence that subcutaneous tumor growth may not replicate intracranial tumor growth. In studying brain tumors, it will be important to find models that replicate the tumor growth pattern that is observed in the human disease.

Drug delivery is a major challenge in the treatment of brain tumors, however these studies suggest that delivery may not be the entire problem. These results, along with literature reports, demonstrate the importance of having adequate models to examine efficacy of experimental therapeutics in the treatment of brain tumors. Subcutaneous models are likely missing important components that preclude efficacy and improving the understanding of the complex nature of brain tumors will be essential in developing preclinical and clinical trials that improve efficacy.

Figure 4.1.A: Elacridar improves the brain delivery of palbociclib.

(A) Brain-to-plasma ratio of palbociclib (150 mg/kg) two hours following p.o. dose of palbociclib and i.p. dose of elacridar (1, 5, 10 or 20 mg/kg), ** indicates $p<0.01$.

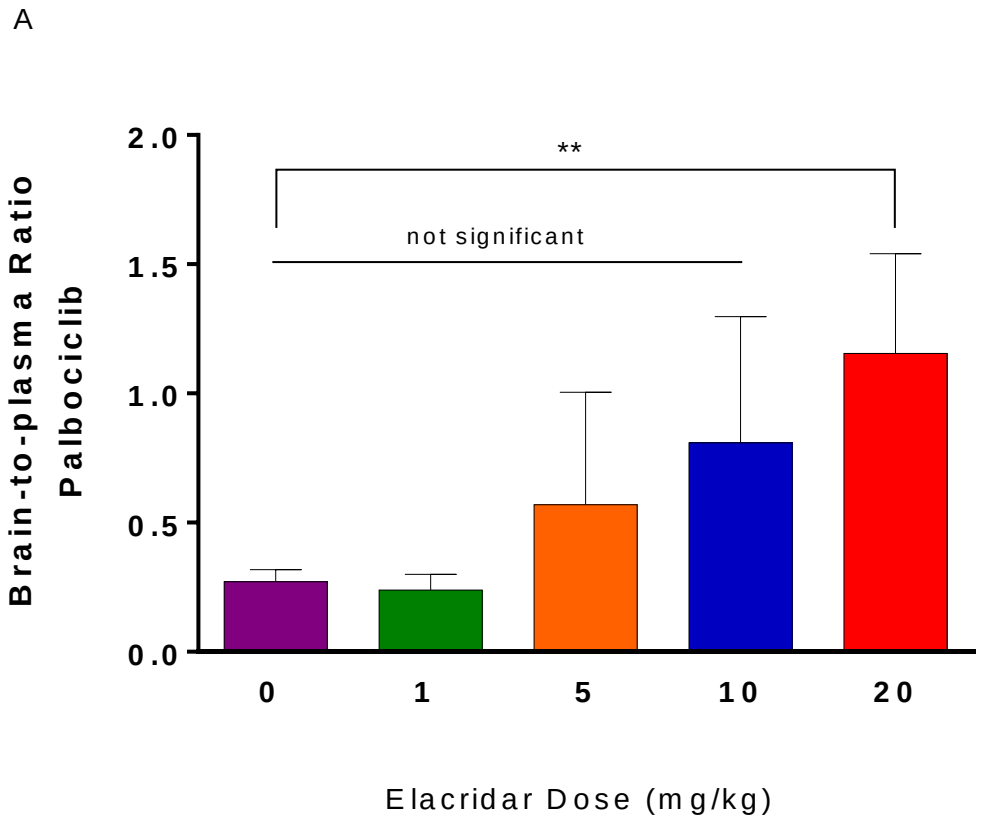

Figure 4.1.B: Palbociclib brain-to-plasma ratio as a function of elacridar plasma concentration.

B

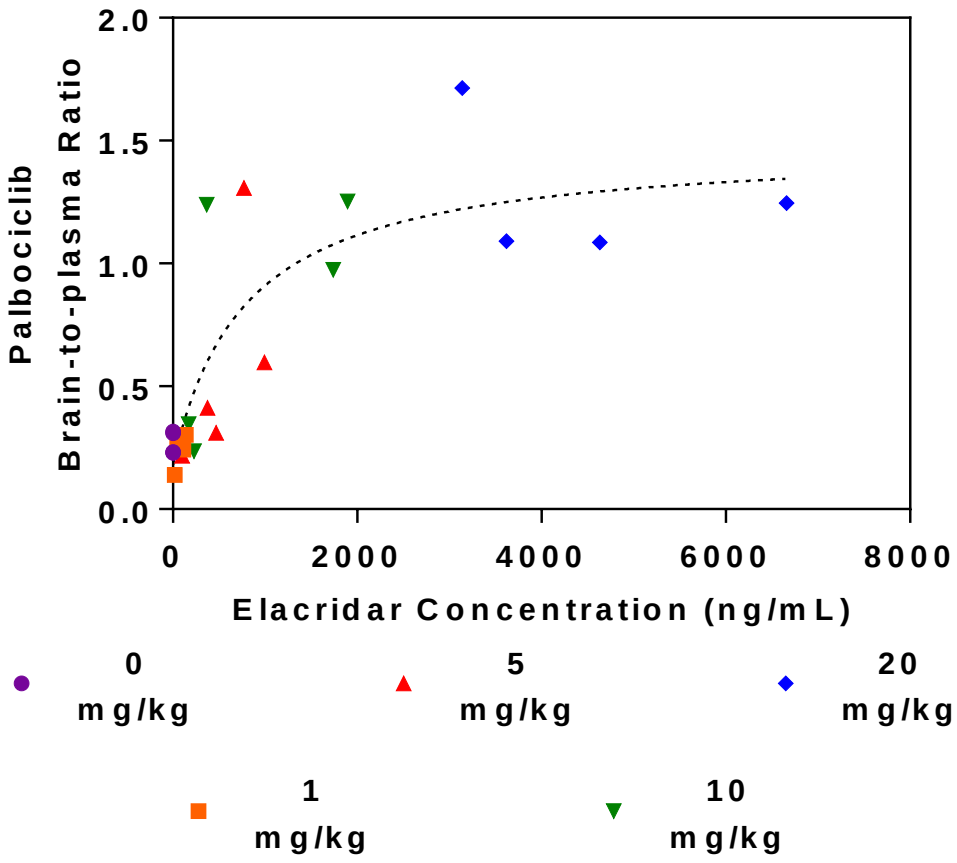

Figure 4.2.A: Body weight to measure tolerability of chronic elacridar treatment.

(A) Body weight measurements during two weeks of elacridar administration (i.p.), n=4-5 per group.

A

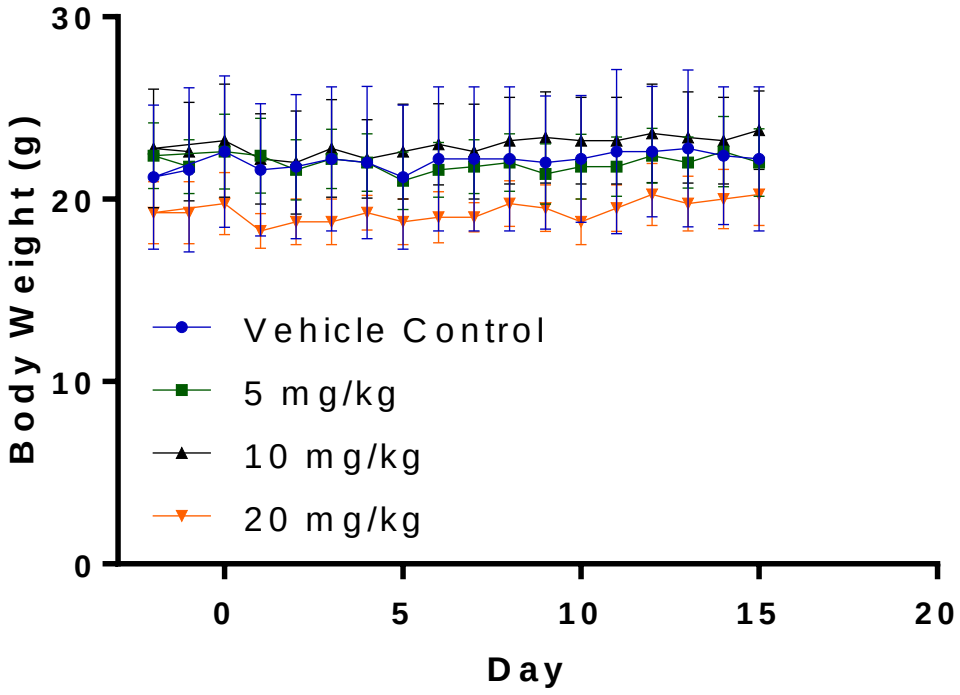

Figure 4.2.B: Latency to fall as a measure of tolerability of chronic elacridar treatment.

(B) Latency to fall measurements by rotorod (300 seconds was used as baseline), n=4-5 per group.

B

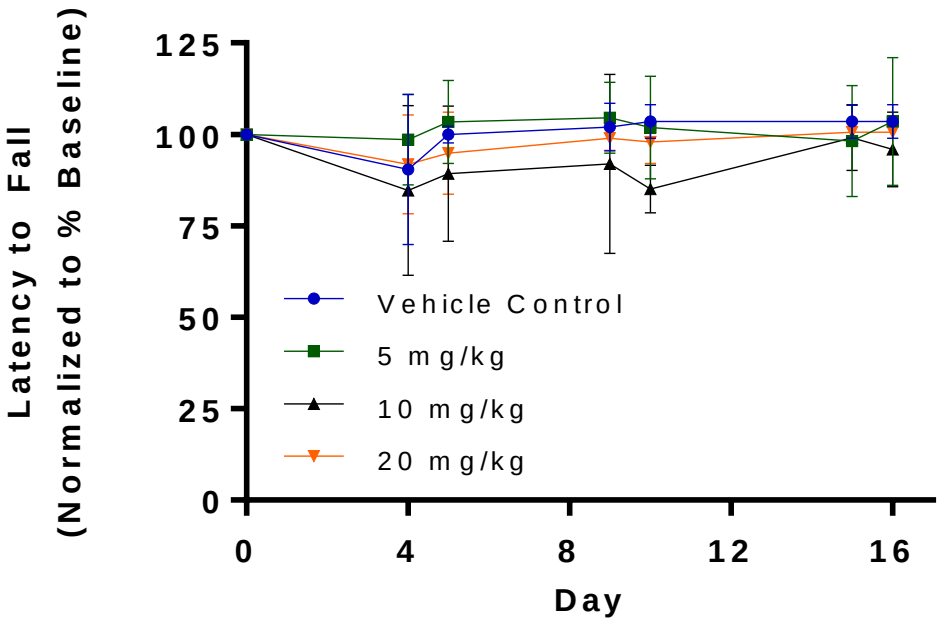

Figure 4.3.A: Chronic administration of elacridar (10 mg/kg and palbociclib (150 mg/kg) is tolerated in FVB mice.

(A) Body weight measurements during 5 days of palbociclib and elacridar administration in FVB mice, n=5.

A

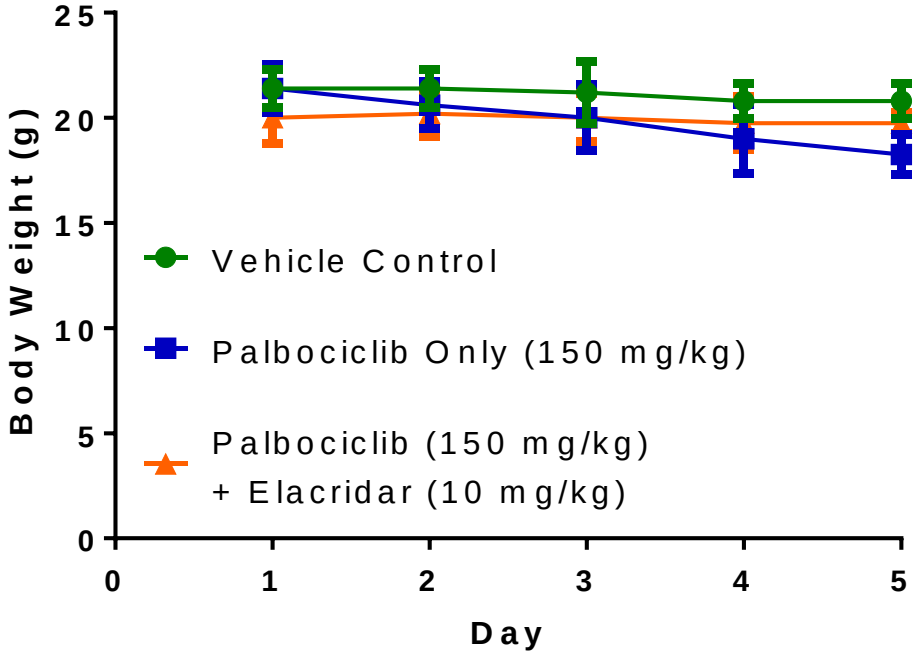

Figure 4.3.B: Chronic administration of elacridar (10 mg/kg and palbociclib (150 mg/kg) is tolerated in FVB mice - brain distribution.

(B) Brain and plasma concentrations two hours following the fifth dose of palbociclib, ns=not significant, n=5.

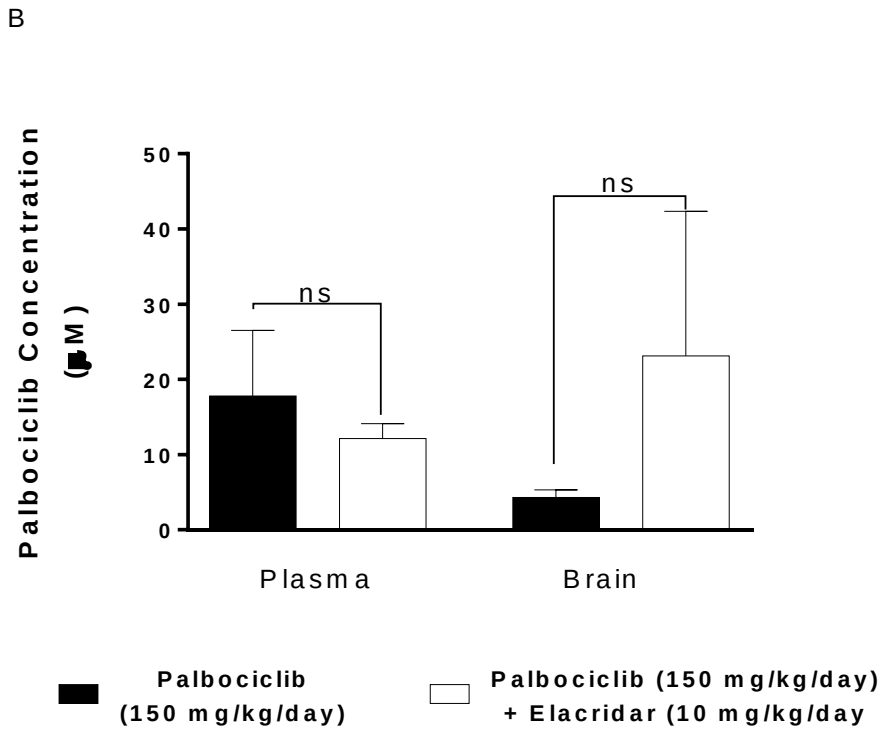

Figure 4.3.C: Chronic administration of elacridar (10 mg/kg and palbociclib (150 mg/kg) is tolerated in FVB mice – brain-to-plasma ratio.

(C) Brain-to-plasma ratio of palbociclib, n=5.

C

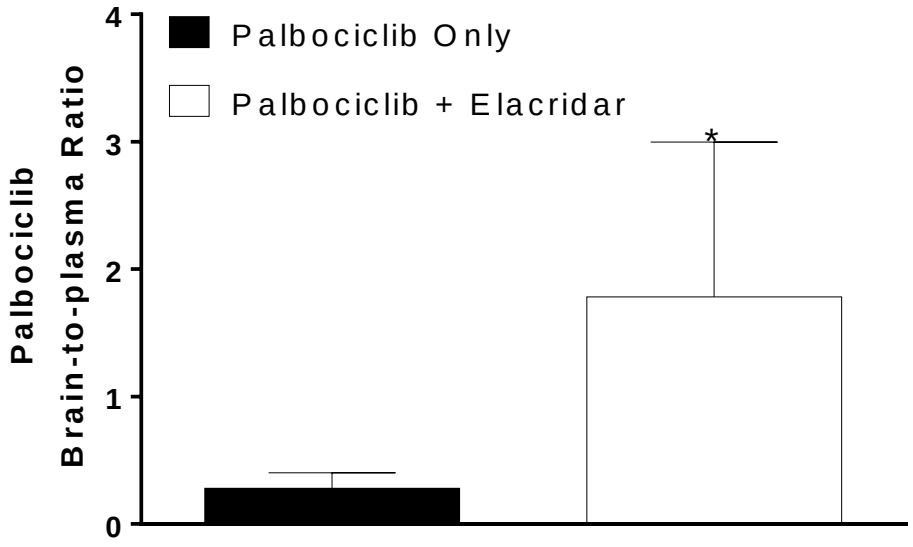

Figure 4.4.A: Tolerability and regional brain and tumor delivery of palbociclib – body weight.

(A) Body weight was measured during treatment to monitor tolerability of therapy in athymic nude mice, n=8-10.

A

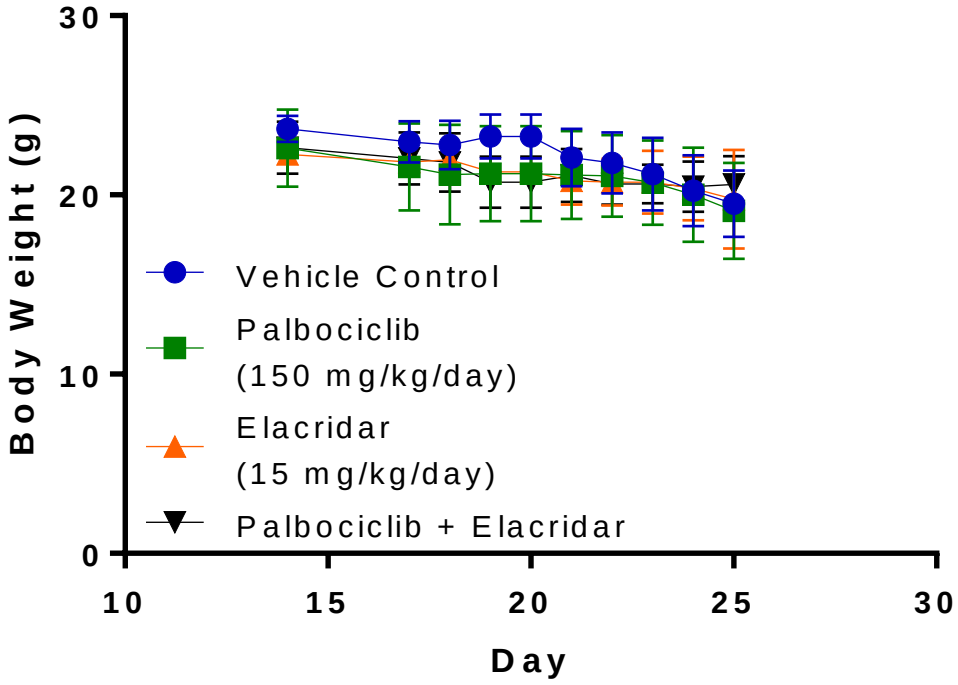

Figure 4.4.B: Tolerability and regional brain and tumor delivery of palbociclib – palbociclib concentrations.

(B) Palbociclib concentrations in normal brain, tumor rim, tumor core and plasma, * and **** indicate p<0.05 and p<0.0001, respectively, n=4-10.

B

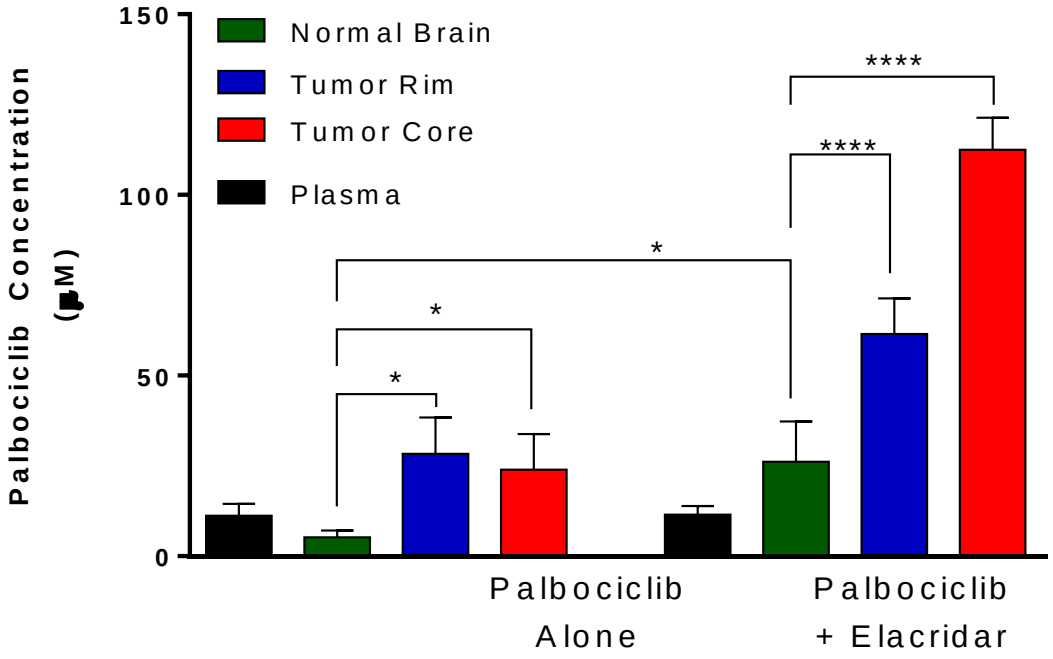

Figure 4.4.C: Tolerability and regional brain and tumor delivery of palbociclib – brain-to-plasma or tumor-to-plasma ratio.

(C) Palbociclib brain-to-plasma ratio or tumor-to-plasma ratio, *, **, and *** indicate $p<0.05$, $p<0.01$ and $p<0.001$, respectively, n=4-5.

C

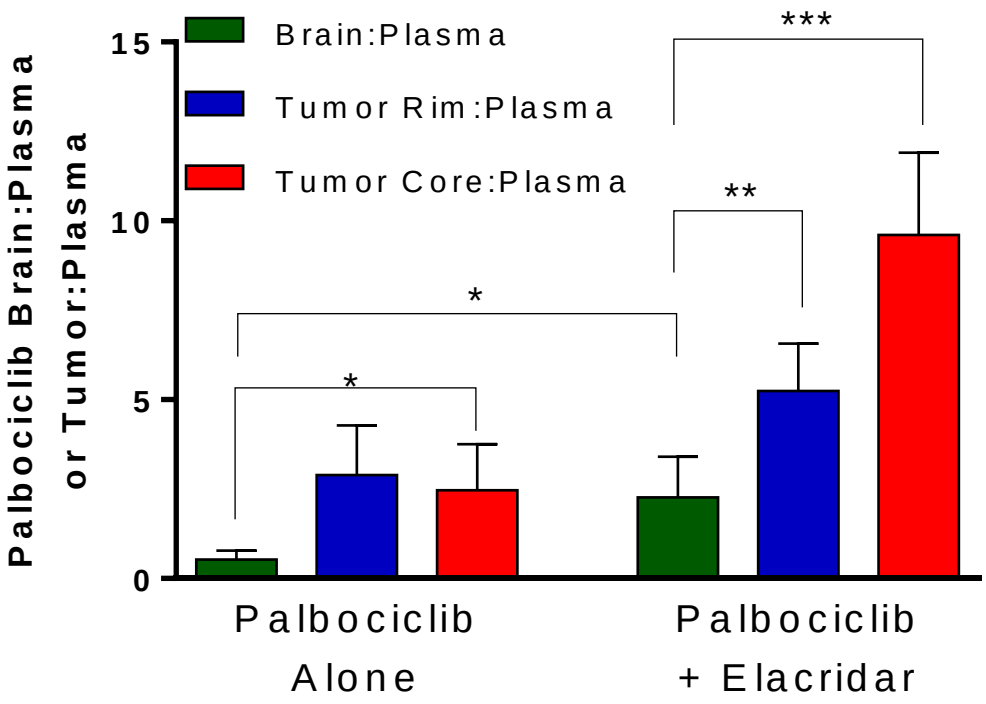

Figure 4.5: Punch biopsies to evaluate regional distribution of palbociclib.

Cresyl violet was used to determine tumor location (A, B) and 2.5 mm diameter punch biopsies were used to sample tumor core, tumor rim, and normal brain (C).

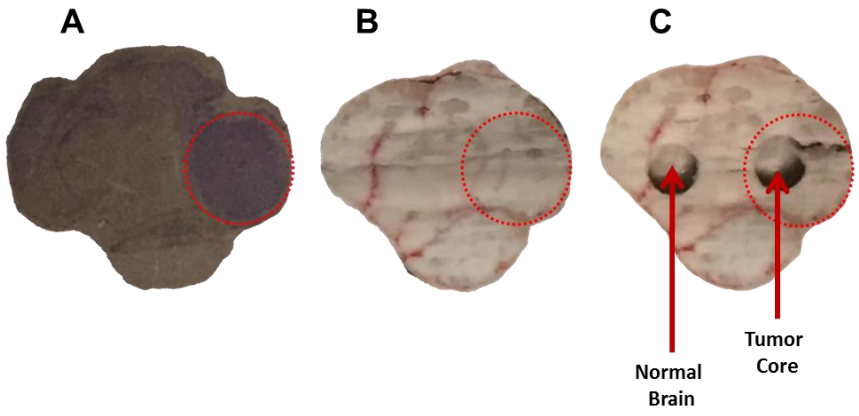

Figure 4.6: Immunohistochemistry to evaluate changes in phospho-RB in treatment groups.

Phospho-RB in vehicle control, elacridar (15 mg/kg/day), palbociclib (150 mg/kg/day) and combination treatment groups.

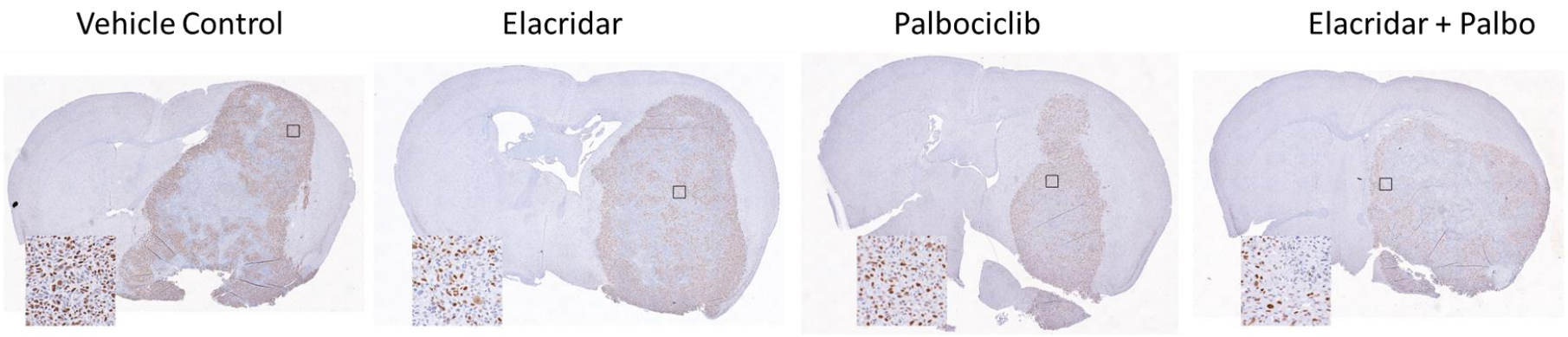

Figure 4.7: Quantification of phospho-RB from IHC analysis

Phospho-RB from IHC samples was quantified using ImageJ and normalized to vehicle control, n=2-4.

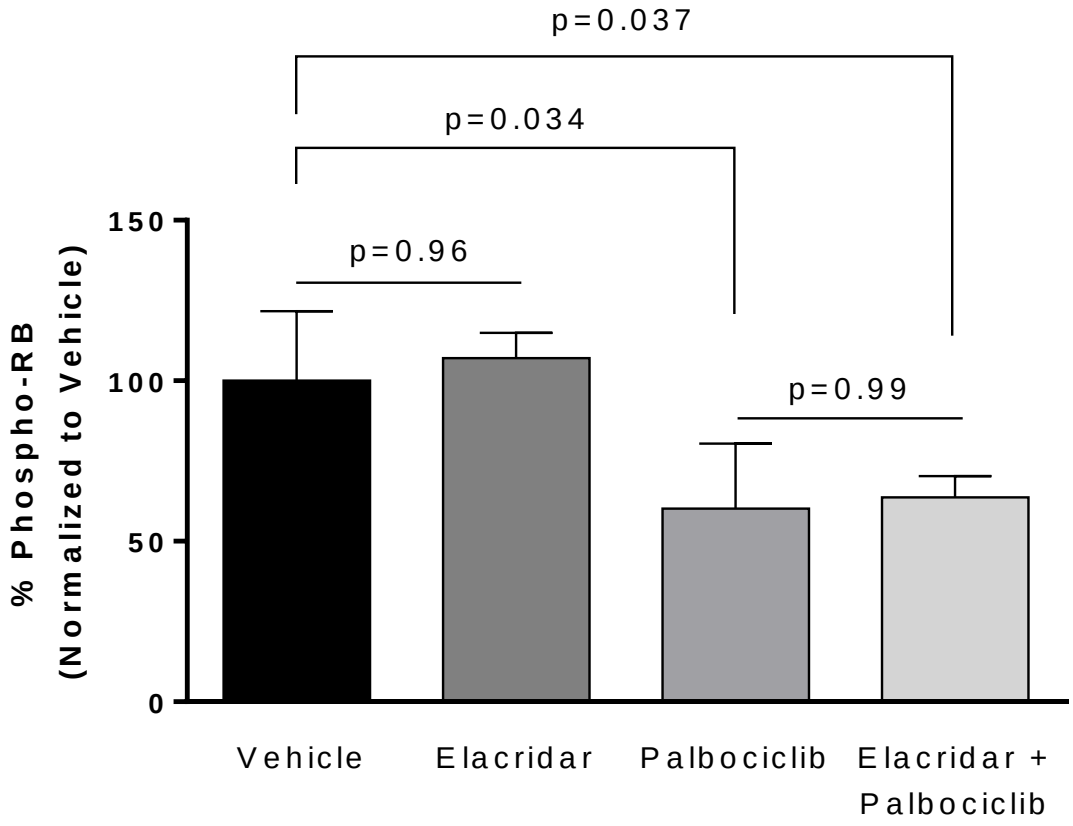

Figure 4.8: Efficacy of palbociclib (150 mg/kg/day) and elacridar (15 mg/kg/day) in patient derived xenograft (GBM22) intracranial model, n=10.

Figure 8

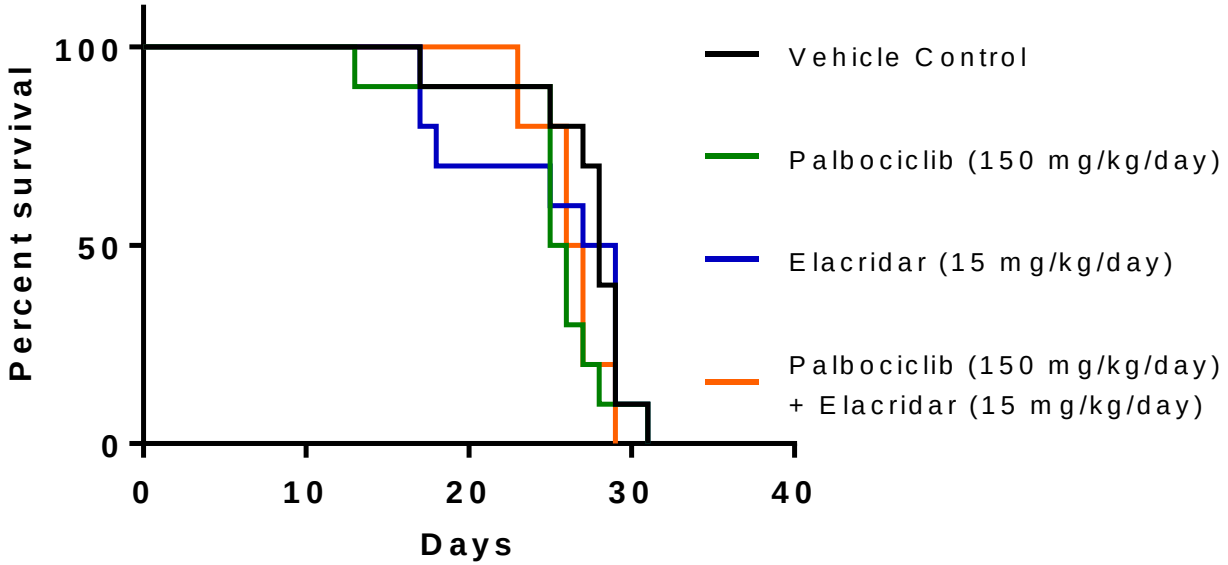

CHAPTER V

CHARACTERIZATION OF THE ROLE OF TRANSPORT AT THE BLOOD-BRAIN BARRIER FOR PALBOCICLIB, RIBOCICLIB AND ABEMACICLIB USING THE *IN SITU* BRAIN PERFUSION TECHNIQUE

ABSTRACT

Preclinical studies were conducted to compare the brain delivery of three CKD4/6 inhibitors that are currently undergoing clinical trials for various solid tumors. Palbociclib, ribociclib and abemaciclib all inhibit CDK4 and CDK6 with nanomolar affinities and have great potential for clinical use in the treatment of cancers such as breast, glioblastoma (GBM), and melanoma. Plasma and brain concentrations following a 48 hour infusion (10 µg/hr) demonstrate that P-glycoprotein (P-gp) and/or breast cancer resistance protein (BCRP) are involved in limiting the brain delivery of all three CDK4/6 inhibitors. Additional *in situ* brain perfusion studies indicate that transporters are involved in the brain distribution of palbociclib, ribociclib and abemaciclib. For all three CDK4/6 inhibitors, there is a suggestion that an uptake transporter may be involved in enhancing the brain delivery when the perfusate concentration is at 100 nM. The uptake process may be saturated at higher concentrations and efflux transporters reduce the transfer coefficient (K_{in}) for brain uptake. Both ribociclib and palbociclib show no evidence of efflux transporter saturation, however the results suggest that abemaciclib may be able to saturate efflux and has an increased K_{in} when the perfusate concentration increases. A simple pharmacokinetic model was developed to demonstrate that an uptake transporter and changes in efflux transport affinity could be responsible for the observed experimental distribution profiles.

5.1 INTRODUCTION

Treatment options for primary and secondary brain tumors remain limited and, due the aggressive nature of most brain tumors, diagnosis is almost always lethal (Ostrom et al., 2014). Current treatment of primary and metastatic disease often entails a combination of local or whole-brain radiation, steroids, surgery, and chemotherapy; however these treatments have provided only a modest improvement in survival (Cloughesy et al., 2014). Lung, breast, and melanoma are the three cancers with the highest likelihood to metastasize to the brain and all three cancers commonly have mutations in the cyclin-dependent kinase (CDK) 4/6 pathway (Asghar et al., 2015; Lin and DeAngelis, 2015). Clinical trials are currently examining the CDK4/6 inhibitors abemaciclib, ribociclib and palbociclib for the treatment of non-small cell lung cancer (NSCLC), melanoma, breast cancer, glioblastoma and a variety of other solid tumors (Sánchez-Martínez et al., 2015). One problem in the treatment of brain tumors is that the tumors remain both unseen and untreated at early stages of tumor development (Parrish et al., 2015a).

One reason for the limited efficacy of current therapeutic options in the treatment of brain tumors is the lack of delivery to tumor cells that reside behind an intact blood-brain barrier (BBB) (Agarwal et al., 2011). At early stages of tumor metastasis as well as at the leading edge of invasive glioblastomas, tumor cells are protected from therapy by the BBB (Oberoi et al., 2015). The BBB provides

both a physical and function barrier to brain delivery and P-glycoprotein (P-gp) and breast cancer resistance protein (BCRP) are two transporters at the BBB that actively transport compounds back into systemic circulation (Sasongko et al., 2005; Uchida et al., 2011; Agarwal et al., 2012). In addition to these two efflux transporters, there are a variety of other transporters that are involved in maintaining the highly regulated environment necessary for efficient neuron function (Abbott, 2013). Influx transporters, for example, are important in the transport of glucose (GLUT1), amino acids (large-neutral amino acid transporter; LAT1), short-chain fatty acids such as lactic acid (monocarboxylate transporters, MCT), organic anions (organic anion transporters, OAT) and cations (organic cation transporters, OCT) (Tamai and Tsuji, 2000; Stenehjem et al., 2009). The *in situ* brain perfusion technique is one approach to understand the role of transport at the BBB in the brain delivery of compounds. In this technique, the brain is perfused with a known concentration of drug over a set interval and transport at the BBB can be evaluated (Smith, 1996; Smith and Allen, 2003; Thomas et al., 2009).

Previous studies have shown that palbociclib has limited brain delivery due to the efflux activity of P-gp and BCRP at the BBB (de Gooijer et al., 2015; Parrish et al., 2015b; Raub et al., 2015) and that abemaciclib, although it is a substrate for efflux transport, has been shown to have enhanced brain delivery due to saturation of BBB efflux transport (Raub et al., 2015). Currently, there are no literature reports about the brain delivery of ribociclib. With this in mind, the

purpose of this study is to understand the role of BBB transporters in the brain delivery of palbociclib, ribociclib and abemaciclib, three CDK4/6 inhibitors that are currently undergoing clinical trials for the treatment of cancers with a high propensity to metastasize to the brain. These studies are intended to provide a means to compare the brain distribution of palbociclib, ribociclib and abemaciclib. Increasing the understanding of the relative brain delivery of these three CDK4/6 inhibitors may guide the clinical development of these compounds for the treatment of primary and metastatic brain tumors.

5.2 METHODS

5.2.1 CHEMICALS AND REAGENTS

Palbociclib (PD-332991) was purchased from ChemieTek (Indianapolis, IN), ribociclib (LEE-011) was purchased from ActiveBiochem (Maplewood, NJ), and abemaciclib (LY2835219) was purchased from Selleckchem (Houston, TX). Dasatinib was purchased from LC Laboratories (Woburn, MA). All other chemicals were purchased from Sigma-Aldrich (St. Louis, MO).

5.2.2 ANIMALS

All animal studies were conducted in Friend leukemia virus B (FVB) male and female mice that were 8-12 weeks old at the time of the experiment. Wild-type (WT) and *Mdr1a/b*$^{-/-}$*Bcrp1*$^{-/-}$ (triple knockout; TKO) mice (Taconic Farms, Germantown, NY) were maintained in a 12-hour light/dark cycle with unlimited access to food and water. All studies were approved by the Institutional Animal Care and Use Committee at the University of Minnesota.

5.2.3 CONSTANT RATE INFUSION (48 HOUR) BRAIN DISTRIBUTION

Alzet osmotic mini pumps (1003D; Durect Corporation, Cupertino, CA) were implanted in the peritoneal cavity of wild-type and *Mdr1a/b*$^{-/-}$*Bcrp1*$^{-/-}$ mice (n=4) as described previously (Parrish et al., 2015b). Palbociclib is included in this

chapter for comparison and a more detailed description can be found in **Chapter 3**). Ribociclib and abemaciclib were prepared in DMSO and delivered at a rate of 10 µg/hr for forty-eight hours. Mini osmotic pumps were primed overnight at 37ºC in saline. The surgical procedure has been described in detail previously (Agarwal et al., 2010; Wang et al., 2012). Briefly, isoflurane was used to anesthetize the mice and the hair was removed from the surgical site. Mice remained on a heating pad for the duration of the surgical procedure until mice were fully recovered. A small incision was made in the lower right abdomen followed by an incision in the peritoneal membrane and the primed pump was inserted. The peritoneal membrane was sutured closed and the abdomen was closed with surgical clips. Following the infusion, brain and whole blood samples were collected. Plasma was isolated from whole blood by centrifugation (3500 rpm for 15 minutes) and brain and plasma samples were stored in -80ºC until analysis via LC-MS/MS.

5.2.4 IN SITU BRAIN PERFUSION TECHNIQUE

In situ brain perfusion allows for the study of BBB transport. In this technique, the brain is perfused with a known concentration of drug and the BBB transport is evaluated without the confounding factor of systemic disposition (Smith, 1996; Dagenais et al., 2000; Smith and Allen, 2003; Zhao et al., 2009a) . Mice were anesthetized with isoflurane throughout the experiment. Oxygenated perfusion fluid (128 mM sodium chloride, 24 mM sodium bicarbonate, 4.2 mM potassium

chloride, 2.4 mM sodium dihydrogen phosphate, 1.5 mM calcium chloride, 0.9 mM magnesium chloride) was prepared with glucose (9 mM) on the day of the experiment. CDK4/6 inhibitor concentrations were 0.1 – 50 µM in the perfusion fluid. Perfusion fluid was warmed to 37ºC and a syringe warmer was used to maintain temperature. An intracardiac perfusion was conducted at 5 mL/min for two minutes and following the perfusion, the brain was isolated and stored at -80ºC until analysis by LC-MS/MS. The amount of drug in the brain vasculature was assumed to be 1.4% for all calculations of brain distribution. The transfer coefficient for brain uptake (K_{in}) was calculated by the following equation:

$$K_{in} = \frac{Q_{total} - V_v C_{pf}}{C_{pf} T_{perfusion}}$$

where Q_{total} is the measured quantity of drug in the brain at the end of the perfusion, V_v is the brain vascular volume, C_{pf} is the concentration of drug in the perfusion fluid, and $T_{perfusion}$ is the time of the perfusion (two minutes). K_{in} represents the total amount of drug that has entered the brain. This technique is an ideal way to examine transport at the BBB because the compounds of interest are delivered to the brain at a known concentration over a defined period of time (Golden and Pollack, 2003). The *in situ* brain perfusion technique has traditionally been used to examine only uptake into the brain, however there are ways to use this technique to examine efflux. One way to examine efflux is through the use of efflux inhibitors in the perfusate (Deguchi et al., 1997). Previous reports have shown that P-gp efflux is active during 10 second

perfusions (Drion et al., 1996) and therefore we can expect that efflux activity is incorporated into the calculated brain uptake value. Efflux transport can also be examined when the concentration of the drug of interest is varied in the perfusate (Drion et al., 1997). Varying the concentration of the compound of interest in the perfusate allows nonlinear brain distribution to be studied and can reveal insights into the role of BBB efflux transport in the brain distribution of these agents. Previous studies have used the *in situ* brain perfusion technique to show that efflux is saturated in the brain delivery of itraconazole and imatinib (Miyama et al., 1998; Bihorel et al., 2007).

5.2.5 LC-MS/MS ANALYSIS

Palbociclib liquid chromatography-tandem mass spectrometry (LC-MS/MS) analysis was conducted as previously described (Parrish et al., 2015b). Ribociclib and abemaciclib LC-MS/MS sample preparation was identical to palbociclib. Briefly, brain samples were prepared by adding three volumes of 5% bovine serum albumin prior to homogenizing using a tissue homogenizer (PowerGen 125; Thermo Fisher Scientific, Waltham, MA). Brain homogenate samples were spiked with internal standard (25 ng dasatinib) and extracted by the addition of 1 volume pH 11 buffer followed by 5 volumes of ethyl acetate. Plasma and perfusate samples were spiked with internal standard and extracted by the addition of 2 volumes pH 11 buffer followed by 10 volumes of ethyl acetate. Samples were then vortexed followed by centrifugation (7500 rpm, 5

minutes) and the supernatant was dried under nitrogen. Samples were reconstituted in mobile phase (abemaciclib – 70:30 :: 1 mM ammonium format with 0.1% formic acid:acetonitrile; ribociclib – 68:32 :: 1 mM ammonium format with 0.1% formic acid:acetonitrile). An AQUITY ultra high performance liquid chromatography system (Waters, Milford, MA) was used with a Phenomenex Synergi Polar 4 micron polar-RP 80Å column (75 x 2 mm; Torrance, CA). All ionization was conducted in positive mode and the *m/z* transitions were 507.1-392.98, 435.07-321.87, 448.34-379.95, and 488.21-400.88 for abemaciclib, ribociclib, palbociclib, and dasatinib, respectively. The mobile phase was delivered at a constant flow rate of 0.25 mL/min for palbociclib and abemaciclib detection (isocratic) and 0.5 mL/min for ribociclib detection (gradient).

5.2.6 EFFLUX SATURATION ANALYSIS

A simple model was used to evaluate the relationship between changes in affinity and saturation in STELLA (10.0.6, isee systems, Lebanon, NH). The active efflux from the brain was modeled as an active clearance process that was saturable:

$$CL_{efflux} = \frac{V_{max,P-gp}}{K_{m,P-gp} + Concentration_{brain}} + \frac{V_{max,BCRP}}{K_{m,BCRP} + Concentration_{brain}}$$

When K_m is significantly less than the concentration in the brain, the rate of active efflux approaches V_{max} and when K_m is significantly greater than the concentration in the brain, the active clearance process is pseudo-linear with a

slope of V_{max}/K_m. Two efflux process were modeled that could be P-gp and BCRP, two BBB efflux transporters.

Similarly, an active uptake process was modeled as a saturable process:

$$CL_{uptake} = \frac{V_{max,\ uptake}}{K_{m,\ uptake} + Concentration_{plasma}}$$

A constant rate infusion was used to examine the possibility of efflux saturation at the BBB. The concentration in the central (plasma) compartment was described by the following equation.

$$V_{plasma} \times \frac{dConcentration_{plasma}}{dt} =$$

$$Infusion\ Rate - CL_{systemic} \times \left(Concentration_{plasma}\right) - CL_{uptake} \times) + CL_{passive} \times$$

$$\left(Concentration_{brain} - Concentration_{plasma}\right) + CL_{efflux} \times (Concentration_{brain})$$

The concentration in the brain was described by the following equation.

$$V_{brain} \times \frac{dConcentration_{brain}}{dt}$$

$$= CL_{passive} \times \left(Concentration_{plasma} - Concentration_{brain}\right)$$

$$+ CL_{uptake} \times (Concentration_{plasma})$$

$$- CL_{efflux} \times (Concentration_{brain})$$

The volumes were fixed to 100 volume units in the central compartment and 1 volume unit in the peripheral (brain) compartment The systemic clearance was fixed to be 20 volume/time. In simulating saturation of efflux transport at the BBB,

six scenarios were evaluated. In the first three scenarios, active uptake was a high affinity, low V_{max} process compared to active efflux, which was a lower affinity, higher V_{max} process. $V_{max,uptake}$ and $K_{m,uptake}$ were kept constant and fixed to 0.1 and 0.00001, respectively for all six simulations. Scenarios 1-3 are described below and the V_{max} parameters used for efflux relate to the relative transporter expression in FVB mice (Agarwal et al., 2012; Sane et al., 2013):

(1) Infusion rate: 1; $V_{max,\ P\text{-}gp} = 150$; $K_{m,\ P\text{-}gp} = 0.1$; $V_{max,\ BCRP} = 50$; $K_{m,\ BCRP} = 0.1$

(2) Infusion rate: 1000; $V_{max,\ P\text{-}gp} = 150$; $K_{m,\ P\text{-}gp} = 0.1$; $V_{max,\ BCRP} = 50$; $K_{m,\ BCRP} = 0.1$

(3) Infusion rate: 25000; $V_{max,\ P\text{-}gp} = 150$; $K_{m,\ P\text{-}gp} = 0.1$; $V_{max,\ BCRP} = 50$; $K_{m,\ BCRP} = 0.1$

In scenarios 4-6, active uptake was kept constant and V_{max} and K_m for P-gp clearance were both decreased, simulating an efflux process that would be saturated at lower concentrations than scenarios 1-3.

(4) Infusion rate: 1; $V_{max,\ P\text{-}gp} = 50$; $K_{m,\ P\text{-}gp} = 0.0001$; $V_{max,\ BCRP} = 50$; $K_{m,\ BCRP} = 0.1$

(5) Infusion rate: 1000; $V_{max,\ P\text{-}gp} = 50$; $K_{m,\ P\text{-}gp} = 0.0001$; $V_{max,\ BCRP} = 50$; $K_{m,\ BCRP} = 0.1$

(6) Infusion rate: 25000; $V_{max,\ P\text{-}gp} = 50$; $K_{m,\ P\text{-}gp} = 0.0001$; $V_{max,\ BCRP} = 50$; $K_{m,\ BCRP} = 0.1$

5.2.7 STATISTICAL ANALYSIS

All statistical analyses were conducted using GraphPad Prism 6.04 (San Diego, CA). Data are represented as the mean ± standard deviation and comparisons between two groups were made using an unpaired t-test. One-way analysis of variance followed by Bonferonni's multiple comparisons test was used for multiple comparisons. For all studies, a significance level of $P < 0.05$ was used.

5.3 RESULTS

5.3.1 48 HOUR INFUSION BRAIN DISTRIBUTION

The brain distribution of palbociclib was published in **Chapter 3** of this thesis, but the steady-state results are summarized here for comparison (Parrish et al., 2015b). Palbociclib has limited brain distribution in wild-type mice (**Figure 5.1.A, Table 5.1**; 3.82 ± 1.1 nM) and this is significantly increased in the *Mdr1a/b*$^{-/-}$ *Bcrp1*$^{-/-}$ mice (**Figure 5.1.A**; 2514 ± 1420 nM; p=0.123). The brain-to-plasma ratio of palbociclib is also significantly increased in the transporter knockout mice (**Figure 5.1.B**; WT: 0.2 ± 0.07 vs. TKO 27.8 ± 5.9; p<0.0001). The efflux transporters P-gp and Bcrp are also involved in the brain delivery of ribociclib following a 48 hour infusion (**Figure 5.2.A**; WT: 51.4 ± 15.1 nM vs. TKO: 2976 ± 1220 nM; p=0.003) that is also reflected in the brain-to-plasma ratio of ribociclib (**Figure 5.2.B**; WT: 0.22 ± 0.1 vs. TKO: 8.74 ± 1.4; p<0.0001). Similarly, efflux transport is involved in the brain delivery of abemaciclib (**Figure 5.3.A**; WT: 96.9 ± 83.7 nM vs. TKO: 7739 ± 7677 nM; p=0.0468) and this results in over a seventy-fold increase in brain-to-plasma in the transporter knockout mice (**Figure 5.3.B**; WT: 0.14 ± 0.12 vs. TKO: 10.1 ± 5.5; p=0.011).

5.3.2 *IN SITU* PERFUSION

The *in situ* brain perfusion technique was used to examine the brain uptake of palbociclib, ribociclib and abemaciclib. Palbociclib uptake (K_{in}) was examined in wild-type and *Mdr1a/b*$^{-/-}$*Bcrp1*$^{-/-}$ mice following a two minute intracardiac perfusion at 5 mL/min. The apparent K_{in} for palbociclib was found to range from 1.1 x 10^{-3} mL/s/g to 34.6 x 10^{-3} mL/s/g (**Figure 5.4**). The perfusate concentration was examined from 0.1 to 50 µM and the highest K_{in} was observed when the perfusate concentration was 0.1 µM. Similarly, the K_{in} for ribociclib ranged from 0.4 x 10-3 mL/s/g to 4.8 mL/s/g and the highest K_{in} was observed when the perfusate concentration was 0.1 µM (**Figure 5.5**). In contrast to palbociclib and ribociclib, *in situ* brain perfusion experiments demonstrated that while abemaciclib has the highest apparent K_{in} at 100 µM in the *Mdr1a/b*$^{-/-}$*Bcrp1*$^{-/-}$ mice, the highest K_{in} value was observed at 50 µM in the wild-type mice (**Figure 5.6**).

5.3.3 MODELING AND SIMULATION

A model was explored to describe the changes in transporter affinity that were observed in the *in situ* perfusion studies (**Figure 5.7**). The model was designed so that efflux transport was not saturated in the first three simulations. The simulated steady-state plasma concentrations were 0.05, 50 and 1250 for infusion rates of 1, 1000, and 25000. The brain concentrations were 0.03, 2.1 and 51.6 (**Table 5.2**). The brain-to-plasma ratio was 0.04 when the infusion rate was 1000 or 25000 and 0.54 when the infusion rate was 1, demonstrating that uptake transport was saturated at the higher infusion rates. The K_m and V_{max} for

P-gp transport were both lowered in simulations 4-6, while the K_m and V_{max} for uptake and BCRP transport were held constant. The simulated plasma concentrations did not change from 0.05, 50 and 1250, however the simulated brain concentration was 642 instead of 51.6 when the infusion rate was 25000, indicating that P-gp efflux transport was saturated (**Table 5.2**). These results suggest that the results observed from the *in situ* perfusion studies can be explained by a high affinity, low V_{max} uptake system and a saturable, lower V_{max}, efflux process.

5.4 DISCUSSION

The treatment of primary and secondary brain tumors has not provided substantial improvement in patient outcomes despite significant advances in the treatment of peripheral tumors in many types of cancers (Davies, 2012; Fidler, 2015). For example, seven new therapies have been approved for metastatic melanoma since 2011, but the median survival following detection of a brain tumor remains six months (Fidler, 2015). In comparison to the treatment of primary brain tumors, the treatment of metastatic brain tumors poses a particularly daunting problem because it is disadvantageous to deliver toxic drugs into the brain under most circumstances, however once brain tumors are found, the diagnosis is almost always lethal. Current imaging techniques are unable to detect brain tumors at the earliest stage and therefore brain tumors grow while unseen and untreated. The development of compounds for the treatment of metastatic disease has somewhat been slowed by the desire to keep these toxic drugs out of the brain and protect the precious nerve cells from damage. This, however, has had major consequences because this has provided a sanctuary site for metastasis with tumor cells residing behind the BBB.

The purpose of this study was to determine the potential problems in the use of CDK4/6 inhibitors in the treatment of primary and metastatic brain tumors. The CDK4/6 pathway is frequently altered in primary brain tumors as well as tumors that have a high propensity to metastasize to the brain (VanArsdale et al., 2015).

Because of this, it is important to understand the mechanisms involved in the delivery of CDK4/6 inhibitors to the brain. Furthermore, there are three CDK4/6 inhibitors currently undergoing clinical development and it is important to understand the potential differences in brain distribution in selecting the best candidate in the treatment of primary and metastatic brain tumors.

Constant rate infusion (48 hours) brain distribution studies revealed that palbociclib, abemaciclib and ribociclib all have limited brain delivery due to the efflux transport activity of P-glycoprotein and/or breast cancer resistance protein. The brain delivery of all three compounds was significantly improved following a 48-hour constant rate (10 µg/hr) infusion in the *Mdr1a/b*$^{-/-}$*Bcrp1*$^{-/-}$ mice (palbociclib, 140-fold (Parrish et al., 2015b); abemaciclib, 70-fold; ribociclib, 40-fold) . In addition, all three CDK4/6 inhibitors have nanomolar IC_{50} values and somewhat similar physicochemical properties. From this information alone, it is impossible to distinguish between these three CDK4/6 inhibitors and in order to understand potential differences in efflux transport and brain distribution, the *in situ* brain perfusion technique was used.

To give context to the apparent K_{in} values observed, diazepam, which is often used as a marker of permeability because it's uptake is perfusion rate limited, has been shown to have an apparent K_{in} of approximately 50 x 10^{-3} mL/s/g (Zhao et al., 2009a). On the other side of the spectrum, fexofenadine, which has a brain-to-plasma ratio of 0.0056, has an apparent K_{in} of 0.083 x 10^{-3} mL/s/g (Zhao

et al., 2009a; Zhao et al., 2009d). The K_{in} values for palbociclib, ribociclib and abemaciclib are in between the reported literature values for fexofenadine and diazepam and were similar at low micromolar concentrations. Interestingly, when the perfusate concentration was 0.1 µM, all three inhibitors had higher apparent K_{in} values than when the perfusate concentration was 1 µM. This could be explained by an influx transporter that is rapidly saturated, but was not further examined in this study. The apparent K_{in} values for ribociclib and palbociclib remained relatively constant when the perfusate concentration increased from 1 µM to 50 µM. This indicates that efflux transport at the BBB is not saturated over this concentration range. Abemaciclib, however, has increasing apparent K_{in} values after 1 µM that could be explained by saturation of BBB efflux transporters. While these results are preliminary, this reaffirms the findings by Raub *et al*. and indicates that abemaciclib may be a better candidate in the treatment of primary and metastatic brain tumors because it has the potential to saturate BBB efflux transport and have improved brain delivery (Raub et al., 2015).

A steady-state model was used to describe the *in situ* brain perfusion observations. Since abemaciclib may be able to saturate efflux transport at the BBB at lower concentrations than palbociclib and ribociclib, the affinity of abemaciclib is likely higher (lower K_m) than palbociclib or ribociclib. If permeability and V_{max} remain constant and affinity, or K_m, is the only parameter that is variable between the three CDK4/6 inhibitors, then the active clearance of abemaciclib

would be higher than or equal to the active clearance of palbociclib or ribociclib at all concentrations. Therefore, we know that the V_{max} of abemaciclib must decrease in order to saturate efflux transport and increase the brain accumulation. Abemaciclib and palbociclib are known substrates of both P-gp and BCRP (Parrish et al., 2015b; Raub et al., 2015). P-gp efflux is expressed at higher levels than BCRP at the murine BBB (Agarwal et al., 2012) and therefore is more sensitive to changes in K_m and V_{max}. The model was able to simulate the observations seen in the *in situ* perfusion studies by reducing the K_m and V_{max} of P-gp. This saturated efflux at the highest simulated infusion rate and increased the brain accumulation. Further *in vitro* and *in vivo* studies are necessary to confirm this preliminary result.

It is important to note here that this saturation of efflux transport by abemaciclib starts to occur when the perfusate concentration is between 10 and 25 µM and that this is the *unbound* concentration. Literature reports that abemaciclib is approximately 95% bound in mouse plasma (Raub et al., 2015) and therefore that must be taken into consideration when determining whether saturation of efflux transport at the BBB is possible.

The likelihood of saturation at the human BBB is important to understand when comparing compounds and the relative brain distribution. The potential for saturation or drug-drug interactions (DDIs) at the BBB has been explored in a recent white paper (Kalvass et al., 2013). In this paper, the authors argue that

DDIs at the human BBB are unlikely because the unbound concentrations of transporter substrates are seldom at relevant concentrations. On the other hand, the expression of P-gp at the human BBB is 2.5-fold lower than the expression at the murine BBB (although the expression of BCRP is 2.5-fold higher at the human BBB) (Uchida et al., 2011; Agarwal et al., 2012). Therefore it will be important for future studies to use techniques that are able to simulate and predict the potential for DDIs to occur at the human BBB in order to understand if saturation of efflux transporters by abemaciclib is probable.

In summary, these studies demonstrate that P-gp and/or Bcrp are involved in limiting the brain delivery of palbociclib, ribociclib and abemaciclib. These are important findings when designing rational clinical trials that examine the use of these CDK4/6 inhibitors in the treatment of primary brain tumors or tumors with a high propensity to metastasize to the brain. Similar to previously published results, abemaciclib demonstrated the ability to saturate efflux transport at concentrations where palbociclib or ribociclib were unable to saturate transport. These preliminary results indicate that abemaciclib may have a greater potential for therapeutic benefit in the treatment of primary or metastatic brain tumors than palbociclib or ribociclib. As expected, the saturation was not seen following a constant rate infusion for 48 hours because the plasma concentrations were approximately 1 μM. Further studies that examine the potential for *in vivo* saturation of efflux transport may provide insight into selecting the best CDK4/6 inhibitor for clinical trials in brain tumor patients.

Figure 5.1.A: Palbociclib brain and plasma distribution.

(A) Palbociclib brain and plasma concentration following 48 hour constant rate infusion (10 µg/hr), ** indicates p<0.01, n=4.

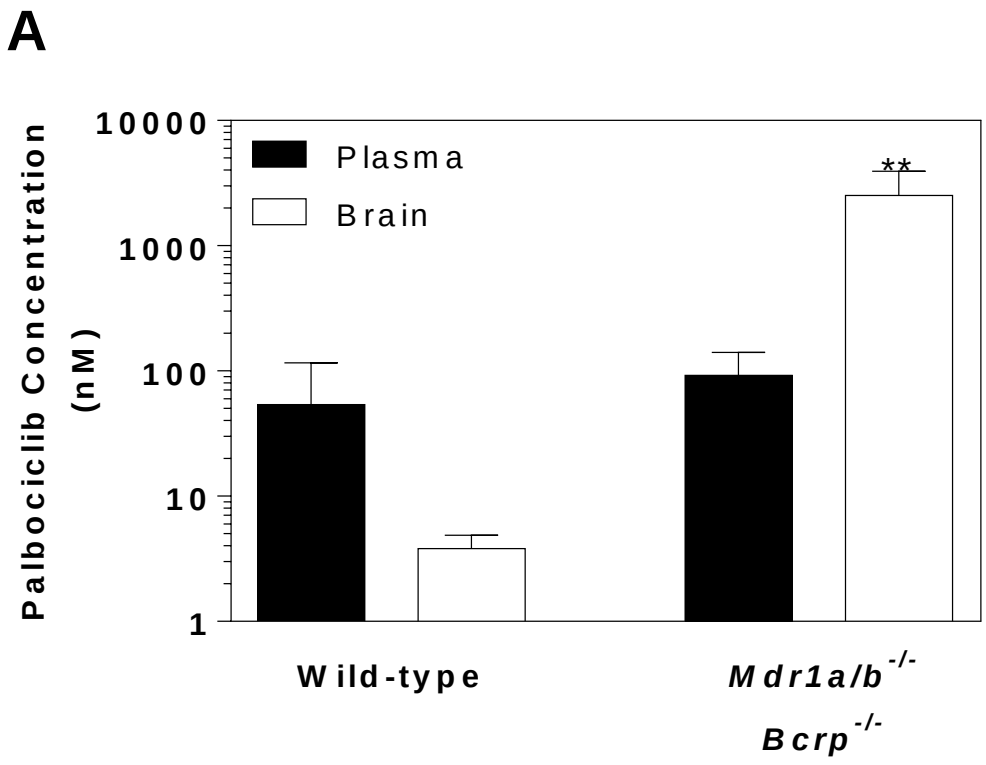

Figure 5.1.B: Palbociclib brain-to-plasma ratio.

(B) Palbociclib brain-to-plasma ratio in wild-type and *Mdr1a/b*$^{-/-}$*Bcrp1*$^{-/-}$ mice following 48 hour constant rate infusion (10 µg/hr), *** indicates p<0.001 n=4.

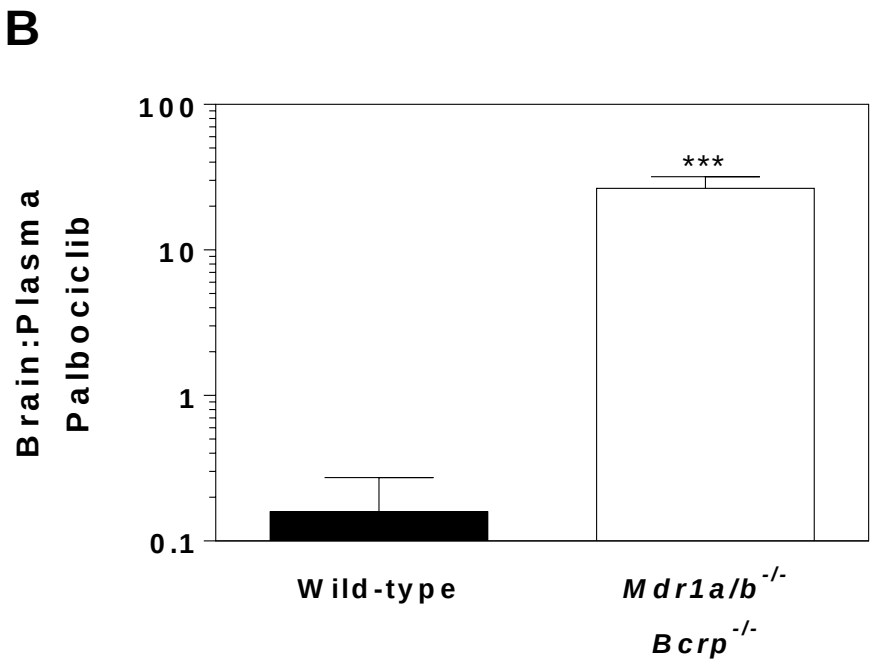

Figure 5.2.A: Ribociclib brain and plasma distribution.

(A) Ribociclib brain and plasma concentration following 48 hour constant rate infusion (10 µg/hr), ** indicates $p<0.01$, n=4.

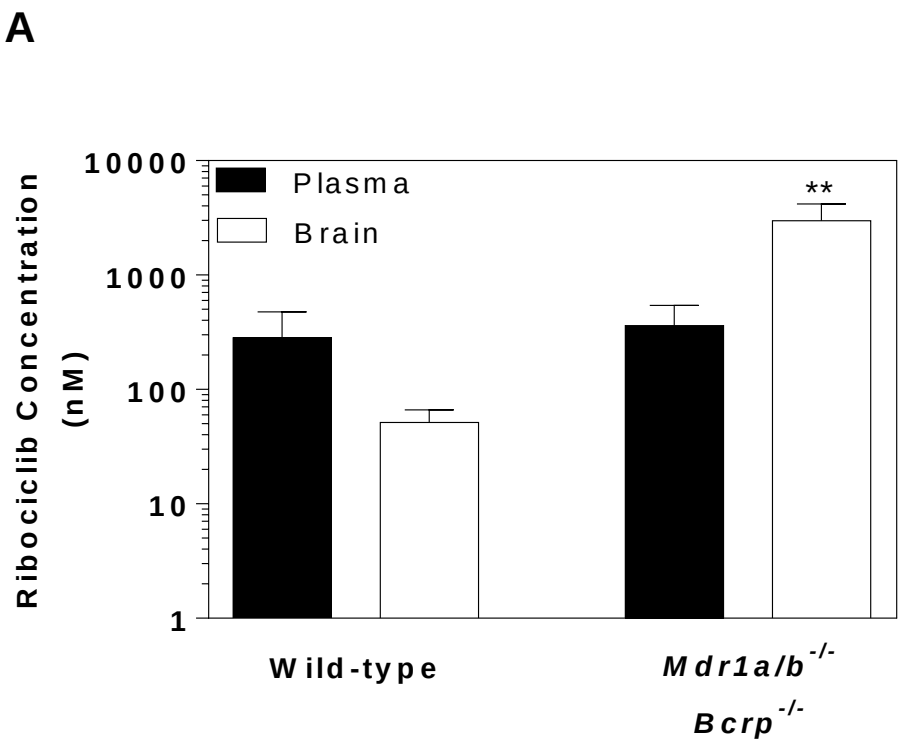

Figure 5.2.B: Ribociclib brain-to-plasma ratio.

(B) Ribociclib brain-to-plasma ratio in wild-type and *Mdr1a/b*$^{-/-}$*Bcrp1*$^{-/-}$ mice following 48 hour constant rate infusion (10 µg/hr), **** indicates p<0.0001, n=4.

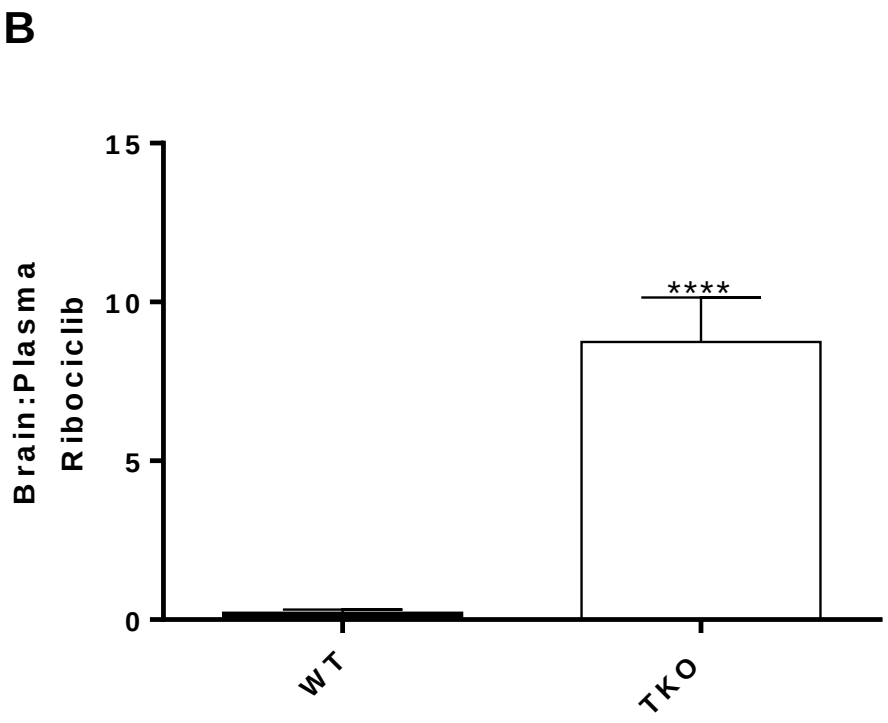

Figure 5.3.A: Abemaciclib brain and plasma distribution.

(A) Abemaciclib brain and plasma concentration following 48 hour constant rate infusion (10 µg/hr), n=4.

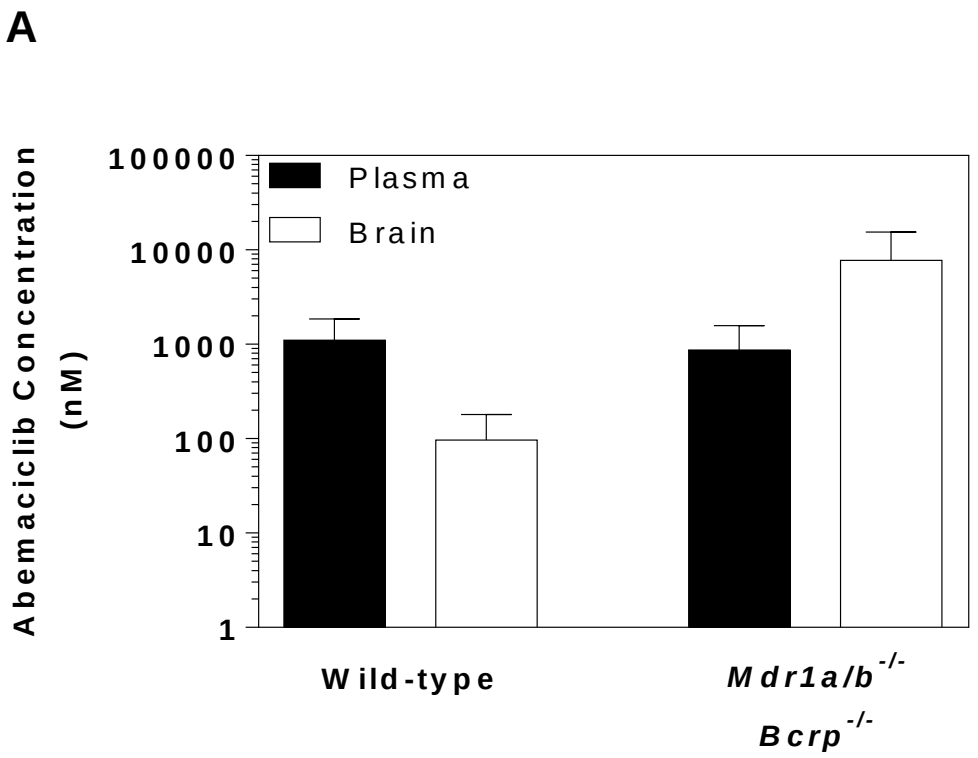

Figure 5.3.B: Abemaciclib brain-to-plasma ratio.

(B) Abemaciclib brain-to-plasma ratio in wild-type and *Mdr1a/b*$^{-/-}$*Bcrp1*$^{-/-}$ mice following 48 hour constant rate infusion (10 µg/hr), * indicates $p<0.05$, n=4.

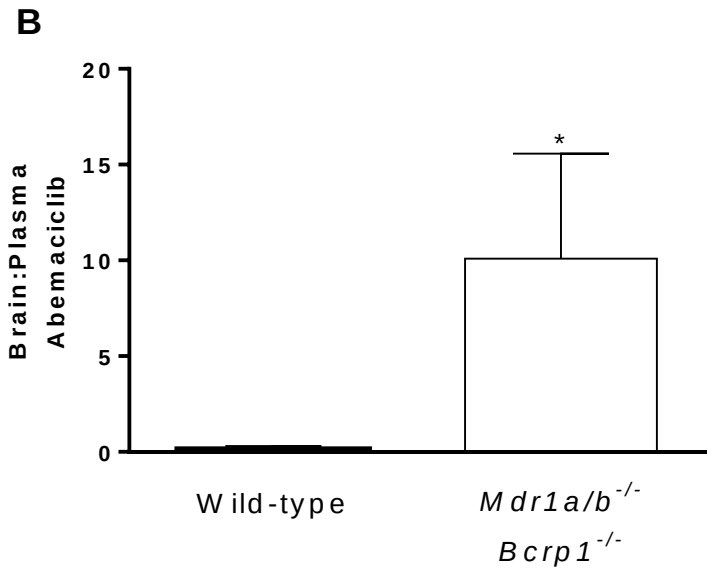

Table 5.1: Summary of constant rate infusion concentrations.

Drug Targeting Index, DTI = $(C_{ss,brain}/C_{ss,plasma})_{knockout}$ / $(C_{ss,brain}/C_{ss,plasma})_{wild\text{-}type}$

Compound	Strain	Plasma Concentration	Brain Concentration	Brain-to-plasma ratio	Drug Targeting Index
Palbociclib	Wild-type	53.8 ± 63	3.82 ± 1.1	0.2 ± 0.07	1
	Mdr1a/b$^{-/-}$*Bcrp1*$^{-/-}$	92.3 ± 49	2514 ± 1420	28 ± 6	140
Ribociclib	Wild-type	283 ± 194	51.4 ± 15.1	0.22 ± 0.1	1
	Mdr1a/b$^{-/-}$*Bcrp1*$^{-/-}$	361 ± 184	2976 ± 1220	8.74 ± 1.4	40
Abemaciclib	Wild-type	1103 ± 745	96.9 ± 83.7	0.14 ± 0.12	1
	Mdr1a/b$^{-/-}$*Bcrp1*$^{-/-}$	874 ± 707	7739 ± 7677	10.1 ± 5.5	70

Figure 5.4: Palbociclib uptake in wild-type and *Mdr1a/b*$^{-/-}$*Bcrp1*$^{-/-}$ mice.

* indicates p<0.05 when compared with 1 µM (wild-type), n=4 per group.

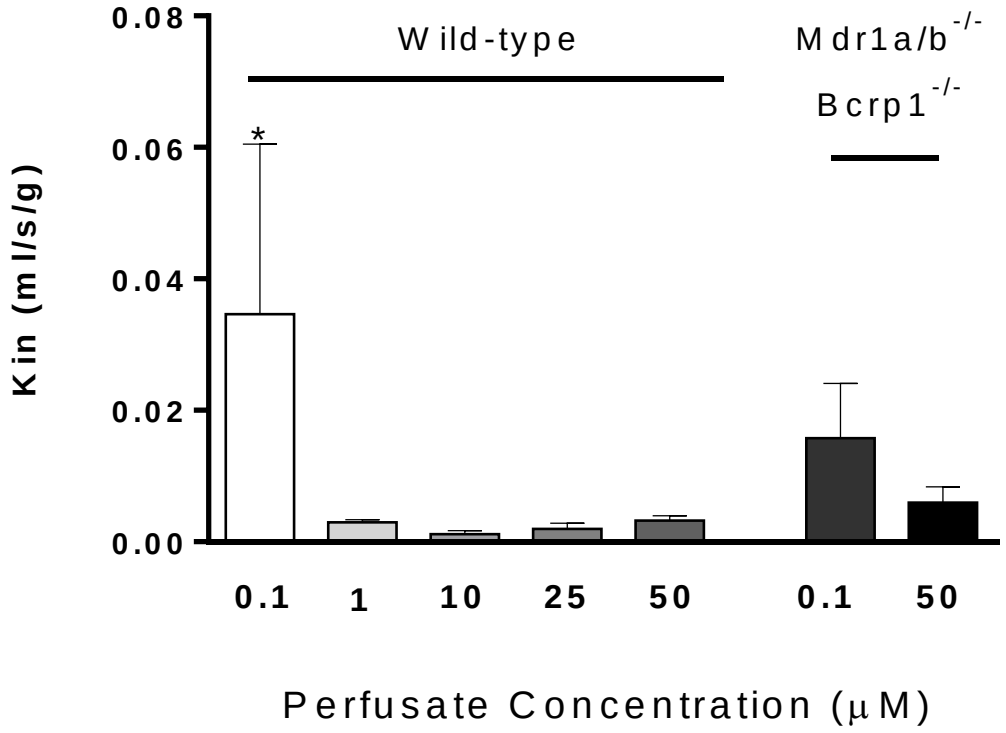

Figure 5.5: Ribociclib uptake in wild-type and *Mdr1a/b*$^{-/-}$*Bcrp1*$^{-/-}$ mice.

* indicates p<0.05 when compared with 1 µM (wild-type), # indicates p<0.05 when comparing between equivalent concentrations in wild-type and *Mdr1a/b*$^{-/-}$ *Bcrp1*$^{-/-}$, n=4 per group.

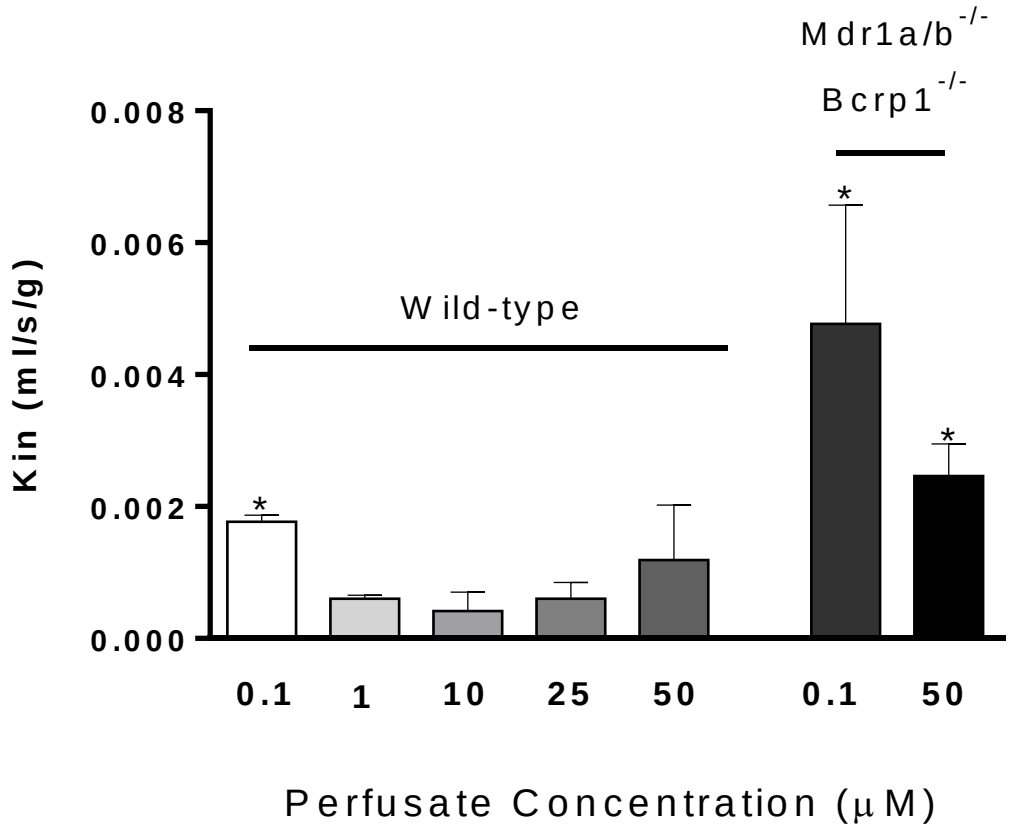

Figure 5.6: Abemaciclib uptake in wild-type and Mdr1a/b-/-Bcrp1-/- mice.

* indicates p<0.05 when compared with 1 µM (wild-type), n=4 per group.

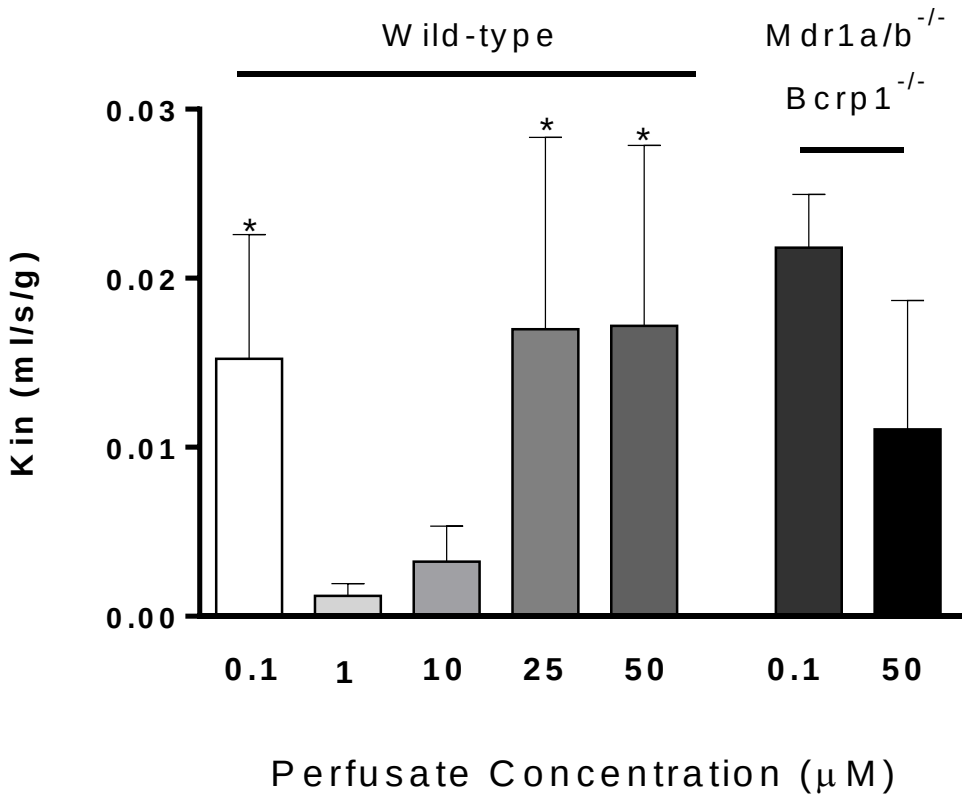

Figure 5.7: Schematic of the constant rate infusion model to evaluate saturation of efflux transport at the BBB.

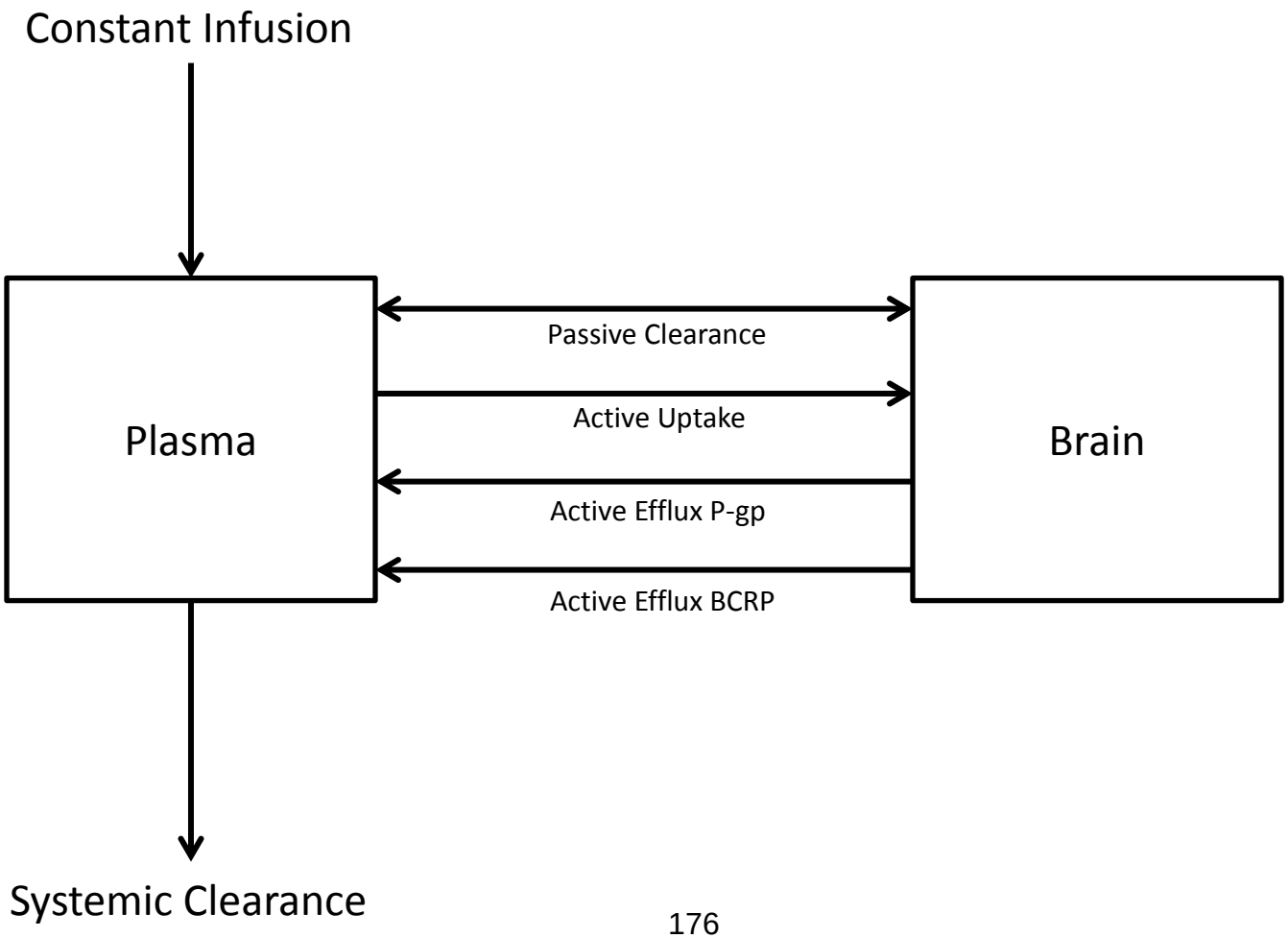

Table 5.2: Steady-state (SS) plasma and brain concentrations and resulting brain-to-plasma ratio following a simulated 48 hour infusion.

$V_{max\ BCRP}$ was held constant at 50 and $V_{max\ P\text{-}gp}$ was 150 for simulations 1-3 and 50 for simulations 4-6.

Simulation #	Infusion Rate	$K_{m,\ uptake}$	$K_{m,\ BCRP}$	$K_{m,\ P\text{-}gp}$	Plasma $Concentration_{ss}$	Brain $Concentration_{ss}$	Brain-to-plasma ratio
1	1	0.00001	0.1	0.1	0.05	0.03	0.54
2	1000	0.00001	0.1	0.1	50.0	2.1	0.04
3	25000	0.00001	0.1	0.1	1250	51.6	0.04
4	1	0.00001	0.1	0.0001	0.05	0.03	0.54
5	1000	0.00001	0.1	0.0001	50.0	2.1	0.04
6	25000	0.00001	0.1	0.0001	1250	642	0.51

CHAPTER VI

RECAPITULATION

Brain tumor treatment options for both primary and metastatic brain tumors are limited. Glioblastoma (GBM) is the most common primary brain tumor in adults and new, more effective treatments are needed to address this devastating disease. Survival is approximately one year following diagnosis and clinical trials continue to fail in patients. The number of patients with metastatic brain tumors is even higher, and this number continues to rise as the treatment of peripheral disease improves. Breast, melanoma and lung cancer are the three most common types of metastatic brain tumors and have extremely poor prognosis and limited treatment options. The treatment of brain tumors is challenging for three main reasons. First, the brain is a delicate organ that is vulnerable to damage by current therapies leading to dose-limiting toxicities. Second, the tumor is comprised of different cell types and this tremendous genetic heterogeneity in tumor drivers makes finding therapies exceedingly difficult. Finally, due to the aggressive and/or infiltrative nature of brain tumors, there are tumor cells that remain untreated behind an intact blood-brain barrier (BBB). The challenges associated with treating primary and metastatic brain tumors are explored in **Chapter 1**.

The BBB serves as a physical barrier to drug delivery as a result of the complex network of tight junctions, and a functional barrier to drug delivery since there are efflux transport proteins that actively prevent drugs from reaching the brain. Although tumors are diagnosed in part by the presence of a disrupted BBB, there are invasive tumor cells that reside behind an intact BBB and this is critical to

understand to achieve the effective treatment of the disease. Compounds that are unable to cross an intact BBB will be unable to reach invasive tumor cells that have migrated into “normal” brain tissue that is adjacent to the tumor core. Therefore, it is paramount to understand the delivery of compounds across an intact BBB to fully explore new treatment options for this difficult disease.

Cyclin-dependent kinases (CDKs) are major regulators of the cell cycle and control cell cycle progression (reviewed in **Chapter 2**). CDK4 and CDK6 are involved in G1-to-S phase cell cycle progression and parts of this pathway are frequently altered in many tumor types. Palbociclib is a potent CDK4/6 inhibitor that was approved in early 2015 by the FDA for the treatment of metastatic breast cancer. Ribociclib and abemaciclib are two other potent CDK4/6 inhibitors that are currently in late-stage clinical trials for a variety of solid tumors such as breast cancer, melanoma and non-small cell lung cancer. This dissertation focuses on studying the brain distribution of CDK4/6 inhibitors across the BBB and the mechanisms that may limit the brain delivery of these agents in preclinical models.

The first part of this project examined the brain delivery of palbociclib and the role of efflux transport at the BBB in limiting brain delivery (**Chapter 3**). P-glycoprotein (P-gp) and breast cancer resistance protein (BCRP) are two ATP-binding cassette (ABC) efflux transporters that are expressed at the BBB and actively transport substrates into systemic circulation, preventing these molecules from reaching the brain. Palbociclib was shown to be a P-gp and

BCRP substrate using both *in vitro* and *in vivo* assays. This experimental paradigm has been reported in the literature from our group and others for a variety of compounds that have been explored for the treatment of GBM. In this part of the project, we examined the brain distribution of palbociclib in FVB wild-type, *Mdr1a/b*$^{-/-}$, *Bcrp1*$^{-/-}$, and *Mdr1a/b*$^{-/-}$*Bcrp1*$^{-/-}$ mice by determining the plasma-concentration profiles in both the plasma and the brain over twenty-four hours. We determined that the normalized brain exposure (AUC ratios) was more than 100-fold higher in the *Mdr1a/b*$^{-/-}$*Bcrp1*$^{-/-}$ mice than the wild-type mice, demonstrating that P-gp and BCRP play a major role in the brain delivery of palbociclib. In athymic nude mice we demonstrated that palbociclib is an effective therapy in a subcutaneously implanted GBM patient-derived xenograft (GBM22) that has homozygous deletion of CDKN2A/B, but does not provide therapeutic benefit in an orthotopic (intracranial) model of GBM.

Chapter 4 builds on these findings and aimed to establish the relationship between P-gp and BCRP efflux inhibition and the brain delivery of palbociclib, by evaluating the link between improved brain delivery and efficacy. We found that elacridar, a dual inhibitor of P-gp and BCRP, significantly improves the brain delivery of palbociclib and that this process is saturable. The effect of chronic administration of elacridar was also assessed by a rotarod assay to measure ataxia. There were no adverse effects of chronic elacridar administration on body weight or ataxia indicating that chronic administration of elacridar is well tolerated up to 20 mg/kg. In order to study the regional delivery of palbociclib in athymic

nude tumor-bearing mice, cresyl violet was used to indicate tumor location and punch biopsies were taken in normal brain, tumor rim and tumor core regions. As was hypothesized, there was enhanced drug delivery in the tumor core, an indication that the BBB was compromised. Elacridar coadministration significantly enhanced palbociclib delivery to the normal brain, tumor rim and tumor core regions. Furthermore, palbociclib concentrations achieved in the critically important tumor rim (brain around tumor that contains invasive glioma cells) and tumor core of the elacridar treated group were comparable to the concentrations achieved in a flank tumor study that significantly delayed GBM22 tumor growth. Despite this improved delivery, there was no further reduction in phosphorylated-RB in the elacridar and palbociclib combination treatment group than in the palbociclib monotherapy group. There was also no improvement in survival with palbociclib monotherapy nor the palbociclib and elacridar combination therapy, indicating that a measure of gross delivery does not entirely explain the lack of efficacy.

Palbociclib is one of three CDK4/6 inhibitors that are currently in clinical trials for a variety of solid tumors. Alterations to the CDK4/6 pathway are commonly observed in GBM, as well as in breast cancer, lung cancer and melanoma, three of the most common cancers to metastasize to the brain. Since CDK4/6 inhibitors are being tested in these types of cancer that have a high rate of brain metastasis, it is important to understand the brain delivery of all three CDK4/6 inhibitors (**Chapter 5**). Brain and plasma concentrations following a 48 hour

constant rate infusion demonstrated that P-gp and BCRP mediated efflux transport is involved in limiting the brain delivery of abemaciclib and ribociclib. The *in situ* brain perfusion technique was used to compare the relative transport activity of P-gp and BCRP in palbociclib, ribociclib and abemaciclib brain distribution. The data suggest that there may be an influx transporter involved in the brain uptake of all three CDK4/6 inhibitors at the lowest concentration tested. Furthermore, these studies suggest that abemaciclib may be able to enhance its own delivery through the saturation of efflux transport at higher concentrations. These preliminary results indicate that abemaciclib may have the greatest potential for use in the treatment of brain tumors or tumors with a propensity to metastasize to the brain, however future studies in models of primary and secondary brain tumors are needed to better understand the differences in the brain delivery, and the ensuing effects on efficacy, of these three CDK4/6 inhibitors.

Taken together, the studies in this dissertation indicate the important role of the BBB in the treatment of brain tumors and demonstrate that active efflux at the BBB limits the brain delivery of ribociclib, palbociclib and abemaciclib. In the treatment of brain tumors there are many interconnected, critical elements: an effective drug (or drugs), heterogeneous targets that drive tumor growth, location and invasion of the heterogeneous tumor cells, and adequate drug delivery of the effective drug(s) to those specific locations that are protected by an intact BBB. These studies have indicated that the selection of the right drug or combination

of drugs may not be as simple as using an *in vitro* (cell lines) or even *in vivo* (subcutaneous) assay. **Chapters 3 and 4** show that palbociclib was effective in inhibiting tumor growth in a subcutaneous tumor model, but provided no therapeutic benefit in the treatment of an intracranial model of GBM despite achieving comparable palbociclib concentrations using elacridar-mediated inhibition of efflux transport. In developing effective therapies for the treatment of brain tumors, it will be essential to deliver the correct drug(s) at adequate concentrations to all tumor cells, some of which reside behind an intact BBB.

Future work on this project will examine the relative distribution of CDK4/6 inhibitors and determine if abemaciclib, through its potential ability to saturate efflux transport, is more effective in the treatment of brain metastases. Additional work that examines combination therapies that include CDK4/6 inhibitors in the treatment of primary or metastatic tumors will also be important. In addition to these studies, it will also be necessary to understand the differences in subcutaneous and intracranial tumor growth in the patient-derived xenografts of GBM. **Chapter 4** reveals that there are significant differences in sensitivity to palbociclib therapy between the flank and intracranial models, and it will be necessary to expand on this finding in order to understand the best preclinical model to test potential therapeutic options. In summary, these current discoveries, and the future answers to the questions they raise, will be important in translating any preclinical findings into the clinic. It will be essential to understand these specific concepts as they are related to the problem of treating

brain tumors in order to conduct preclinical studies that will be therapeutically relevant to patients.

BIBLIOGRAPHY

CHAPTER I

(2014) New Drugs at FDA: CDER's New Molecular Entities and New Therapeutic Biological Products of 2014, in, FDA.

Abbott NJ (2013) Blood-brain barrier structure and function and the challenges for CNS drug delivery. *Journal of inherited metabolic disease* **36**:437-449.

Agarwal S, Mittapalli RK, Zellmer DM, Gallardo JL, Donelson R, Seiler C, Decker Sa, Santacruz KS, Pokorny JL, Sarkaria JN, Elmquist WF and Ohlfest JR (2012) Active efflux of Dasatinib from the brain limits efficacy against murine glioblastoma: broad implications for the clinical use of molecularly targeted agents. *Molecular cancer therapeutics* **11**:2183-2192.

Agarwal S, Sane R, Gallardo JL, Ohlfest JR and Elmquist WF (2010) Distribution of Gefitinib to the Brain Is Limited by P-glycoprotein (ABCB1) and Breast Cancer Resistance Protein (ABCG2) -Mediated Active Efflux. **334**:147-155.

Agarwal S, Sane R, Oberoi R, Ohlfest JR and Elmquist WF (2011) Delivery of molecularly targeted therapy to malignant glioma, a disease of the whole brain. *Expert reviews in molecular medicine* **13**:e17-e17.

Anders CK, Adamo B, Karginova O, Deal AM, Rawal S, Darr D, Schorzman A, Santos C, Bash R, Kafri T, Carey L, Miller CR, Perou CM, Sharpless N and Zamboni WC (2013) Pharmacokinetics and efficacy of PEGylated liposomal doxorubicin in an intracranial model of breast cancer. *PloS one* **8**:e61359-e61359.

Angelov L, Doolittle ND, Kraemer DF, Siegal T, Barnett GH, Peereboom DM, Stevens G, McGregor J, Jahnke K, Lacy Ca, Hedrick Na, Shalom E, Ference S, Bell S, Sorenson L, Tyson RM, Haluska M and Neuwelt Ea (2009) Blood-brain barrier disruption and intra-arterial methotrexate-based therapy for newly diagnosed primary CNS lymphoma: a multi-institutional experience. *Journal of clinical oncology : official journal of the American Society of Clinical Oncology* **27**:3503-3509.

Bellavance M-A, Blanchette M and Fortin D (2008) Recent advances in blood-brain barrier disruption as a CNS delivery strategy. *The AAPS journal* **10**:166-177.

Berens ME and Giese a (1999) "...those left behind." Biology and oncology of invasive glioma cells. *Neoplasia (New York, NY)* **1**:208-219.

Blakeley JO, Olson J, Grossman Sa, He X, Weingart J and Supko JG (2009) Effect of blood brain barrier permeability in recurrent high grade gliomas on the intratumoral pharmacokinetics of methotrexate: a microdialysis study. *Journal of neuro-oncology* **91**:51-58.

Brandsma D, Kerklaan BM, Dieras V, Altintas S, Anders CK, Ballester MA, Gelderblom H, Soetekouw PMMB, Gladdines W, Lonnqvist F, Jager A, van Linde ME, Schellens J and Aftimos P (2014) 472P: Phase 1/2a study of glutathione PEGylated liposomal doxorubicin (2B3-101) in patients with brain metastases (BM) from solid tumors or recurrent high grade gliomas

(HGG) [abstract], in *European society of medical oncology 2014 Congress*, Madrid, Spain.

Bregy A, Shah AH, Diaz MV, Pierce HE, Ames PL, Diaz D and Komotar RJ (2013) The role of Gliadel wafers in the treatment of high-grade gliomas. *Expert review of anticancer therapy* **13**:1453-1461.

Brem H, Piantadosi S, Burger PC, Walker M, Selker R, Vick Na, Black K, Sisti M, Brem S, Mohr G, Muller P, Morawetz R and Schold SC (1995) Placebo-controlled trial of safety and efficacy of intraoperative controlled delivery by biodegradable polymers of chemotherapy for recurrent gliomas. *The Lancet* **345**:1008-1012.

Carlson BL, Pokorny JL, Schroeder MA and Sarkaria JN (2011) Establishment, maintenance and in vitro and in vivo applications of primary human glioblastoma multiforme (GBM) xenograft models for translational biology studies and drug discovery. *Current protocols in pharmacology / editorial board, SJ Enna (editor-in-chief) [et al]* **Chapter 14**:Unit 14.16-Unit 14.16.

Chamberlain MC (2011) Bevacizumab for the treatment of recurrent glioblastoma. *Clinical Medicine Insights Oncology* **5**:117-129.

Cloughesy TF, Cavenee WK and Mischel PS (2014) Glioblastoma: from molecular pathology to targeted treatment. *Annual review of pathology* **9**:1-25.

de Vries Na, Beijnen JH and van Tellingen O (2009) High-grade glioma mouse models and their applicability for preclinical testing. *Cancer treatment reviews* **35**:714-723.

del Amo EM, Urtti A and Yliperttula M (2008) Pharmacokinetic role of L-type amino acid transporters LAT1 and LAT2. *European journal of pharmaceutical sciences : official journal of the European Federation for Pharmaceutical Sciences* **35**:161-174.

Demeule M, Currie J-C, Bertrand Y, Ché C, Nguyen T, Régina A, Gabathuler R, Castaigne J-P and Béliveau R (2008) Involvement of the low-density lipoprotein receptor-related protein in the transcytosis of the brain delivery vector angiopep-2. *Journal of neurochemistry* **106**:1534-1544.

Dickens D, Webb SD, Antonyuk S, Giannoudis A, Owen A, Rädisch S, Hasnain SS and Pirmohamed M (2013) Transport of gabapentin by LAT1 (SLC7A5). *Biochemical pharmacology* **85**:1672-1683.

Fan C-H, Lin W-H, Ting C-Y, Chai W-Y, Yen T-C, Liu H-L and Yeh C-K (2014) Contrast-Enhanced Ultrasound Imaging for the Detection of Focused Ultrasound-Induced Blood-Brain Barrier Opening. *Theranostics* **4**:1014-1025.

Fazeny-Dörner B, Wenzel C, Veitl M, Piribauer M, Rössler K, Dieckmann K, Ungersböck K and Marosi C (2003) Survival and prognostic factors of patients with unresectable glioblastoma multiforme. *Anti-cancer drugs* **14**:305-312.

Fokas E, Steinbach JP and Rödel C (2013) Biology of brain metastases and novel targeted therapies: time to translate the research. *Biochimica et biophysica acta* **1835**:61-75.

Franceschi E, Stupp R, van den Bent MJ, van Herpen C, Laigle Donadey F, Gorlia T, Hegi M, Lhermitte B, Strauss LC, Allgeier A, Lacombe D and Brandes Aa (2012) EORTC 26083 phase I/II trial of dasatinib in combination with CCNU in patients with recurrent glioblastoma. *Neuro-oncology* **14**:1503-1510.

Friden PM, Walus LR, Musso GF, Taylor Ma, Malfroy B and Starzyk RM (1991) Anti-transferrin receptor antibody and antibody-drug conjugates cross the blood-brain barrier. *Proceedings of the National Academy of Sciences of the United States of America* **88**:4771-4775.

Gaillard PJ, Appeldoorn CCM, Dorland R, van Kregten J, Manca F, Vugts DJ, Windhorst B, van Dongen GaMS, de Vries HE, Maussang D and van Tellingen O (2014) Pharmacokinetics, brain delivery, and efficacy in brain tumor-bearing mice of glutathione pegylated liposomal doxorubicin (2B3-101). *PloS one* **9**:e82331-e82331.

Gállego Pérez-Larraya J and Hildebrand J (2014) Brain metastases. *Handbook of clinical neurology* **121**:1143-1157.

Gilbert MR, Dignam JJ, Armstrong TS, Wefel JS, Blumenthal DT, Vogelbaum Ma, Colman H, Chakravarti A, Pugh S, Won M, Jeraj R, Brown PD, Jaeckle Ka, Schiff D, Stieber VW, Brachman DG, Werner-Wasik M,

Tremont-Lukats IW, Sulman EP, Aldape KD, Curran WJ and Mehta MP (2014) A randomized trial of bevacizumab for newly diagnosed glioblastoma. *The New England journal of medicine* **370**:699-708.

Gomes P and Soares-da-Silva P (1999) L-DOPA transport properties in an immortalised cell line of rat capillary cerebral endothelial cells, RBE 4. *Brain research* **829**:143-150.

Grossman R, Tyler B, Rudek Ma, Kim E, Zadnik P, Khan U, Blakeley JO, Pathak AP and Brem H (2013) Microdialysis measurement of intratumoral temozolomide concentration after cediranib, a pan-VEGF receptor tyrosine kinase inhibitor, in a U87 glioma model. *Cancer chemotherapy and pharmacology* **72**:93-100.

Gynther M, Ropponen J, Laine K, Leppänen J, Haapakoski P, Peura L, Järvinen T and Rautio J (2009) Glucose promoiety enables glucose transporter mediated brain uptake of ketoprofen and indomethacin prodrugs in rats. *Journal of medicinal chemistry* **52**:3348-3353.

Heffron TP, Salphati L, Alicke B, Cheong J, Dotson J, Edgar K, Goldsmith R, Gould SE, Lee LB, Lesnick JD, Lewis C, Ndubaku C, Nonomiya J, Olivero AG, Pang J, Plise EG, Sideris S, Trapp S, Wallin J, Wang L and Zhang X (2012) The design and identification of brain penetrant inhibitors of phosphoinositide 3-kinase α. *Journal of medicinal chemistry* **55**:8007-8020.

Hofer S and Frei K (2007) Gefitinib concentrations in human glioblastoma tissue. *Journal of neuro-oncology* **82**:175-176.

Kalvass JC, Polli JW, Bourdet DL, Feng B, Huang SM, Liu X, Smith QR, Zhang LK and Zamek-Gliszczynski MJ (2013) Why clinical modulation of efflux transport at the human blood-brain barrier is unlikely: the ITC evidence-based position. *Clinical pharmacology and therapeutics* **94**:80-94.

Keles GE, Anderson B and Berger MS (1999) The effect of extent of resection on time to tumor progression and survival in patients with glioblastoma multiforme of the cerebral hemisphere. *Surgical Neurology* **52**:371-379.

Kreuter J (2014) Drug delivery to the central nervous system by polymeric nanoparticles: what do we know? *Advanced drug delivery reviews* **71**:2-14.

Kunwar S, Chang S, Westphal M, Vogelbaum M, Sampson J, Barnett G, Shaffrey M, Ram Z, Piepmeier J, Prados M, Croteau D, Pedain C, Leland P, Husain SR, Joshi BH and Puri RK (2010) Phase III randomized trial of CED of IL13-PE38QQR vs Gliadel wafers for recurrent glioblastoma. *Neuro-oncology* **12**:871-881.

Liu H-L, Fan C-H, Ting C-Y and Yeh C-K (2014) Combining microbubbles and ultrasound for drug delivery to brain tumors: current progress and overview. *Theranostics* **4**:432-444.

Lonser RR, Sarntinoranont M, Morrison PF and Oldfield EH (2014) Convection-enhanced delivery to the central nervous system. *Journal of neurosurgery*:1-10.

Maher Ea, Mietz J, Arteaga CL, DePinho Ra and Mohla S (2009) Brain metastasis: opportunities in basic and translational research. *Cancer research* **69**:6015-6020.

Mitragotri S (2005) Healing sound: the use of ultrasound in drug delivery and other therapeutic applications. *Nature reviews Drug discovery* **4**:255-260.

Mittapalli RK, Vaidhyanathan S, Sane R and Elmquist WF (2012) Impact of P-glycoprotein (ABCB1) and breast cancer resistance protein (ABCG2) on the brain distribution of a novel BRAF inhibitor: vemurafenib (PLX4032). *The Journal of pharmacology and experimental therapeutics* **342**:33-40.

Morrison PF, Laske DW, Bobo H, Oldfield EH and Dedrick RL (1994) High-flow microinfusion: tissue penetration and pharmacodynamics. *The American journal of physiology* **266**:R292-305.

Nayak L, Lee EQ and Wen PY (2012) Epidemiology of brain metastases. *Current oncology reports* **14**:48-54.

Neuwelt EA, Diehl JT, Vu LH, Hill SA, Michael AJ and Frenkel EP (1981) Monitoring of methotrexate delivery in patients with malignant brain tumors after osmotic blood-brain barrier disruption. *Annals of internal medicine* **94**:449-454.

O'Sullivan CC and Smith KL (2014) Therapeutic Considerations in Treating HER2-Positive Metastatic Breast Cancer. *Current breast cancer reports* **6**:169-182.

Ostrom QT, Gittleman H, Liao P, Rouse C, Chen Y, Dowling J, Wolinsky Y, Kruchko C and Barnholtz-Sloan J (2014) CBTRUS Statistical Report: Primary Brain and Central Nervous System Tumors Diagnosed in the United States in 2007-2011. *Neuro-oncology* **16 Suppl 4**:iv1-iv63.

Pafundi DH, Laack NN, Youland RS, Parney IF, Lowe VJ, Giannini C, Kemp BJ, Grams MP, Morris JM, Hoover JM, Hu LS, Sarkaria JN and Brinkmann DH (2013) Biopsy validation of 18F-DOPA PET and biodistribution in gliomas for neurosurgical planning and radiotherapy target delineation: results of a prospective pilot study. *Neuro-oncology* **15**:1058-1067.

Pardridge WM (2012) Drug transport across the blood-brain barrier. *Journal of cerebral blood flow and metabolism : official journal of the International Society of Cerebral Blood Flow and Metabolism* **32**:1959-1972.

Parsons DW, Jones S, Zhang X, Lin JC-H, Leary RJ, Angenendt P, Mankoo P, Carter H, Siu IM, Gallia GL, Olivi A, McLendon R, Rasheed BA, Keir S, Nikolskaya T, Nikolsky Y, Busam Da, Tekleab H, Diaz La, Hartigan J, Smith DR, Strausberg RL, Marie SKN, Shinjo SMO, Yan H, Riggins GJ, Bigner DD, Karchin R, Papadopoulos N, Parmigiani G, Vogelstein B, Velculescu VE and Kinzler KW (2008) An integrated genomic analysis of human glioblastoma multiforme. *Science (New York, NY)* **321**:1807-1812.

Peereboom DM, Shepard DR, Ahluwalia MS, Brewer CJ, Agarwal N, Stevens GHJ, Suh JH, Toms Sa, Vogelbaum Ma, Weil RJ, Elson P and Barnett GH (2010) Phase II trial of erlotinib with temozolomide and radiation in patients with newly diagnosed glioblastoma multiforme. *Journal of neuro-oncology* **98**:93-99.

Peuvrel L, Saint-Jean M, Quéreux G, Brocard a, Khammari a, Knol aC and Dréno B (2014) Incidence and characteristics of melanoma brain metastases developing during treatment with vemurafenib. *Journal of neuro-oncology* **120**:147-154.

Rapoport SI, Hori M and Klatzo I (1972) Testing of a hypothesis for osmotic opening of the blood-brain barrier. *The American journal of physiology* **223**:323-331.

Reardon Da, Vredenburgh JJ, Desjardins A, Peters KB, Sathornsumetee S, Threatt S, Sampson JH, Herndon JE, Coan A, McSherry F, Rich JN, McLendon RE, Zhang S and Friedman HS (2012) Phase 1 trial of dasatinib plus erlotinib in adults with recurrent malignant glioma. *Journal of neuro-oncology* **108**:499-506.

Rochet NM, Dronca RS, Kottschade La, Chavan RN, Gorman B, Gilbertson JR and Markovic SN (2012) Melanoma brain metastases and vemurafenib: need for further investigation. *Mayo Clinic proceedings* **87**:976-981.

Roth P and Weller M (2014) Challenges to targeting epidermal growth factor receptor in glioblastoma: escape mechanisms and combinatorial treatment strategies. *Neuro-oncology* **16**:viii14-viii19.

Salphati L, Shahidi-latham S, Quiason C, Barck K, Nishimura M, Alicke B, Pang J, Carano RA, Olivero AG and Phillips HS (2014) Accelerated Communication Distribution of the Phosphatidylinositol 3-Kinase Inhibitors Pictilisib (GDC-0941) and GNE-317 in U87 and GS2 Intracranial Glioblastoma Models — Assessment by Matrix-Assisted Laser Desorption Ionization Imaging.1110-1116.

Sampson JH, Archer G, Pedain C, Wembacher-Schröder E, Westphal M, Kunwar S, Vogelbaum Ma, Coan A, Herndon JE, Raghavan R, Brady ML, Reardon Da, Friedman AH, Friedman HS, Rodríguez-Ponce MI, Chang SM, Mittermeyer S, Croteau D and Puri RK (2010) Poor drug distribution as a possible explanation for the results of the PRECISE trial. *Journal of neurosurgery* **113**:301-309.

Shi L, Palacio-mancheno P, Badami J, Zeng M, Cardoso L, Tu R and Fu BM (2014) Quantification of transient increase of the blood – brain barrier permeability to macromolecules by optimized focused ultrasound combined with microbubbles.4437-4448.

Stemmler H-J and Heinemann V (2008) Central nervous system metastases in HER-2-overexpressing metastatic breast cancer: a treatment challenge. *The oncologist* **13**:739-750.

Stupp R, Mason WP, van den Bent MJ, Weller M, Fisher B, Taphoorn MJB, Belanger K, Brandes AA, Marosi C, Bogdahn U, Curschmann J, Janzer RC, Ludwin SK, Gorlia T, Allgeier A, Lacombe D, Cairncross JG, Eisenhauer E and Mirimanoff RO (2005) Radiotherapy plus concomitant and adjuvant temozolomide for glioblastoma. *The New England journal of medicine* **352**:987-996.

Szerlip NJ, Pedraza A, Chakravarty D, Azim M, McGuire J, Fang Y, Ozawa T, Holland EC, Huse JT, Jhanwar S, Leversha Ma, Mikkelsen T and Brennan CW (2012) Intratumoral heterogeneity of receptor tyrosine kinases EGFR and PDGFRA amplification in glioblastoma defines subpopulations with distinct growth factor response. *Proceedings of the National Academy of Sciences of the United States of America* **109**:3041-3046.

Thompson EM, Frenkel EP and Neuwelt Ea (2011) The paradoxical effect of bevacizumab in the therapy of malignant gliomas. *Neurology* **76**:87-93.

Trunzer K, Pavlick AC, Schuchter L, Gonzalez R, McArthur Ga, Hutson TE, Moschos SJ, Flaherty KT, Kim KB, Weber JS, Hersey P, Long GV, Lawrence D, Ott Pa, Amaravadi RK, Lewis KD, Puzanov I, Lo RS, Koehler A, Kockx M, Spleiss O, Schell-Steven A, Gilbert HN, Cockey L, Bollag G, Lee RJ, Joe AK, Sosman Ja and Ribas A (2013) Pharmacodynamic effects and mechanisms of resistance to vemurafenib in patients with metastatic melanoma. *Journal of clinical oncology : official journal of the American Society of Clinical Oncology* **31**:1767-1774.

Uchida Y, Ohtsuki S, Katsukura Y, Ikeda C, Suzuki T, Kamiie J and Terasaki T (2011) Quantitative targeted absolute proteomics of human blood-brain barrier transporters and receptors. *Journal of neurochemistry* **117**:333-345.

Uhm JH, Ballman KV, Wu W, Giannini C, Krauss JC, Buckner JC, James CD, Scheithauer BW, Behrens RJ, Flynn PJ, Schaefer PL, Dakhill SR and Jaeckle Ka (2011) Phase II evaluation of gefitinib in patients with newly diagnosed Grade 4 astrocytoma: Mayo/North Central Cancer Treatment Group Study N0074. *International journal of radiation oncology, biology, physics* **80**:347-353.

Vitucci M, Hayes DN and Miller CR (2011) Gene expression profiling of gliomas: merging genomic and histopathological classification for personalised therapy. *British journal of cancer* **104**:545-553.

Wen PY and Kesari S (2008) Malignant gliomas in adults. *The New England journal of medicine* **359**:492-507.

Westphal M, Hilt DC, Bortey E, Delavault P, Olivares R, Warnke PC, Whittle IR, Jääskeläinen J and Ram Z (2003) A phase 3 trial of local chemotherapy with biodegradable carmustine (BCNU) wafers (Gliadel wafers) in patients with primary malignant glioma. *Neuro-oncology* **5**:79-88.

Wiesner SM, Decker Sa, Larson JD, Ericson K, Forster C, Gallardo JL, Long C, Demorest ZL, Zamora Ea, Low WC, SantaCruz K, Largaespada Da and

Ohlfest JR (2009) De novo induction of genetically engineered brain tumors in mice using plasmid DNA. *Cancer research* **69**:431-439.

Yoon DJ, Kwan BH, Chao FC, Nicolaides TP, Phillips JJ, Lam GY, Mason AB, Weiss Wa and Kamei DT (2010) Intratumoral therapy of glioblastoma multiforme using genetically engineered transferrin for drug delivery. *Cancer research* **70**:4520-4527.

Youland RS, Kitange GJ, Peterson TE, Pafundi DH, Ramiscal Ja, Pokorny JL, Giannini C, Laack NN, Parney IF, Lowe VJ, Brinkmann DH and Sarkaria JN (2013) The role of LAT1 in (18)F-DOPA uptake in malignant gliomas. *Journal of neuro-oncology* **111**:11-18.

Yu YJ, Zhang Y, Kenrick M, Hoyte K, Luk W, Lu Y, Atwal J, Elliott JM, Prabhu S, Watts RJ and Dennis MS (2011) Boosting brain uptake of a therapeutic antibody by reducing its affinity for a transcytosis target. *Science translational medicine* **3**:84ra44-84ra44.

Zhang P, Hu L, Yin Q, Feng L and Li Y (2012) Transferrin-modified c[RGDfK]-paclitaxel loaded hybrid micelle for sequential blood-brain barrier penetration and glioma targeting therapy. *Molecular pharmaceutics* **9**:1590-1598.

Zollinger R (1935) Removal of Left Cerebral Hemisphere. *Archives of Neurology and Psychiatry* **34**:1055-1064.

(2008) Comprehensive genomic characterization defines human glioblastoma genes and core pathways. *Nature* **455**:1061-1068.

Abbott NJ (2013) Blood-brain barrier structure and function and the challenges for CNS drug delivery. *Journal of inherited metabolic disease* **36**:437-449.

Agarwal S, Hartz AMS, Elmquist WF and Bauer B (2011) Breast cancer resistance protein and P-glycoprotein in brain cancer: two gatekeepers team up. *Current pharmaceutical design* **17**:2793-2802.

Agarwal S, Manchanda P, Vogelbaum Ma, Ohlfest JR and Elmquist WF (2013) Function of the blood-brain barrier and restriction of drug delivery to invasive glioma cells: Findings in an orthotopic rat xenograft model of glioma. *Drug Metabolism and Disposition* **41**:33-39.

Agarwal S, Sane R, Gallardo JL, Ohlfest JR and Elmquist WF (2010) Distribution of Gefitinib to the Brain Is Limited by P-glycoprotein (ABCB1) and Breast Cancer Resistance Protein (ABCG2) -Mediated Active Efflux. **334**:147-155.

Akhavan D, Cloughesy TF and Mischel PS (2010) mTOR signaling in glioblastoma: lessons learned from bench to bedside. *Neuro-oncology* **12**:882-889.

Alifieris C and Trafalis DT (2015) Glioblastoma multiforme: Pathogenesis and treatment. *Pharmacology & Therapeutics* **152**:63-82.

Asghar U, Witkiewicz AK, Turner NC and Knudsen ES (2015) The history and future of targeting cyclin-dependent kinases in cancer therapy. *Nature reviews Drug discovery* **14**:130-146.

Barton KL, Misuraca K, Cordero F, Dobrikova E, Min HD, Gromeier M, Kirsch DG and Becher OJ (2013) PD-0332991, a CDK4/6 Inhibitor, Significantly Prolongs Survival in a Genetically Engineered Mouse Model of Brainstem Glioma. *PLoS ONE* **8**:1-7.

Berens ME and Giese a (1999) "...those left behind." Biology and oncology of invasive glioma cells. *Neoplasia (New York, NY)* **1**:208-219.

Brennan Cameron W, Verhaak Roel GW, McKenna A, Campos B, Noushmehr H, Salama Sofie R, Zheng S, Chakravarty D, Sanborn JZ, Berman Samuel H, Beroukhim R, Bernard B, Wu C-J, Genovese G, Shmulevich I, Barnholtz-Sloan J, Zou L, Vegesna R, Shukla Sachet A, Ciriello G, Yung WK, Zhang W, Sougnez C, Mikkelsen T, Aldape K, Bigner Darell D, Van Meir Erwin G, Prados M, Sloan A, Black Keith L, Eschbacher J, Finocchiaro G, Friedman W, Andrews David W, Guha A, Iacocca M, O'Neill Brian P, Foltz G, Myers J, Weisenberger Daniel J, Penny R, Kucherlapati R, Perou Charles M, Hayes DN, Gibbs R, Marra M, Mills Gordon B, Lander E, Spellman P, Wilson R, Sander C, Weinstein J, Meyerson M, Gabriel S, Laird Peter W, Haussler D, Getz G and Chin L (2013) The Somatic Genomic Landscape of Glioblastoma. *Cell* **155**:462-477.

Brower V (2014) Cell cycle inhibitors make progress. *Journal of the National Cancer Institute* **106**:dju225-dju225.

Cadoo Ka, Gucalp A and Traina Ta (2014) Palbociclib : an evidence-based review of its potential in the treatment of breast cancer. *Breast Cancer (Dove Med Press)* **4**:123-133.

Chamberlain MC (2011) Bevacizumab for the treatment of recurrent glioblastoma. *Clinical Medicine Insights Oncology* **5**:117-129.

Cicenas J, Kalyan K, Sorokinas A, Jatulyte A, Valiunas D, Kaupinis A and Valius M (2014) Highlights of the Latest Advances in Research on CDK Inhibitors. *Cancers*:2224-2242.

Cloughesy TF, Cavenee WK and Mischel PS (2014) Glioblastoma: from molecular pathology to targeted treatment. *Annual review of pathology* **9**:1-25.

Cohen MH, Shen YL, Keegan P and Pazdur R (2009) FDA drug approval summary: bevacizumab (Avastin) as treatment of recurrent glioblastoma multiforme. *The oncologist* **14**:1131-1138.

de Gooijer MC, Zhang P, Thota N, Mayayo-Peralta I, Buil LCM, Beijnen JH and van Tellingen O (2015) P-glycoprotein and breast cancer resistance protein restrict the brain penetration of the CDK4/6 inhibitor palbociclib. *Investigational New Drugs*.

Dhermain FG, Hau P, Lanfermann H, Jacobs AH and van den Bent MJ (2010) Advanced MRI and PET imaging for assessment of treatment response in patients with gliomas. *The Lancet Neurology* **9**:906-920.

Dhillon S (2015) Palbociclib: First Global Approval. *Drugs* **75**:543-551.

Dickson Ma (2014) Molecular Pathways: CDK4 Inhibitors for Cancer Therapy. *Clinical cancer research : an official journal of the American Association for Cancer Research* **20**:3379-3383.

Duzgun Z, Eroglu Z and Biray Avci C (2016) Role of mTOR in glioblastoma. *Gene* **575**:187-190.

Flaherty KT, LoRusso PM, DeMichele A, Abramson VG, Courtney R, Randolph SS, Shaik MN, Wilner KD, O'Dwyer PJ and Schwartz GK (2012) Phase I, dose-escalation trial of the oral cyclin-dependent kinase 4/6 inhibitor PD 0332991, administered using a 21-day schedule in patients with advanced cancer. *Clinical Cancer Research* **18**:568-576.

Hanahan D and Weinberg RA (2000) The hallmarks of cancer. *Cell* **100**:57-70.

Jhanwar-Uniyal M, Albert L, McKenna E, Karsy M, Rajdev P, Braun A and Murali R (2011) Deciphering the signaling pathways of cancer stem cells of glioblastoma multiforme: Role of Akt/mTOR and MAPK pathways. *Advances in Enzyme Regulation* **51**:164-170.

Jhanwar-Uniyal M, Labagnara M, Friedman M, Kwasnicki A and Murali R (2015) Glioblastoma: Molecular Pathways, Stem Cells and Therapeutic Targets. *Cancers* **7**:538-555.

Karar J and Maity A (2011) PI3K/AKT/mTOR Pathway in Angiogenesis. *Frontiers in molecular neuroscience* **4**:51-51.

Kodaira H, Kusuhara H, Ushiki J, Fuse E and Sugiyama Y (2010) Kinetic analysis of the cooperation of P-glycoprotein (P-gp/Abcb1) and breast cancer resistance protein (Bcrp/Abcg2) in limiting the brain and testis penetration of erlotinib, flavopiridol, and mitoxantrone. *The Journal of pharmacology and experimental therapeutics* **333**:788-796.

Malumbres M (2014) Cyclin-dependent kinases. *Genome Biology* **15**:122-122.

Malumbres M and Barbacid M (2005) Mammalian cyclin-dependent kinases. *Trends in Biochemical Sciences* **30**:630-641.

Malumbres M, Harlow E, Hunt T, Hunter T, Lahti JM, Manning G, Morgan DO, Tsai L-H and Wolgemuth DJ (2009) Cyclin-dependent kinases: a family portrait. *Nature cell biology* **11**:1275-1276.

Mariaule G and Belmont P (2014) Cyclin-Dependent Kinase Inhibitors as Marketed Anticancer Drugs: Where Are We Now? A Short Survey. *Molecules* **19**:14366-14382.

Michaud K, Solomon Da, Oermann E, Kim J-S, Zhong W-Z, Prados MD, Ozawa T, James CD and Waldman T (2010) Pharmacologic inhibition of cyclin-dependent kinases 4 and 6 arrests the growth of glioblastoma multiforme intracranial xenografts. *Cancer research* **70**:3228-3238.

Oberoi RK, Parrish KE, Sio TT, Mittapalli RK, Elmquist WF and Sarkaria JN (2015) Strategies to improve delivery of anticancer drugs across the blood–brain barrier to treat glioblastoma. *Neuro-Oncology*:nov164-nov164.

Onishi M, Ichikawa T, Kurozumi K and Date I (2011) Angiogenesis and invasion in glioma. *Brain tumor pathology* **28**:13-24.

Pafundi DH, Laack NN, Youland RS, Parney IF, Lowe VJ, Giannini C, Kemp BJ, Grams MP, Morris JM, Hoover JM, Hu LS, Sarkaria JN and Brinkmann DH (2013) Biopsy validation of 18F-DOPA PET and biodistribution in gliomas for neurosurgical planning and radiotherapy target delineation: results of a prospective pilot study. *Neuro-oncology* **15**:1058-1067.

Pandey V, Bhaskara VK and Babu PP (2015) Implications of mitogen-activated protein kinase signaling in glioma. *Journal of Neuroscience Research* **00**:n/a-n/a.

Parrish K, Sarkaria J and Elmquist W (2015) Improving drug delivery to primary and metastatic brain tumors: Strategies to overcome the blood-brain barrier. *Clinical Pharmacology & Therapeutics* **97**:336-346.

Peyressatre M, Prével C, Pellerano M and Morris M (2015) Targeting Cyclin-Dependent Kinases in Human Cancers: From Small Molecules to Peptide Inhibitors. *Cancers* **7**:179-237.

Prados MD, Byron SA, Tran NL, Phillips JJ, Molinaro AM, Ligon KL, Wen PY, Kuhn JG, Mellinghoff IK, de Groot JF, Colman H, Cloughesy TF, Chang SM, Ryken TC, Tembe WD, Kiefer JA, Berens ME, Craig DW, Carpten JD

and Trent JM (2015a) Toward precision medicine in glioblastoma: the promise and the challenges. *Neuro-Oncology* **17**:1051-1063.

Prados MD, Byron Sa, Tran NL, Phillips JJ, Molinaro aM, Ligon KL, Wen PY, Kuhn JG, Mellinghoff IK, de Groot JF, Colman H, Cloughesy TF, Chang SM, Ryken TC, Tembe WD, Kiefer Ja, Berens ME, Craig DW, Carpten JD and Trent JM (2015f) Toward precision medicine in glioblastoma: the promise and the challenges. *Neuro-Oncology* **17**:1051-1063.

Puyol M, Martín A, Dubus P, Mulero F, Pizcueta P, Khan G, Guerra C, Santamaría D and Barbacid M (2010) A Synthetic Lethal Interaction between K-Ras Oncogenes and Cdk4 Unveils a Therapeutic Strategy for Non-small Cell Lung Carcinoma. *Cancer Cell* **18**:63-73.

Raub TJ, Gelbert LM, Wishart GN, Sanchez-Martinez C, Kulanthaivel P, Staton Ba, Ajamie RT, Sawada Ga, Shannon HE and De Dios a (2015) Brain Exposure of Two Selective Dual CDK4 and CDK6 Inhibitors and the Antitumor Activity of CDK4 and 6 Inhibition in Combination with Temozolomide in an Intracranial Glioblastoma Xenograft. *Drug Metabolism and Disposition*.

Reardon DA, Desjardins A, Rich JN and Vredenburgh JJ (2008a) The emerging role of anti-angiogenic therapy for malignant glioma. *Current treatment options in oncology* **9**:1-22.

Reardon DA, Ligon KL, Chiocca EA and Wen PY (2015) One size should not fit all: advancing toward personalized glioblastoma therapy. *Discovery medicine* **19**:471-477.

Reardon DA, Wen PY, Desjardins A, Batchelor TT and Vredenburgh JJ (2008b) Glioblastoma multiforme: an emerging paradigm of anti-VEGF therapy. *Expert opinion on biological therapy* **8**:541-553.

Rivadeneira DB, Mayhew CN, Thangavel C, Sotillo E, Reed Ca, Graña X and Knudsen ES (2010) Proliferative suppression by CDK4/6 inhibition: complex function of the retinoblastoma pathway in liver tissue and hepatoma cells. *Gastroenterology* **138**:1920-1930.

Ruas M and Peters G (1998) The p16INK4a/CDKN2A tumor suppressor and its relatives. *Biochimica et biophysica acta* **1378**:F115-F177.

Salphati L, Heffron TP, Alicke B, Nishimura M, Barck K, Carano Ra, Cheong J, Edgar Ka, Greve J, Kharbanda S, Koeppen H, Lau S, Lee LB, Pang J, Plise EG, Pokorny JL, Reslan HB, Sarkaria JN, Wallin JJ, Zhang X, Gould SE, Olivero AG and Phillips HS (2012) Targeting the PI3K pathway in the brain--efficacy of a PI3K inhibitor optimized to cross the blood-brain barrier. *Clinical cancer research : an official journal of the American Association for Cancer Research* **18**:6239-6248.

Salphati L, Shahidi-latham S, Quiason C, Barck K, Nishimura M, Alicke B, Pang J, Carano RA, Olivero AG and Phillips HS (2014) Accelerated Communication Distribution of the Phosphatidylinositol 3-Kinase Inhibitors

Pictilisib (GDC-0941) and GNE-317 in U87 and GS2 Intracranial Glioblastoma Models — Assessment by Matrix-Assisted Laser Desorption Ionization Imaging.1110-1116.

Sánchez-Martínez C, Gelbert LM, Lallena MJ and Dios AD (2015) Cyclin Dependent Kinase (CDK) inhibitors as anticancer drugs. *Bioorganic & Medicinal Chemistry Letters* **25**:3420-3435.

Schmidt EE, Ichimura K, Reifenberger G and Collins VP (1994) CDKN2 (p16/MTS1) gene deletion or CDK4 amplification occurs in the majority of glioblastomas. *Cancer Research* **54**:6321-6324.

Schröder LBW and McDonald KL (2015) CDK4/6 Inhibitor PD0332991 in Glioblastoma Treatment: Does It Have a Future? *Frontiers in oncology* **5**:259-259.

Sherr CJ and Roberts JM (1999) CDK inhibitors: positive and negative regulators of G1-phase progression. *Genes & development* **13**:1501-1512.

Sherr CJ and Roberts JM (2004) Living with or without cyclins and cyclin-dependent kinases. *Genes & development* **18**:2699-2711.

Stupp R, Mason WP, van den Bent MJ, Weller M, Fisher B, Taphoorn MJB, Belanger K, Brandes AA, Marosi C, Bogdahn U, Curschmann J, Janzer RC, Ludwin SK, Gorlia T, Allgeier A, Lacombe D, Cairncross JG, Eisenhauer E and Mirimanoff RO (2005) Radiotherapy plus concomitant and adjuvant temozolomide for glioblastoma. *The New England journal of medicine* **352**:987-996.

Takano S, Yamashita T and Ohneda O (2010) Molecular therapeutic targets for glioma angiogenesis. *Journal of oncology* **2010**:351908-351908.

Takano S, Yoshii Y, Kondo S, Suzuki H, Maruno T, Shirai S and Nose T (1996) Concentration of vascular endothelial growth factor in the serum and tumor tissue of brain tumor patients. *Cancer Res* **56**:2185-2190.

Taylor TE, Furnari FB and Cavenee WK (2012) Targeting EGFR for treatment of glioblastoma: molecular basis to overcome resistance. *Current cancer drug targets* **12**:197-209.

van Tellingen O, Yetkin-Arik B, de Gooijer MC, Wesseling P, Wurdinger T and de Vries HE (2015) Overcoming the blood-brain tumor barrier for effective glioblastoma treatment. *Drug Resistance Updates*:1-12.

VanArsdale T, Boshoff C, Arndt KT and Abraham RT (2015) Molecular Pathways: Targeting the Cyclin D-CDK4/6 Axis for Cancer Treatment. *Clinical cancer research : an official journal of the American Association for Cancer Research* **21**:2905-2910.

Vidula N and Rugo HS (2015) Cyclin-Dependent Kinase 4/6 Inhibitors for the Treatment of Breast Cancer: A Review of Preclinical and Clinical Data. *Clinical Breast Cancer*:1-10.

Vredenburgh JJ, Desjardins A, Ii JEH, Dowell JM, Reardon DA, Quinn J, Rich JN, Sathornsumetee S, Gururangan S, Wagner M, Bigner DD and Friedman AH (2007) Cancer Therapy : Clinical Phase II T rial of

Bevacizumab and Irinotecan in Recurrent Malignant Glioma. **13**:1253-1260.

Wong MLH, Prawira A, Kaye AH and Hovens CM (2009) Tumour angiogenesis : Its mechanism and therapeutic implications in malignant gliomas. *Journal of Clinical Neuroscience* **16**:1119-1130.

Yadav V, Burke TF, Huber L, Van Horn RD, Zhang Y, Buchanan SG, Chan EM, Starling JJ, Beckmann RP and Peng S-B (2014a) The CDK4/6 inhibitor LY2835219 overcomes vemurafenib resistance resulting from MAPK reactivation and cyclin D1 upregulation. *Molecular cancer therapeutics* **13**:2253-2263.

Yadav V, Chen S-H, Yue YG, Buchanan S, Beckmann RP and Peng S-B (2014b) Co-targeting BRAF and cyclin dependent kinases 4/6 for BRAF mutant cancers. *Pharmacology & Therapeutics* **149**:139-149.

Young RJ, Waldeck K, Martin C, Foo JH, Cameron DP, Kirby L, Do H, Mitchell C, Cullinane C, Liu W, Fox SB, Dutton-Regester K, Hayward NK, Jene N, Dobrovic A, Pearson RB, Christensen JG, Randolph S, McArthur Ga and Sheppard KE (2014) Loss of CDKN2A expression is a frequent event in primary invasive melanoma and correlates with sensitivity to the CDK4/6 inhibitor PD0332991 in melanoma cell lines. *Pigment Cell and Melanoma Research* **27**:590-600.

Yu Q, Sicinska E, Geng Y, Ahnström M, Zagozdzon A, Kong Y, Gardner H, Kiyokawa H, Harris LN, Stål O and Sicinski P (2006) Requirement for CDK4 kinase function in breast cancer. *Cancer Cell* **9**:23-32.

Zuo L, Weger J, Yang Q, Goldstein AM, Tucker MA, Walker GJ, Hayward N and Dracopoli NC (1996) Germline mutations in the p16INK4a binding domain of CDK4 in familial melanoma. *Nature Genetics* **12**:97-99.

CHAPTER III

Abbott NJ (2013) Blood-brain barrier structure and function and the challenges for CNS drug delivery. *Journal of inherited metabolic disease* **36**:437-449.

Agarwal S, Hartz AMS, Elmquist WF and Bauer B (2011a) Breast cancer resistance protein and P-glycoprotein in brain cancer: two gatekeepers team up. *Current pharmaceutical design* **17**:2793-2802.

Agarwal S, Sane R, Gallardo JL, Ohlfest JR and Elmquist WF (2010) Distribution of Gefitinib to the Brain Is Limited by P-glycoprotein (ABCB1) and Breast Cancer Resistance Protein (ABCG2) -Mediated Active Efflux. **334**:147-155.

Agarwal S, Sane R, Oberoi R, Ohlfest JR and Elmquist WF (2011b) Delivery of molecularly targeted therapy to malignant glioma, a disease of the whole brain. *Expert reviews in molecular medicine* **13**:e17-e17.

Agarwal S, Sane R, Ohlfest JR and Elmquist WF (2011d) The Role of the Breast Cancer Resistance Protein (ABCG2) in the Distribution of Sorafenib to the Brain. **336**:223-233.

Barton KL, Misuraca K, Cordero F, Dobrikova E, Min HD, Gromeier M, Kirsch DG and Becher OJ (2013) PD-0332991, a CDK4/6 Inhibitor, Significantly Prolongs Survival in a Genetically Engineered Mouse Model of Brainstem Glioma. *PLoS ONE* **8**:1-7.

Baughn LB, Di Liberto M, Wu K, Toogood PL, Louie T, Gottschalk R, Niesvizky R, Cho H, Ely S, Moore MaS and Chen-Kiang S (2006) A novel orally active small molecule potently induces G1 arrest in primary myeloma cells and prevents tumor growth by specific inhibition of cyclin-dependent kinase 4/6. *Cancer Research* **66**:7661-7667.

Cancer Genome Atlas Research N (2008) Comprehensive genomic characterization defines human glioblastoma genes and core pathways. *Nature* **455**:1061-1068.

Carlson BL, Pokorny JL, Schroeder MA and Sarkaria JN (2011) Establishment, maintenance and in vitro and in vivo applications of primary human glioblastoma multiforme (GBM) xenograft models for translational biology studies and drug discovery. *Current protocols in pharmacology / editorial board, SJ Enna (editor-in-chief) [et al]* **Chapter 14**:Unit 14.16-Unit 14.16.

Cen L, Carlson BL, Schroeder Ma, Ostrem JL, Kitange GJ, Mladek AC, Fink SR, Decker Pa, Wu W, Kim J-S, Waldman T, Jenkins RB and Sarkaria JN (2012) p16-Cdk4-Rb axis controls sensitivity to a cyclin-dependent kinase inhibitor PD0332991 in glioblastoma xenograft cells. *Neuro-oncology* **14**:870-881.

de Gooijer MC, Zhang P, Thota N, Mayayo-Peralta I, Buil LCM, Beijnen JH and van Tellingen O (2015) P-glycoprotein and breast cancer resistance protein restrict the brain penetration of the CDK4/6 inhibitor palbociclib. *Investigational New Drugs*.

de Vries Na, Beijnen JH and van Tellingen O (2009) High-grade glioma mouse models and their applicability for preclinical testing. *Cancer treatment reviews* **35**:714-723.

Fife KM, Colman MH, Stevens GN, Firth IC, Moon D, Shannon KF, Harman R, Petersen-Schaefer K, Zacest aC, Besser M, Milton GW, McCarthy WH and Thompson JF (2004) Determinants of outcome in melanoma patients with cerebral metastases. *Journal of Clinical Oncology* **22**:1293-1300.

Finn RS, Crown JP, Lang I, Boer K, Bondarenko IM, Kulyk SO, Ettl J, Patel R, Pinter T, Schmidt M, Shparyk Y, Thummala AR, Voytko NL, Fowst C, Huang X, Kim ST, Randolph S and Slamon DJ (2014) The cyclin-dependent kinase 4/6 inhibitor palbociclib in combination with letrozole versus letrozole alone as first-line treatment of oestrogen receptor-positive, HER2-negative, advanced breast cancer (PALOMA-1/TRIO-18): a randomised phase 2 study. *The Lancet Oncology* **16**:25-35.

Fry DW, Harvey PJ, Keller PR, Elliott WL, Meade M, Trachet E, Albassam M, Zheng X, Leopold WR, Pryer NK and Toogood PL (2004) Specific inhibition of cyclin-dependent kinase 4/6 by PD 0332991 and associated antitumor activity in human tumor xenografts. *Molecular cancer therapeutics* **3**:1427-1438.

Gállego Pérez-Larraya J and Hildebrand J (2014) Brain metastases. *Handbook of clinical neurology* **121**:1143-1157.

Maher Ea, Mietz J, Arteaga CL, DePinho Ra and Mohla S (2009) Brain metastasis: opportunities in basic and translational research. *Cancer research* **69**:6015-6020.

Michaud K, Solomon Da, Oermann E, Kim J-S, Zhong W-Z, Prados MD, Ozawa T, James CD and Waldman T (2010) Pharmacologic inhibition of cyclin-dependent kinases 4 and 6 arrests the growth of glioblastoma multiforme intracranial xenografts. *Cancer research* **70**:3228-3238.

Mittapalli RK, Vaidhyanathan S, Sane R and Elmquist WF (2012) Impact of P-glycoprotein (ABCB1) and breast cancer resistance protein (ABCG2) on the brain distribution of a novel BRAF inhibitor: vemurafenib (PLX4032). *The Journal of pharmacology and experimental therapeutics* **342**:33-40.

Musgrove Ea, Caldon CE, Barraclough J, Stone A and Sutherland RL (2011) Cyclin D as a therapeutic target in cancer. *Nature reviews Cancer* **11**:558-572.

O'Sullivan CC and Smith KL (2014) Therapeutic Considerations in Treating HER2-Positive Metastatic Breast Cancer. *Current breast cancer reports* **6**:169-182.

Parrish K, Sarkaria J and Elmquist W (2015) Improving drug delivery to primary and metastatic brain tumors: Strategies to overcome the blood-brain barrier. *Clinical Pharmacology & Therapeutics* **97**:336-346.

Peuvrel L, Saint-Jean M, Quéreux G, Brocard a, Khammari a, Knol aC and Dréno B (2014) Incidence and characteristics of melanoma brain

metastases developing during treatment with vemurafenib. *Journal of neuro-oncology* **120**:147-154.

Peyressatre M, Prével C, Pellerano M and Morris M (2015) Targeting Cyclin-Dependent Kinases in Human Cancers: From Small Molecules to Peptide Inhibitors. *Cancers* **7**:179-237.

Pokorny JL, Calligaris D, Gupta SK, Iyekegbe DO, Mueller D, Bakken KK, Carlson BL, Schroeder Ma, Evans DL, Lou Z, Decker Pa, Eckel-Passow J, Pucci V, Ma B, Shumway SD, Elmquist WF, Agar NY and Sarkaria JN (2015) The efficacy of the Wee1 inhibitor MK-1775 combined with temozolomide is limited by heterogeneous distribution across the blood-brain barrier in glioblastoma. *Clinical Cancer Research* **21**:1916-1925.

Raub TJ, Gelbert LM, Wishart GN, Sanchez-Martinez C, Kulanthaivel P, Staton Ba, Ajamie RT, Sawada Ga, Shannon HE and De Dios a (2015) Brain Exposure of Two Selective Dual CDK4 and CDK6 Inhibitors and the Antitumor Activity of CDK4 and 6 Inhibition in Combination with Temozolomide in an Intracranial Glioblastoma Xenograft. *Drug Metabolism and Disposition*.

Salphati L, Shahidi-latham S, Quiason C, Barck K, Nishimura M, Alicke B, Pang J, Carano RA, Olivero AG and Phillips HS (2014) Accelerated Communication Distribution of the Phosphatidylinositol 3-Kinase Inhibitors Pictilisib (GDC-0941) and GNE-317 in U87 and GS2 Intracranial

Glioblastoma Models — Assessment by Matrix-Assisted Laser Desorption Ionization Imaging.1110-1116.

Sane R, Mittapalli RK and Elmquist WF (2013) Development and evaluation of a novel microemulsion formulation of elacridar to improve its bioavailability. *Journal of Pharmaceutical Sciences* **102**:1343-1354.

Stupp R, Mason WP, van den Bent MJ, Weller M, Fisher B, Taphoorn MJB, Belanger K, Brandes AA, Marosi C, Bogdahn U, Curschmann J, Janzer RC, Ludwin SK, Gorlia T, Allgeier A, Lacombe D, Cairncross JG, Eisenhauer E and Mirimanoff RO (2005) Radiotherapy plus concomitant and adjuvant temozolomide for glioblastoma. *The New England journal of medicine* **352**:987-996.

Thangavel C, Boopathi E, Ertel A, Lim M, Addya S, Fortina P, Witkiewicz AK and Knudsen ES (2013) Regulation of miR106b cluster through the RB pathway: mechanism and functional targets. *Cell cycle (Georgetown, Tex)* **12**:98-111.

Turner NC, Ro J, André F, Loi S, Verma S, Iwata H, Harbeck N, Loibl S, Huang Bartlett C, Zhang K, Giorgetti C, Randolph S, Koehler M and Cristofanilli M (2015) Palbociclib in Hormone-Receptor–Positive Advanced Breast Cancer. *New England Journal of Medicine*:150601063747007-150601063747007.

Uchida Y, Ohtsuki S, Katsukura Y, Ikeda C, Suzuki T, Kamiie J and Terasaki T (2011) Quantitative targeted absolute proteomics of human blood-brain

barrier transporters and receptors. *Journal of neurochemistry* **117**:333-345.

VanArsdale T, Boshoff C, Arndt KT and Abraham RT (2015) Molecular Pathways: Targeting the Cyclin D-CDK4/6 Axis for Cancer Treatment. *Clinical Cancer Research*.

Wang T, Agarwal S and Elmquist WF (2012) Brain distribution of cediranib is limited by active efflux at the blood-brain barrier. *The Journal of pharmacology and experimental therapeutics* **341**:386-395.

(2008) Comprehensive genomic characterization defines human glioblastoma genes and core pathways. *Nature* **455**:1061-1068.

Abbott NJ (2013) Blood-brain barrier structure and function and the challenges for CNS drug delivery. *J Inherit Metab Dis* **36**:437-449.

Agarwal S, Hartz AM, Elmquist WF and Bauer B (2011) Breast cancer resistance protein and P-glycoprotein in brain cancer: two gatekeepers team up. *Curr Pharm Des* **17**:2793-2802.

Agarwal S, Manchanda P, Vogelbaum MA, Ohlfest JR and Elmquist WF (2013) Function of the blood-brain barrier and restriction of drug delivery to invasive glioma cells: findings in an orthotopic rat xenograft model of glioma. *Drug Metab Dispos* **41**:33-39.

Alonso-Camino V, Rajani K, Kottke T, Rommelfanger-Konkol D, Zaidi S, Thompson J, Pulido J, Ilett E, Donnelly O, Selby P, Pandha H, Melcher A, Harrington K, Diaz RM and Vile R (2014) The profile of tumor antigens which can be targeted by immunotherapy depends upon the tumor's anatomical site. *Mol Ther* **22**:1936-1948.

Asghar U, Witkiewicz AK, Turner NC and Knudsen ES (2015) The history and future of targeting cyclin-dependent kinases in cancer therapy. *Nat Rev Drug Discov* **14**:130-146.

Berens ME and Giese a (1999) "...those left behind." Biology and oncology of invasive glioma cells. *Neoplasia (New York, NY)* **1**:208-219.

Blouw B, Song HQ, Tihan T, Bosze J, Ferrara N, Gerber HP, Johnson RS and Bergers G (2003) The hypoxic response of tumors is dependent on their microenvironment. *Cancer Cell* **4**:133-146.

Carlson BL, Pokorny JL, Schroeder MA and Sarkaria JN (2011) Establishment, maintenance and in vitro and in vivo applications of primary human glioblastoma multiforme (GBM) xenograft models for translational biology studies and drug discovery. *Current protocols in pharmacology / editorial board, SJ Enna (editor-in-chief) [et al]* **Chapter 14**:Unit 14.16-Unit 14.16.

Cen L, Carlson BL, Schroeder Ma, Ostrem JL, Kitange GJ, Mladek AC, Fink SR, Decker Pa, Wu W, Kim J-S, Waldman T, Jenkins RB and Sarkaria JN (2012) p16-Cdk4-Rb axis controls sensitivity to a cyclin-dependent kinase inhibitor PD0332991 in glioblastoma xenograft cells. *Neuro-oncology* **14**:870-881.

Chen EI, Hewel J, Krueger JS, Tiraby C, Weber MR, Kralli A, Becker K, Yates JR, 3rd and Felding-Habermann B (2007) Adaptation of energy metabolism in breast cancer brain metastases. *Cancer Res* **67**:1472-1486.

Da Silva L, Simpson PT, Smart CE, Cocciardi S, Waddell N, Lane A, Morrison BJ, Vargas AC, Healey S, Beesley J, Pakkiri P, Parry S, Kurniawan N, Reid L, Keith P, Faria P, Pereira E, Skalova A, Bilous M, Balleine RL, Do H, Dobrovic A, Fox S, Franco M, Reynolds B, Khanna KK, Cummings M,

Chenevix-Trench G and Lakhani SR (2010) HER3 and downstream pathways are involved in colonization of brain metastases from breast cancer. *Breast Cancer Res* **12**:R46.

de Gooijer MC, Zhang P, Thota N, Mayayo-Peralta I, Buil LCM, Beijnen JH and van Tellingen O (2015) P-glycoprotein and breast cancer resistance protein restrict the brain penetration of the CDK4/6 inhibitor palbociclib. *Investigational new drugs* **33**:1012-1019.

de Vries NA, Beijnen JH and van Tellingen O (2009) High-grade glioma mouse models and their applicability for preclinical testing. *Cancer Treat Rev* **35**:714-723.

Dhillon S (2015) Palbociclib: First Global Approval. *Drugs* **75**:543-551.

Dickson Ma (2014) Molecular Pathways: CDK4 Inhibitors for Cancer Therapy. *Clinical cancer research : an official journal of the American Association for Cancer Research* **20**:3379-3383.

Fairbanks CA, Kitto KF, Nguyen HO, Stone LS and Wilcox GL (2009) Clonidine and dexmedetomidine produce antinociceptive synergy in mouse spinal cord. *Anesthesiology* **110**:638-647.

Finn RS, Crown JP, Lang I, Boer K, Bondarenko IM, Kulyk SO, Ettl J, Patel R, Pinter T, Schmidt M, Shparyk Y, Thummala AR, Voytko NL, Fowst C, Huang X, Kim ST, Randolph S and Slamon DJ (2015) The cyclin-dependent kinase 4/6 inhibitor palbociclib in combination with letrozole versus letrozole alone as first-line treatment of oestrogen receptor-

positive, HER2-negative, advanced breast cancer (PALOMA-1/TRIO-18): a randomised phase 2 study. *The Lancet Oncology* **16**:25-35.

Maxwell PH, Dachs GU, Gleadle JM, Nicholls LG, Harris AL, Stratford IJ, Hankinson O, Pugh CW and Ratcliffe PJ (1997) Hypoxia-inducible factor-1 modulates gene expression in solid tumors and influences both angiogenesis and tumor growth. *Proceedings of the National Academy of Sciences of the United States of America* **94**:8104-8109.

Mayer A, Schneider F, Vaupel P, Sommer C and Schmidberger H (2012) Differential expression of HIF-1 in glioblastoma multiforme and anaplastic astrocytoma. *Int J Oncol* **41**:1260-1270.

Ostrom QT, Gittleman H, Liao P, Rouse C, Chen Y, Dowling J, Wolinsky Y, Kruchko C and Barnholtz-Sloan J (2014) CBTRUS statistical report: primary brain and central nervous system tumors diagnosed in the United States in 2007-2011. *Neuro Oncol* **16 Suppl 4**:iv1-63.

Parrish KE, Pokorny J, Mittapalli RK, Bakken K, Sarkaria JN and Elmquist WF (2015a) Efflux Transporters at the Blood-Brain Barrier Limit Delivery and Efficacy of Cyclin-Dependent Kinase 4/6 Inhibitor Palbociclib (PD-0332991) in an Orthotopic Brain Tumor Model. *The Journal of pharmacology and experimental therapeutics* **355**:264-271.

Parrish KE, Sarkaria JN and Elmquist WF (2015h) Improving drug delivery to primary and metastatic brain tumors: strategies to overcome the blood-brain barrier. *Clin Pharmacol Ther* **97**:336-346.

Peyressatre M, Prével C, Pellerano M and Morris M (2015) Targeting Cyclin-Dependent Kinases in Human Cancers: From Small Molecules to Peptide Inhibitors. *Cancers* **7**:179-237.

Pokorny JL, Calligaris D, Gupta SK, Iyekegbe DO, Mueller D, Bakken KK, Carlson BL, Schroeder Ma, Evans DL, Lou Z, Decker Pa, Eckel-Passow J, Pucci V, Ma B, Shumway SD, Elmquist WF, Agar NY and Sarkaria JN (2015) The efficacy of the Wee1 inhibitor MK-1775 combined with temozolomide is limited by heterogeneous distribution across the blood-brain barrier in glioblastoma. *Clinical Cancer Research* **21**:1916-1925.

Raub TJ, Wishart GN, Kulanthaivel P, Staton BA, Ajamie RT, Sawada GA, Gelbert LM, Shannon HE, Sanchez-Martinez C and De Dios A (2015) Brain Exposure of Two Selective Dual CDK4 and CDK6 Inhibitors and the Antitumor Activity of CDK4 and CDK6 Inhibition in Combination with Temozolomide in an Intracranial Glioblastoma Xenograft. *Drug Metab Dispos* **43**:1360-1371.

Ryan HE, Lo J and Johnson RS (1998) HIF-1alpha is required for solid tumor formation and embryonic vascularization. *EMBO Journal* **17**:3005-3015.

Sane R, Agarwal S and Elmquist WF (2012) Brain distribution and bioavailability of elacridar after different routes of administration in the mouse. *Drug Metab Dispos* **40**:1612-1619.

Sane R, Mittapalli RK and Elmquist WF (2013) Development and evaluation of a novel microemulsion formulation of elacridar to improve its bioavailability. *J Pharm Sci* **102**:1343-1354.

Stone LS, German JP, Kitto KF, Fairbanks CA and Wilcox GL (2014) Morphine and clonidine combination therapy improves therapeutic window in mice: synergy in antinociceptive but not in sedative or cardiovascular effects. *PLoS One* **9**:e109903.

Svokos KA, Salhia B and Toms SA (2014) Molecular biology of brain metastasis. *Int J Mol Sci* **15**:9519-9530.

Vartanian A, Singh SK, Agnihotri S, Jalali S, Burrell K, Aldape KD and Zadeh G (2014) GBM's multifaceted landscape: highlighting regional and microenvironmental heterogeneity. *Neuro Oncol* **16**:1167-1175.

Wang J, Klem J, Wyrick JB, Ozawa T, Cunningham E, Golinveaux J, Allen MJ, Lamborn KR and Deen DF (2003) Detection of Hypoxia in Human Brain Tumor Xenografts Using a Modified Comet Assay1. *Neoplasia* **5**:288-296.

CHAPTER V

Abbott NJ (2013) Blood-brain barrier structure and function and the challenges for CNS drug delivery. *J Inherit Metab Dis* **36**:437-449.

Agarwal S, Sane R, Gallardo JL, Ohlfest JR and Elmquist WF (2010) Distribution of gefitinib to the brain is limited by P-glycoprotein (ABCB1) and breast cancer resistance protein (ABCG2)-mediated active efflux. *J Pharmacol Exp Ther* **334**:147-155.

Agarwal S, Sane R, Oberoi R, Ohlfest JR and Elmquist WF (2011) Delivery of molecularly targeted therapy to malignant glioma, a disease of the whole brain. *Expert Rev Mol Med* **13**:e17.

Agarwal S, Uchida Y, Mittapalli RK, Sane R, Terasaki T and Elmquist WF (2012) Quantitative Proteomics of Transporter Expression in Brain Capillary Endothelial Cells Isolated from P-Glycoprotein (P-gp), Breast Cancer Resistance Protein (Bcrp), and P-gp / Bcrp Knockout Mice. *Drug Metab Dispos* **40**:1164-1169.

Asghar U, Witkiewicz AK, Turner NC and Knudsen ES (2015) The history and future of targeting cyclin-dependent kinases in cancer therapy. *Nat Rev Drug Discov* **14**:130-146.

Bihorel S, Camenisch G, Lemaire M and Scherrmann JM (2007) Influence of breast cancer resistance protein (Abcg2) and p-glycoprotein (Abcb1a) on

the transport of imatinib mesylate (Gleevec) across the mouse blood-brain barrier. *J Neurochem* **102**:1749-1757.

Cloughesy TF, Cavenee WK and Mischel PS (2014) Glioblastoma: from molecular pathology to targeted treatment. *Annu Rev Pathol* **9**:1-25.

Dagenais C, Rousselle C, Pollack GM and Scherrmann JM (2000) Development of an in situ mouse brain perfusion model and its application to mdr1a P-glycoprotein-deficient mice. *J Cereb Blood Flow Metab* **20**:381-386.

Davies Ma (2012) *Targeted therapy for brain metastases*. Elsevier Inc.

de Gooijer MC, Zhang P, Thota N, Mayayo-Peralta I, Buil LC, Beijnen JH and van Tellingen O (2015) P-glycoprotein and breast cancer resistance protein restrict the brain penetration of the CDK4/6 inhibitor palbociclib. *Invest New Drugs* **33**:1012-1019.

Deguchi Y, Nozawa K, Yamada S, Yokoyama Y and Kimura R (1997) Quantitative evaluation of brain distribution and blood-brain barrier efflux transport of probenecid in rats by microdialysis: possible involvement of the monocarboxylic acid transport system. *J Pharmacol Exp Ther* **280**:551-560.

Drion N, Lemaire M, Lefauconnier JM and Scherrmann JM (1996) Role of P-glycoprotein in the blood-brain transport of colchicine and vinblastine. *J Neurochem* **67**:1688-1693.

Drion N, Risede P, Cholet N, Chanez C and Scherrmann JM (1997) Role of P-170 glycoprotein in colchicine brain uptake. *J Neurosci Res* **49**:80-88.

Fidler IJ (2015) The Biology of Brain Metastasis: Challenges for Therapy. *Cancer J* **21**:284-293.

Golden PL and Pollack GM (2003) Blood-brain barrier efflux transport. *J Pharm Sci* **92**:1739-1753.

Kalvass JC, Polli JW, Bourdet DL, Feng B, Huang SM, Liu X, Smith QR, Zhang LK, Zamek-Gliszczynski MJ and International Transporter C (2013) Why clinical modulation of efflux transport at the human blood-brain barrier is unlikely: the ITC evidence-based position. *Clin Pharmacol Ther* **94**:80-94.

Lin X and DeAngelis LM (2015) Treatment of Brain Metastases. *J Clin Oncol* **33**:3475-3484.

Miyama T, Takanaga H, Matsuo H, Yamano K, Yamamoto K, Iga T, Naito M, Tsuruo T, Ishizuka H, Kawahara Y and Sawada Y (1998) P-glycoprotein-mediated transport of itraconazole across the blood-brain barrier. *Antimicrob Agents Chemother* **42**:1738-1744.

Oberoi RK, Parrish KE, Sio TT, Mittapalli RK, Elmquist WF and Sarkaria JN (2016) Strategies to improve delivery of anticancer drugs across the blood-brain barrier to treat glioblastoma. *Neuro Oncol* **18**:27-36.

Ostrom QT, Gittleman H, Liao P, Rouse C, Chen Y, Dowling J, Wolinsky Y, Kruchko C and Barnholtz-Sloan J (2014) CBTRUS statistical report: primary brain and central nervous system tumors diagnosed in the United States in 2007-2011. *Neuro Oncol* **16 Suppl 4**:iv1-63.

Parrish KE, Pokorny J, Mittapalli RK, Bakken K, Sarkaria JN and Elmquist WF (2015a) Efflux Transporters at the Blood-Brain Barrier Limit Delivery and Efficacy of Cyclin-Dependent Kinase 4/6 Inhibitor Palbociclib (PD-0332991) in an Orthotopic Brain Tumor Model. *J Pharmacol Exp Ther* **355**:264-271.

Parrish KE, Sarkaria JN and Elmquist WF (2015g) Improving drug delivery to primary and metastatic brain tumors: strategies to overcome the blood-brain barrier. *Clin Pharmacol Ther* **97**:336-346.

Raub TJ, Gelbert LM, Wishart GN, Sanchez-Martinez C, Kulanthaivel P, Staton Ba, Ajamie RT, Sawada Ga, Shannon HE and De Dios a (2015a) Brain Exposure of Two Selective Dual CDK4 and CDK6 Inhibitors and the Antitumor Activity of CDK4 and 6 Inhibition in Combination with Temozolomide in an Intracranial Glioblastoma Xenograft. *Drug Metabolism and Disposition*.

Raub TJ, Wishart GN, Kulanthaivel P, Staton BA, Ajamie RT, Sawada GA, Gelbert LM, Shannon HE, Sanchez-Martinez C and De Dios A (2015b) Brain Exposure of Two Selective Dual CDK4 and CDK6 Inhibitors and the Antitumor Activity of CDK4 and CDK6 Inhibition in Combination with Temozolomide in an Intracranial Glioblastoma Xenograft. *Drug Metab Dispos* **43**:1360-1371.

Sanchez-Martinez C, Gelbert LM, Lallena MJ and de Dios A (2015) Cyclin dependent kinase (CDK) inhibitors as anticancer drugs. *Bioorg Med Chem Lett* **25**:3420-3435.

Sane R, Agarwal S, Mittapalli RK and Elmquist WF (2013) Saturable active efflux by p-glycoprotein and breast cancer resistance protein at the blood-brain barrier leads to nonlinear distribution of elacridar to the central nervous system. *J Pharmacol Exp Ther* **345**:111-124.

Sasongko L, Link JM, Muzi M, Mankoff DA, Yang X, Collier AC, Shoner SC and Unadkat JD (2005) Imaging P-glycoprotein transport activity at the human blood-brain barrier with positron emission tomography. *Clin Pharmacol Ther* **77**:503-514.

Smith QR (1996) Brain perfusion systems for studies of drug uptake and metabolism in the central nervous system. *Pharm Biotechnol* **8**:285-307.

Smith QR and Allen DD (2003) In situ brain perfusion technique. *Methods Mol Med* **89**:209-218.

Stenehjem DD, Hartz AM, Bauer B and Anderson GW (2009) Novel and emerging strategies in drug delivery for overcoming the blood-brain barrier. *Future Med Chem* **1**:1623-1641.

Tamai I and Tsuji A (2000) Transporter-mediated permeation of drugs across the blood-brain barrier. *J Pharm Sci* **89**:1371-1388.

Thomas FC, Taskar K, Rudraraju V, Goda S, Thorsheim HR, Gaasch JA, Mittapalli RK, Palmieri D, Steeg PS, Lockman PR and Smith QR (2009)

Uptake of ANG1005, a novel paclitaxel derivative, through the blood-brain barrier into brain and experimental brain metastases of breast cancer. *Pharm Res* **26**:2486-2494.

Uchida Y, Ohtsuki S, Katsukura Y, Ikeda C, Suzuki T, Kamiie J and Terasaki T (2011) Quantitative targeted absolute proteomics of human blood-brain barrier transporters and receptors. *J Neurochem* **117**:333-345.

VanArsdale T, Boshoff C, Arndt KT and Abraham RT (2015) Molecular Pathways: Targeting the Cyclin D-CDK4/6 Axis for Cancer Treatment. *Clin Cancer Res* **21**:2905-2910.

Wang T, Agarwal S and Elmquist WF (2012) Brain distribution of cediranib is limited by active efflux at the blood-brain barrier. *J Pharmacol Exp Ther* **341**:386-395.

Zhao R, Kalvass JC and Pollack GM (2009a) Assessment of blood-brain barrier permeability using the in situ mouse brain perfusion technique. *Pharm Res* **26**:1657-1664.

Zhao R, Kalvass JC, Yanni SB, Bridges AS and Pollack GM (2009d) Fexofenadine brain exposure and the influence of blood-brain barrier P-glycoprotein after fexofenadine and terfenadine administration. *Drug Metab Dispos* **37**:529-535.